UNIVERSIDADE DO PORTO

MASTER'S THESIS

Aspects of superradiant scattering off Kerr black holes

Author:
José SÁ

Supervisor:
João ROSA

Co-supervisor:
Orfeu BERTOLAMI

A thesis submitted in fulfilment of the requirements
for the degree of Master of Science

at the

Faculdade de Ciências da Universidade do Porto
Departamento de Física e Astronomia

September 2017

Acknowledgements

First and foremost, I would like to thank my father, Domingo, and my mother, Rosa, for all the support and care given and for all the sacrifices made all these years, which allowed me to be in the privileged position I am today. I want to thank my brother, Cristiano, for the all laughs and joy shared on the weekends. I would like to thank Carlos and Carmo, Sara and Inês for being like a second family to me. I want to offer a special word to Carlos for truly treating me like a son.

Thank you Mara, for all the love and care, for always pushing me to be better and always believing in me.

I wish express the utmost gratitude to my supervisor, Professor João Rosa, for the availabilty, help and invaluable advice he provided during this year. It is been an incredible experience working with you. Also want leave a word of appreciation for my cosupervisor, Professor Orfeu Bertolami, for being a supportive and present figure during my academic years.

I want to thank Artur, Luís and Pedro for the help, friendship and for all the great moments spent this academic year. I would like to thank, among many others, Carlos Nunes e Vitor Bessa for all the incredible and funny moments shared during these years.

Last but not least, I want to thank all the professors who shared their knowledge in physics and mathematics throughout my collage years. I want to express a word of gratitude for all the colleges I shared the classroom with.

UNIVERSIDADE DO PORTO

Abstract

Faculdade de Ciências da Universidade do Porto
Departamento de Física e Astronomia

Master of Science

Aspects of superradiant scattering off Kerr black holes

by José SÁ

In this work we study the phenomena of superradiance in the context of General Relativity, with particular focus on scattering of electromagnetic waves by rotating black hole. We give a short introduction to Kerr black holes, specifying some of their symmetries and properties. We then introduce the Newman-Penrose formalism to study wave perturbations in a Kerr background, and obtain the electromagnetic case of Teukolsky's master equation. This equation is both solved using approximate analytical methods and numerical techniques that are presented in detail. We obtain the amplification/absorption factor for each multipole mode with high precision, obtaining a very good agreement with those found in the literature. Finally, we discuss the scattering of realistic electromagnetic waves by a Kerr BH, which are superpositions of these different modes.

UNIVERSIDADE DO PORTO

Resumo

Faculdade de Ciências da Universidade do Porto
Departamento de Física e Astronomia

Mestre de Ciência

Aspects of superradiant scattering off Kerr black holes

por José SÁ

Neste trabalho, estudamos os fenómenos de superradiância no contexto da Relatividade Geral, com foco particular na dispersão de ondas eletromagnéticas por buracos negros em rotação. Apresentamos uma pequena introdução aos buracos negros de Kerr, especificando algumas das suas simetrias e propriedades. De seguida, introduzimos o formalismo de Newman-Pensore para estudar perturbações em espaço-tempo de Kerr, e obtemos o caso electromagético da equação de Teukolsky. Esta equação é resolvida usando métodos analíticos aproximados e técnicas numéricas que são apresentadas em detalhe. Obtemos o fator de amplificação/absorção para cada modo multipolar com elevada precisão, obtendo uma boa concordância com os que são encontrados na literatura. Por fim, é discutida a dispersão de uma onda electromagnéria realista pelo buraco negro de Kerr, composta por uma sobreposição de modos diferentes.

Contents

Acknowledgements iii

Abstract v

Resumo vii

Contents ix

List of Figures xi

List of Tables xiii

Abbreviations xv

1 Superradiance 1
- 1.1 Introduction . . . 1
- 1.2 Klein paradox as a first example . . . 3
  - 1.2.1 Bosons . . . 3
  - 1.2.2 Fermions . . . 4

2 Kerr black hole 7
- 2.1 General Relativity . . . 7
- 2.2 Spacetime symmetries . . . 9
- 2.3 Kerr-Schild coordinates . . . 11
- 2.4 Boyer-Lindquist coordinates . . . 14
- 2.5 Ergoregion and the Penrose process . . . 17

3 Teukolsky's master equation 21
- 3.1 Newman-Penrose formalism . . . 21
  - 3.1.1 Kinnersley tetrad . . . 22
  - 3.1.2 Maxwell equations . . . 24
- 3.2 Spin-Weighted Spheroidal Harmonics . . . 31
- 3.3 Analytic radial approximations . . . 34
- 3.4 Amplification factor ${}_sZ_{\ell m}$ . . . 38

4 Numerical methods 43
- 4.1 Angular Eigenvalues . . . 43

4.1.1 Leaver method . . . 44
4.1.2 Spectral method . . . 45
4.2 Amplification factor . . . 48

5 Superradiant scattering of plane waves **55**
5.1 Harmonics decomposition . . . 56
5.2 Scattering theory . . . 58
5.3 Phase-shifts . . . 59

6 Discussion and future work **63**

A Tetrad techniques **65**
A.1 Noncoordinate representation . . . 65
A.2 Spin connection . . . 66

B Additional Newman-Penrose definitions and computations **69**
B.1 Spin coefficients . . . 69

C Spin-weighted spherical harmonics **73**

D Eigenvalue small-c expansion **77**

Bibliography **79**

List of Figures

2.1 Contour plots of the surface $r(x,y,z)/a$ for constant values of 0, 1/2, 1, 3/2, in the Kerr-Schild coordinates. The left plot is the intersection of the $y = 0$ plane with the 3D representation (right) that spotlights the ring singularity. Dashed curves representing orthogonal constant $\theta(x,y,z)$ hypersufaces become asymptotically affine. 13

2.2 Illustration of the Schwarzschild (A,C) and Kerr (B,D) null equatorial infalling geodesics given by Eqs. (2.26), for $r(0) = 20M$, with emphasis on $L \neq 0$. Even starting with opposite angular momentum, the Kerr geodesic (D) is forced to co-rotate with the BH once crossed the ergoregion (dotted). . 17

2.3 Illustration of the Penrose process, with ergoregion (dotted) and event horizon surfaces parameterized in Kerr-Schild cartesian coordinates. 18

4.1 Showcasing discontinuities in the values of ${}_{\pm1}\mathcal{E}_{\ell 1}$ for $m = 1, 2$ when using an incorrect implementation of the Leaver method. Real values of the eigenvalues are shown as dashed lines ($m = 1, 2, 3$) of the same color. 44

4.2 Eigenvalues for $\ell = 1$ (left) and $\ell = 2$ (right) for typical values of c, using the spectral method. 47

4.3 Plots of all spin-weighted spheroidal harmonics ${}_{-1}S_{\ell m}(\theta, 0)$ with $\ell = 1$ (left) and $\ell = 2$ (right) for $s = -1$ and $c = 0.4$. This plot shares the same legend coloring as the above (Figure 4.2). Dotted curves represent the values of the ${}_{-1}Y_{\ell m}$, when $c \to 0$. 47

4.4 Amplification factor of an extremal BH ($\mathcal{J} = 0.9999$) for modes with $\ell = 1$. In this figure, superradiance occurs only for $m = 1$ as predicted. 50

4.5 Log plot demonstrating error propagation for ${}_{\pm1}Z_{53}$ when computing the factor using both numerical solutions for the radial part of ϕ_0 and ϕ_2. 51

4.6 Log plot of ${}_{\pm1}Z_{\ell m}$ as a function of $\bar{\omega}/m\bar{\omega}_H$ [32]. Each color represents the same value of ℓ, while different dashing corresponds to grouping the modes as $|\ell - m| = 0, 1, 2$. 53

5.1 Plot of the scattering function $|f(\theta, 0)|^2$ truncated at different $\ell_{\max}$, for values of $\mathcal{J} = 0.99$ and $\bar{\omega} = 0.4$, showing divergence in $\theta = \theta_0 = 0$. 60

5.2 Plots of the phase-shifts δ_ℓ compared with the newtonian shifts δ_N summed with a given adjustment constant δ_0 (fitted), for two given BH configurations and modes. 62

5.3 Plots of the regularized partial wave sum, $|f_D(\theta, 0)|^2$, for the same configurations of Figure 5.2. 62

List of Tables

3.1 Newman-Penrose fields that obey the Teukolsky master equation for different spin-weights [29] 30

3.2 Radial function solutions (ϕ_0 and ϕ_2) for near-horizon and far-horizon approximations 41

Abbreviations

BH	Black Hole
BL	Boyer-Lindquist
EF	Eddington-Finkelstein
GR	General Relativity
GW	Gravitational Wave
NP	Newman-Penrose
QFT	Quantum Field Theory
SWSH	Spin-Weighted Spheroidal Harmonic

Chapter 1

Superradiance

1.1 Introduction

The first direct observation of gravitational waves (GWs) by the Laser Interferometer Gravitational Wave Observatory (LIGO) was in 2015 and later announced in 2016. The recorded event matched the predictions of General Relativity (GR) for a binary system of black holes (BHs) merging together in an inward spiral into a single BH [1]. These observations demonstrated not only the existence of GWs but also existence of binary stellar-mass BH systems and that these systems could merge in a time less than the known Universe age. Since then, two more similar events were detected, which assured the inauguration of a new era of GW cosmology.

Naturally, this sparked new interest in the study of binary systems and GW-related phenomena. One of these phenomena is the possibility of amplification in waves scattered off rotating and/or charged BHs, which can occur under certain conditions for scalar, electromagnetic (EM) and gravitational bosonic waves. Such effect is one of many that encompass a wide range of phenomena generally known as *superradiance*. In this work, we aim to study in detail the effects of superradiance for EM waves scattering off rotating BHs, paving the way for future observational studies of this phenomenon.

Historically, the first appearance of the concept of superradiance appeared in 1954, in a publication by Dicke [2]. Almost two decades later, Zel'dovich [3, 4] showed that an absorbing cylinder rotating with an angular velocity Ω could amplify an incident wave, $\psi \sim e^{-i\omega t + im\phi}$, with frequency ω if

$$\omega < m\,\Omega \tag{1.1}$$

were satisfied, where m is the usual azimuthal number of the monochromatic plane wave relative to the rotation axis. In his work, he noticed that superradiance was related with dissipation of rotational energy from the absorbing object, possibly due to spontaneous pair creation at the surface. Hawking later showed [5] that the presence of strong electromagnetic or gravitational fields could indeed generate bosonic and fermionic pairs spontaneously. This result was possible by the efforts of Starobinsky and Deruelle [6–9], which also laid the groundwork necessary for the discovery of BH evaporation.

Among other possible cases of radiation amplification, the phenomena worked out throughout this work is an example of *rotational superradiance*. As the name suggests, it occurs in the presence of "rotating" objects, as is the famous example of Zel'dovich cylinder. The condition Eq. (1.1) also appears in the context of general relativity, but in this case Ω represents the angular velocity of a Kerr BH event horizon. This geometry is the simplest solution for a static but non-stationary BH, which breaks spherical symmetry. In Chapter 2 we describe many features of the Kerr BH, the most important for this work being the existence of an *ergoregion* where is possible for an infalling particle (or wave) to have negative energy [10] when measured by a static observer in asymptotic flat space. As a result, under certain conditions it is possible for a particle to extract energy from the BH through the *Penrose process* [11], which is a counterpart to wave amplification.

In the case of superradiance, it is was shown by Teukolsky that all types of wave perturbations propagating in the Kerr background are described using the same master equation [12, 13]. This generalization is only possible by recurring to the Newman-Pensore (NP) formalism, which is a form of spinor calculus in GR [14], introduced in Chapter 3. Certain modes in bosonic waves (scalar, electromagnetic, gravitational) can be amplified while others are partially or totally absorbed by the BH. Also, it can be shown that fermionic waves cannot be amplified [15]. Therefore we will focus primarily on EM waves in the case of a neutral rotating BH, which needs less algebraic computations to achieve to the same master equation. However, this study provides a close parallel to the gravitational case as it provides insight to the same physical process.

The effects of superradiance can be computed for each mode by solving the radial part of Teukolsky's equation using approximate analytical methods [6, 7]. Since no other analytical methods that solve this problem have been found, the only other way of tackling the problem is by taking a numerical approach. All steps necessary to implement this method are explained in detail in Chapter 4, including some results.

In Chapter 5 it is addressed a we address the scattering of EM plane waves. Plane waves are a composition superposition of harmonic modes that are scattered independently by the black hole, with different amplification/absorption factors and phase-shifts. We discuss how these different effects add up in the overall scattered wave.

We summarize and make an overall appreciation of our results and conclusions in Chapter 6, along with discussing the prospects for future observational tests of black hole superradiance.

1.2 Klein paradox as a first example

Radiation amplification can be traced to the birth of Quantum Mechanics, in the beginning of the 20th century. First studies of the Dirac equation by Klein [16] revealed the possibility of electrons propagating in a region with a sufficiently large potential barrier without the expected dampening from non-relativistic tunnel effect. Due to some confusion, this result was wrongly interpreted by some authors as fermionic superradiance, as if the current reflected by the barrier could be greater than the incident current. The problem was named *Klein paradox* by Sauter [17] and this misleading result was due to an incorrect calculation of the group velocities of the reflected and transmitted waves.

Today, it is known that fermionic currents cannot be amplified for this particular problem [16, 18], a result that was correctly obtained by Klein in is original paper. On the contrary, superradiant scattering can indeed occur for bosonic fields.

1.2.1 Bosons

The equation that governs bosonic wave function is the Klein-Gordon equation, which for a minimally coupled electromagnetic potential takes the form

$$(D^\nu D_\nu - \mu^2)\Phi = 0\,, \tag{1.2}$$

where the usual partial derivative becomes $D_\nu \equiv \partial_\nu + ieA_\nu$ and μ is the boson mass.

The problem is greatly simplified by considering flat space-time in (1+1)-dimensions and a step potential $A_t(x) = V\,\theta(x)$, for constant $V > 0$ and wave solutions $\Phi = e^{-i\omega t}\phi$. For $x < 0$, the solution can be divided as incident and reflected, taking the form

$$\phi_{\text{inc}}(x) = \mathcal{I}\, e^{ikx}\,, \qquad \phi_{\text{refl}}(x) = \mathcal{R}\, e^{-ikx}\,, \tag{1.3}$$

in which the dispersion relation states that $k = \sqrt{\omega^2 - \mu^2}$. For $x > 0$, the transmitted wave is naturally given by

$$\psi_{\text{inc}}(x) = \mathcal{T} e^{iqx} \,, \tag{1.4}$$

but in this case the root sign for the momentum must be carefully chosen so that the group velocity sign of the transmitted wave matches that of the incoming wave [18], *i.e.*

$$\left.\frac{\partial\omega}{\partial p}\right|_{p=q} = \frac{q}{\omega - eV} > 0 \,, \tag{1.5}$$

therefore we must have that

$$q = \text{sgn}(\omega - eV)\sqrt{(\omega - eV)^2 - \mu^2} \,. \tag{1.6}$$

After obtaining the continuity relations at the barrier, $x = 0$, we follow by computing the ratios of the transmitted and reflected currents relative to the incident one, which yield

$$\frac{j_{\text{refl}}}{j_{\text{inc}}} = -\left|\frac{\mathcal{R}}{\mathcal{I}}\right|^2 = -\left|\frac{1-r}{1+r}\right|^2 \,, \qquad \frac{j_{\text{trans}}}{j_{\text{inc}}} = \text{Re}(r)\left|\frac{\mathcal{T}}{\mathcal{I}}\right|^2 = \frac{4\,\text{Re}(r)}{|1+r|^2} \,, \tag{1.7}$$

written as a function of the coefficient

$$r = \frac{q}{k} = \text{sgn}(\omega - eV)\sqrt{\frac{(\omega - eV)^2 - \mu^2}{\omega^2 - \mu^2}} \,. \tag{1.8}$$

Hence, in the case of strong potential limit, $eV > \omega + \mu > 2\mu$, we may have $r < 0$ real and the reflected current is larger (in magnitude) than the incident wave and therefore we have amplification.

1.2.2 Fermions

Dirac noticed that the Klein-Gordon equation masked internal degrees of freedom, so he devised his own equation which describes fermions. Considering that scalar potentials do not have any impact on spin orientation [19], we need only to consider half of the spinor components in the Dirac equation

$$(i\gamma^\nu D_\nu - \mu)\Psi = 0 \,, \tag{1.9}$$

where μ is the fermion mass, for which a valid representation of the gamma matrices is

$$\gamma^0 = \begin{pmatrix} 1 & 0 \\ 0 & -1 \end{pmatrix}, \qquad \gamma^1 = \begin{pmatrix} 0 & 1 \\ -1 & 0 \end{pmatrix}. \tag{1.10}$$

Probing wave solutions $\Psi = e^{-i\omega t}\psi$, the incident and reflected solutions are

$$\psi_{\text{inc}}(x) = \mathcal{I}\, e^{ikx} \begin{pmatrix} 1 \\ \dfrac{k}{\omega+\mu} \end{pmatrix}, \qquad \psi_{\text{refl}}(x) = \mathcal{R}\, e^{-ikx} \begin{pmatrix} 1 \\ \dfrac{-k}{\omega+\mu} \end{pmatrix}, \tag{1.11}$$

while for $x > 0$, the transmitted wave function is written as

$$\psi_{\text{trans}}(x) = \mathcal{T}\, e^{iqx} \begin{pmatrix} 1 \\ \dfrac{q}{\omega - eV + \mu} \end{pmatrix}, \tag{1.12}$$

where we followed the same procedure as before, obtaining the same results from Eq. (1.5) through (1.7). Due to the structure of the spinor components, the coefficient in Eq. (1.8) is modified to

$$r = \operatorname{sgn}(\omega - eV)\frac{\omega+\mu}{\omega - eV + \mu}\sqrt{\frac{(\omega - eV)^2 - \mu^2}{\omega^2 - \mu^2}}, \tag{1.13}$$

and now, in the same region, $\omega > \mu$, superradiance does not occur.

Even though superradiance and spontaneous pair creation are two distinct phenomena, this result is usually interpreted using the latter, from a Quantum Field Theory (QFT) stand point. All incident particles are completely reflected, as well as some extra due to pair creation at the barrier as a result of stimulation by the incident radiation and the presence of a strong electromagnetic field, while the resultant anti-particles are transmitted in the opposite direction, accounting for the change of sign in the transmitted current in Eq. (1.7), owing to the opposite charge they carry. This also explains the undamped transmission part.

One may think that this difference between bosons and fermions arises from the potential barrier shape, but work by other authors [17, 18, 20] shows that only the difference between the asymptotic values of the potential at infinity is essential for the process. The difference comes from intrinsic properties of these particles. The amount of fermion pairs

produced in a given state, *i.e.* for a given ω, is limited by Pauli's exclusion principle, while such limitation does not occur for bosons [15]. Additionally, fermionic current densities are always positive definite, while bosons can change sign because of the ambiguity in the wave function describing positive and negative energy solutions.

The minimum necessary energy for this to occur, 2μ, leaves evidence that superradiance is accompanied with spontaneous pair creation and some sort of dissipation by the battery maintaining the strong electromagnetic potential, in order to maintain energy balance.

Chapter 2

Kerr black hole

2.1 General Relativity

General Relativity is the theory of space, time and gravitation developed by Einstein in 1915. It introduces a new viewpoint on gravity and its relation with the fabric of spacetime, a *manifold* that bounds our three spatial dimensions with time. The concept challenged our deeply ingrained and intuitive notions of nature, partially because the mathematical background needed to understand the precise formulation of the theory was unfamiliar to much of the physics community at the time. This formulation corresponds to a field theory with the dynamical object of study being the metric of spacetime, $\boldsymbol{g} = g_{\mu\nu}\mathrm{d}x^\mu \mathrm{d}x^\nu$, connecting geometry with mass and energy through Einstein's field equations. The theory inherits diffeomorphism invariance, *i.e.* remains the same theory by an active change of coordinates, which was at the core of definition of manifolds.

Immediately after, in 1916, Schwarzschild found the first solution [21], describing a static spherical isolated object. Then, the theory was left aside because of the numerous coupled nonlinear equations, but the astronomical discovery of compact and highly energetic objects in the 1950s breaded new interest into the somewhat dormant GR, mainly because it was thought that these quasars and compact X-ray sources had suffered some form of gravitational collapse or that strong gravitational fields were present. Soon after, the modern theory of gravitational collapse was developed in the mid-1960s, including other BH solutions, for example Kerr's [22].

The theory of GR can be elegantly described in the form of the Hilbert action,

$$S_H = \frac{1}{16\pi}\int \mathrm{d}^4x\sqrt{-g}\,R\,, \tag{2.1}$$

where $g = \det(g_{\mu\nu})$ and $R = g_{\alpha\beta}R^{\alpha\beta}$ corresponds to the Ricci scalar. Naturally, the first solutions corresponded to pure gravity, usually designated as vacuum solutions [10], which obey

$$R_{\mu\nu} = 0\,. \tag{2.2}$$

Despite their simplicity, they enjoy some very fascinating nontrivial properties. One of which is the existence of an event horizon, a surface that separates two causally disconnected regions of spacetime.

The underlying technique behind the study of superradiance is the linearization of Einstein and/or Maxwell equations around known BHs in stationary equilibrium. These perturbations will obey a series of partial differential equations whose dynamical variables are components of the Weyl tensor, $C_{\mu\nu\rho\sigma}$, or the Maxwell field tensor, $F_{\mu\nu}$. Thanks to the NP formalism we will be able to decouple and separate the equations for both GWs and EM waves, revealing decoupled variables which contain all the information needed about the nontrivial perturbations, instead of working with all components of the field tensors.

For the gravitational case, a straightforward way of obtaining a linearized theory is to consider a background stationary BH solution, ${g_{\mu\nu}}^B$, and then expanding the field equations (2.2) using the metric

$${g_{\mu\nu}} = {g_{\mu\nu}}^B + {h_{\mu\nu}}^P\,, \tag{2.3}$$

keeping only terms that are $\mathcal{O}({h_{\mu\nu}}^B)$. The indices B and P refer to the background and perturbations, respectively. As a result we are left with a wave equation in the given background.

In this work we will focus on (massless, neutral) electromagnetic waves and perturbations are performed including EM interactions through the Maxwell action

$$S_{EM} = -\frac{1}{4}\int \mathrm{d}^4x\sqrt{-g}\,F_{\alpha\beta}F^{\alpha\beta}\,, \tag{2.4}$$

where $F_{\mu\nu}$ is the Maxwell tensor. Variation of both actions, $\delta(S_H + S_{EM}) = 0$, result in two field equations

$$\nabla_\mu F^{\mu\nu} = 0 \,, \tag{2.5}$$

$$R_{\mu\nu} - \frac{R}{2} g_{\mu\nu} = 8\pi T_{\mu\nu} \,. \tag{2.6}$$

The first equation is just the usual of Maxwell equation in curved spacetime. The latter are the Einstein field equations, reflecting the backreaction of the electromagnetic waves into the geometry through the presence of the EM stress-energy tensor

$$T_{\mu\nu} = F_{\mu\alpha} F_\nu{}^\alpha - \frac{1}{4} g_{\mu\nu} F^2 \,. \tag{2.7}$$

These equations completely describe the system, but the problem is analytically untreatable, so we will resort to perturbation theory, considering the field A^μ to be small. This is a very good approximation, as the gravitational field near a stellar-mass BHs is considerably stronger then the radiation emitted by nearby astrophysical sources. As the stress-energy tensor is quadratic in the fields, $T_{\mu\nu} \sim \mathcal{O}(A^2)$, then we can ignore the backreaction and the field equations for the metric $g_{\mu\nu}$ reduce to Eq. (2.2).

2.2 Spacetime symmetries

It was generally accepted that a perfectly spherical symmetrical star would collapse to a Schwarzschild BH, although at the time the effect of a slightest amount of angular momentum on a gravitational collapse was not known. Finding a metric with intrinsic rotation could give insight into such a problem. Due to the lack of spherical symmetry, the problem became much harder, and took roughly 50 years after Schwarzschild's discovery to find a metric for a rotating body. Imposing symmetries to the final metric was essential to solve the field equations.

If we represent our spacetime and corresponding fields by $(\mathcal{M}, g_{\mu\nu}, \psi)$, then the pull-back f^* of the diffeomorphism $f : \mathcal{M} \to \mathcal{M}$ would give us the same physical system $(\mathcal{M}, f^* g_{\mu\nu}, f^* \psi)$. Since diffeomorphisms are just active coordinate transformations, such concept may raise some confusion, as we do not seem to obtain any new information to work with. Almost all physical theories are coordinate invariant, as is Newtonian mechanics and Special Relativity, but in such theories there is a preferable coordinate system

(inertial), while the same does not hold true for GR. An analogy can be made with the path integral formalism in QFT, where special consideration is taken when summing all field configurations in the case of gauge field theories in order to not overcount indistinguishable configurations. A similar ambiguity can occur in GR, where two apparently different solutions can be related by a diffeomorphism and are actually "the same", so we must be careful when deriving and analyzing any geometries.

Despite the added complexity of Einstein's field equations, it is still possible to find exact nontrivial solutions in a systematic way by considering spacetimes with symmetries with the use of Killing vector fields. A vector field $\boldsymbol{\xi}$ that obeys

$$\left(\mathcal{L}_{\xi}\, \boldsymbol{g}\right)_{\mu\nu} = 0 \tag{2.8}$$

is called a Killing field. Locally, this expression reduces to $\nabla_\mu \xi_\nu + \nabla_\nu \xi_\mu = 0$.

A *stationary* solution implies the existence of a Killing vector $\boldsymbol{k}$ that is asymptotically timelike, $\boldsymbol{k}^2 > 0$, therefore allowing us to normalize our vector such that $\boldsymbol{k}^2 \to 1$. Unlike the case of the static spacetime, a stationary metric does not show invariance under reversal of the time coordinate, which is natural considering a system with angular momentum. Futhermore, a solution is also *axisymmetric* if there is an asymptotically spacelike Killing field $\boldsymbol{m}$ whose integral curves are closed. A solution is stationary and axisymmetric if both symmetries are present, along with commuting fields, $[\boldsymbol{k}, \boldsymbol{m}] = 0$, *i.e.* rotations about the axis of symmetry commute with time translations [10]. The commutativity of the fields implies the existence of a set of coordinates, (t, r, θ, φ), such that

$$\boldsymbol{k} = \frac{\partial}{\partial t}\,, \qquad \boldsymbol{m} = \frac{\partial}{\partial \varphi}\,. \tag{2.9}$$

As a direct implication of this choice of chart, components of the metric stay independent of (t, φ), in virtue of Eq. (2.8),

$$\left(\mathcal{L}_{\boldsymbol{m}}\, \boldsymbol{g}\right)_{\mu\nu} = \frac{\partial g_{\mu\nu}}{\partial \varphi} = 0\,, \tag{2.10}$$

with the same holding true for $\boldsymbol{k}$, hence we can write $g_{\mu\nu} = g_{\mu\nu}(r, \theta)$.

One of the major applications of Killing vectors is to find conserved charges associated with the motion along a geodesic spanned by the field. These quantities are defined by taking the geodesics to regions of space that are asymptotical flat, where the geometry

does not affect the observer. In the case of the Kerr solution, we have two Killing vectors, $\boldsymbol{k}$ and $\boldsymbol{m}$, which are naturally associated with the total mass M and angular momentum J of the BH, respectively. This is usually done by evaluating the Komar integrals [11, 23], which can be written in a covariant way as

$$M = \frac{1}{8\pi}\int_{S^2_\infty} \star \mathrm{d}\boldsymbol{k}^\flat = -\frac{1}{4}\lim_{r\to\infty}\int_0^\pi \mathrm{d}\theta \sqrt{-g}\, g^{t\alpha} g^{r\beta} g_{t[\alpha,\beta]} \,, \tag{2.11}$$

$$J = -\frac{1}{16\pi}\int_{S^2_\infty} \star \mathrm{d}\boldsymbol{m}^\flat = \frac{1}{8}\lim_{r\to\infty}\int_0^\pi \mathrm{d}\theta \sqrt{-g}\, g^{t\alpha} g^{r\beta} g_{\varphi[\alpha,\beta]} \,, \tag{2.12}$$

where the usual notation $\boldsymbol{k}^\flat \equiv g_{\mu\nu}k^\mu \mathrm{d}x^\nu$ transforms a vector into a one-form and the operator $\star : \Omega^p(\mathcal{M}) \to \Omega^{4-p}(\mathcal{M})$ is the Hodge dual map for p-forms. In order to complete the integration in the last step are assumed (2.9) and (2.10), keeping (t, r) constant. According to the widely accepted *no-hair conjecture* [24], these two quantities completely define a stationary (neutral) BH.

2.3 Kerr-Schild coordinates

Naturally, Kerr was not the only one looking for such solution. Many presented other geometries to approximately describe a rotating star. Most of the solutions were one-parameter modifications to Schwarzschild that were not asymptotically flat. Simply using stationary and axisymmetric symmetries and then solving Einstein equations clearly did not suffice.

Kerr's success originated in of Petrov's classification of spacetimes, which used the algebraic properties of the Weyl tensor to distinguish the solutions in 3 types, with some subcases. He assumed that his solution would have the same classification as Schwarzschild's, associated with the geometry of isolated central objects, such as stars and BHs. From this assumption, using GR spinor techniques and only then imposing the Killing vectors in Eq. (2.9) was possible to find a new solution. Kerr's metric appear in his original paper [22] in the form

$$\begin{aligned} \boldsymbol{g} = &\left(1 - \frac{2Mr}{\rho^2}\right)(\mathrm{d}v - a\sin^2\theta \mathrm{d}\chi)^2 \\ &- 2(\mathrm{d}v - a\sin^2\theta\mathrm{d}\chi)(\mathrm{d}r - a\sin^2\theta\mathrm{d}\chi) \\ &- \rho^2(\mathrm{d}\theta^2 + \sin^2\theta \mathrm{d}\chi^2) \,, \end{aligned} \tag{2.13}$$

where a is a parameter, M is the BH mass and $\rho^2 = r^2 + a^2\cos^2\theta$. Naturally the time Killing vector is ∂_v and ∂_χ is the axial field, entailing that $J = aM$.

Taking the limit of $a \to 0$, we reduce the metric to the Schwarzschild solution in ingoing Eddington-Finkelstein (EF) coordinates, (v, r, θ, χ), which are useful to study ingoing (to the horizon) geodesics and remove the horizon coordinate singularity. When a given metric has singularities it is not trivial to identify if they are physical singularities or an artifact resultant of choice of chart, removable by a better choice of coordinates. That being said, this raises the difficulty of finding the essential singularities. The best way to look for these singularities is to compute curvature scalar quantities, and if they diverge in one particular chart, then they diverge in all charts. Since any BH is just a vacuum solution, then the Ricci scalar vanishes, $R = 0$, so we resort to the Kretschmann scalar,

$$R_{\alpha\beta\gamma\delta}R^{\alpha\beta\gamma\delta} = \frac{48M(r^2 - a^2\cos^2\theta)\left[(r^2 - a^2\cos^2\theta)^2 - 16r^2M^2a^2\cos^2\theta\right]}{(r^2 + a^2\cos^2\theta)^6}\,, \tag{2.14}$$

that clearly diverges for $\rho^2 = 0$. The Schwarzschild singularity, $r = 0$, is replaced with the Kerr singularity $(r, \theta) = (0, \pi/2)$. It is not clear what is the geometry of the Kerr singularity if we interpret r and θ as being part of the ordinary spherical coordinates. Although the metric is singular, we can draw some insight considering (r, θ) constant and then the limit of $r \to 0$ through the equatorial plane,

$$g|_{\text{singularity}} \sim \mathrm{d}v^2 - a^2\mathrm{d}\chi^2\,. \tag{2.15}$$

Hence the metric is reduced to the line element of the circle, S^1, confirming a *ring singularity* of radius a. This result implies that we may only reach the singularity, $\rho^2 = 0$, by approaching the Kerr BH through the equatorial plane.

The Kerr-Schild theory provides the "cartesian" form [25],

$$\begin{aligned} g = {} & \mathrm{d}\tilde{t}^2 - \mathrm{d}x^2 - \mathrm{d}y^2 - \mathrm{d}z^2 \\ & - \frac{2Mr^3}{r^4 + a^2z^2}\left[\mathrm{d}\tilde{t} + \frac{r(x\mathrm{d}x + y\mathrm{d}y) + a(y\mathrm{d}x - x\mathrm{d}y)}{r^2 + a^2} + \frac{z}{r}\mathrm{d}z\right]^2\,, \end{aligned} \tag{2.16}$$

which is particularly useful to understand the singularity geometry. In this metric, r is no longer a coordinate but a function of this chart coordinates $(\tilde{t}, x, y, z)$. We can relate the

The Kerr-Schild metric to the original Kerr solution, using

$$\tilde{t} = v - r\,, \qquad x + iy = (r - ia)e^{i\chi}\sin\theta\,, \qquad z = r\cos\theta\,, \tag{2.17}$$

which implies that $r(x, y, z)$ is implicitly given by

$$r^4 - (x^2 + y^2 + z^2 - a^2)r^2 - a^2z^2 = 0\,. \tag{2.18}$$

This condition deserves a more in-depth analysis. For increasing r, the surfaces obeying Eq. (2.18) approximates perfect spheres as the geometry gets more and more flat. Minkowsky flat space is immediately also guaranteed for $M = 0$. On the other hand, as we approach the singularity on $z = 0$ and $x^2 + y^2 = a^2$, rotation effects deform the surfaces into oblate spheroids ($\theta \neq \pi/2$ for the strict inequality). Such remarks are visually demonstrated in Figure 2.1.

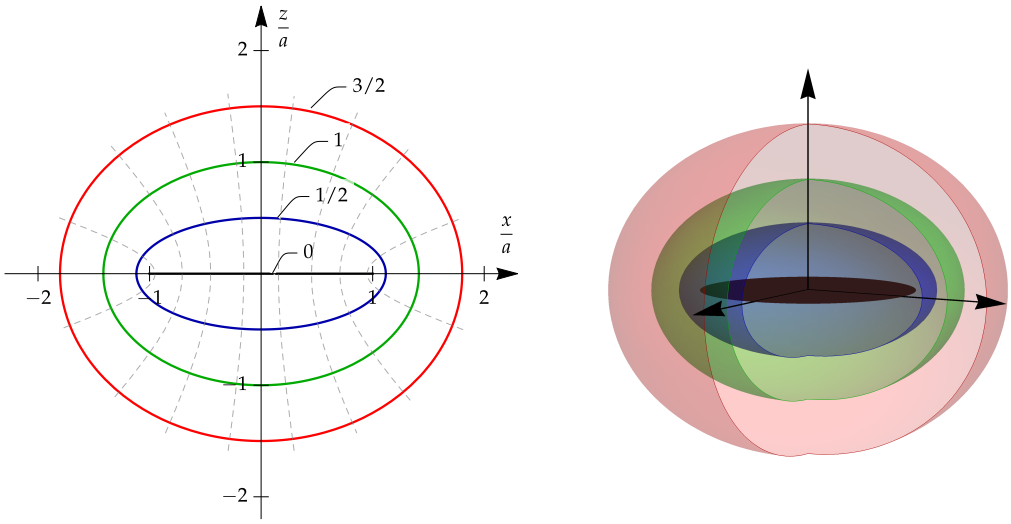

FIGURE 2.1: Contour plots of the surface $r(x, y, z)/a$ for constant values of 0, 1/2, 1, 3/2, in the Kerr-Schild coordinates. The left plot is the intersection of the $y = 0$ plane with the 3D representation (right) that spotlights the ring singularity. Dashed curves representing orthogonal constant $\theta(x, y, z)$ hypersufaces become asymptotically affine.

Even though the Kerr-Schild metric takes $r > 0$ values, there is no mathematical reason to restrict r strictly to positive values. Thus, hypersurfaces of constant r can also be represented by $-r$. This means that this chart can be analytically extended to regions where $r < 0$. It is possible to obtain a *maximally extended* solution by analytic continuation and a proper collage of charts [11]. This gives mathematical access to new spacetime regions, even tough most of them show unphysical properties.

2.4 Boyer-Lindquist coordinates

Considering the problem in hand, the most suitable coordinates for work with the Newman-Penrose (NP) formalism, are the Boyer-Lindquist (BL) coordinates [26],

$$\begin{aligned} g = &\left(1 - \frac{2Mr}{\rho^2}\right) \mathrm{d}t^2 - 2a\sin^2\theta \frac{(r^2 + a^2 - \Delta)}{\rho^2} \mathrm{d}t\mathrm{d}\varphi \\ &- \frac{(r^2 + a^2)^2 - \Delta a^2 \sin^2\theta}{\rho^2} \sin^2\theta \mathrm{d}\varphi^2 - \frac{\rho^2}{\Delta}\mathrm{d}r^2 - \rho^2 \mathrm{d}\theta^2 \,, \end{aligned} \tag{2.19}$$

where we define $\Delta = r^2 - 2Mr + a^2$. In order to show that these correspond to the same solution, the change of coordinates

$$\mathrm{d}v = \mathrm{d}(t + r_*) \,, \qquad \mathrm{d}\chi = \mathrm{d}\varphi + \frac{a}{\Delta}\,\mathrm{d}r \,, \tag{2.20}$$

takes us back to the original Kerr form (2.13). The coordinate v is given by the known ingoing EF transformation, defined by the Regge-Wheeler coordinate, also named *tortoise* coordinate, which is very useful to construct null directions. In the case of the Kerr BL metric, it holds that

$$\frac{\mathrm{d}r_*}{\mathrm{d}r} = \frac{r^2 + a^2}{\Delta} \,. \tag{2.21}$$

These coordinates are usually referred as "Schwarzschild like", as they lead to the spherical static case in standard curvature coordinates when setting $a = 0$. Time inversion symmetry is characteristic of the static Schwarzschild spacetime, but the same does not hold for Kerr's. Nevertheless, this specific form is invariant under the inversion $(t, \varphi) \to (-t, -\varphi)$, also known as the *circular condition*, an intuitive notion from physical systems with angular momentum [10, 23]. This discrete symmetry eliminates most of the off-diagonal components of the BL metric, $g_{tr} = g_{\varphi r} = g_{t\theta} = g_{\varphi\theta} = 0$, making it the simplest to perform calculations.

To study the possible horizons of the Kerr BH, we will consider $\boldsymbol{n} = (\mathrm{d}r)^\sharp \equiv (g^{\mu\nu}\nabla_\nu r)\partial_\mu$ which defines a normal vector to constant radial hypersurfaces. It is easy to show that $\boldsymbol{n}^2 = g^{rr}$, which implies that $\boldsymbol{n}$ is null when $\Delta = 0$, defining null hypersurfaces at

$$r_\pm = M \pm \sqrt{M^2 - a^2} \,, \tag{2.22}$$

singularities of g_{rr} which we know to be removable. As a consequence, for a static observer a massless particle on an ingoing null geodesic would spiral around the BH for a infinite time, as the coordinate $t \to \infty$, never reaching $r = r_+$. This surface is the event horizon of the Kerr BH, as it separates two causally disconnected regions of spacetime, *i.e* any information from inside this surface will never reach any asymptotic observer. The expression for the event horizon surface also raises limitations for the amount of angular momentum a physical BH can have. We must have

$$|a| < M \,, \tag{2.23}$$

otherwise Δ would lack any real roots and would lead to an essential *naked singularity*, reachable in a finite time, which is forbidden by the *Weak Cosmic Censorship* conjecture [11].

The surface at $r = r_-$, on the other hand, is called a Cauchy horizon. In GR, a spacelike surface containing all initial conditions of spacetime (Cauchy surface) would suffice to predict all past and future events, but a Cauchy horizon separates the domain of validity of such initial conditions. Despite no information ever escaping the event horizon, it is still possible to predict events inside $r_- < r < r_+$, but such thing it is not guaranteed after crossing the Cauchy horizon. Due to this and some other unphysical features (for example, closed timelike curves and instabilities under perturbations), we need only to focus on the region outside the event horizon $r > r_+$, since only information on that region is physically reachable from an asymptotic observer's point of view.

Event tough most of the Kerr BH basic properties were demonstrated, there is still no result so far showing some kind of rotation. First, consider the quantity $\boldsymbol{\xi} \cdot \boldsymbol{u} \equiv \xi_\alpha u^\alpha$, where $\boldsymbol{u}$ is the four-velocity of a point-particle and $\boldsymbol{\xi}$ is any Killing field. Taking into account the geodesic equation, $u^\beta \nabla_\beta u^\alpha = 0$, it is easy to show that this quantity is conserved along geodesics,

$$u^\beta \nabla_\beta (\xi_\alpha u^\alpha) = u^\alpha u^\beta \nabla_\beta \xi_\alpha = \frac{u^\alpha u^\beta}{2} \left(\nabla_\alpha \xi_\beta + \nabla_\beta \xi_\alpha \right) = 0 \,, \tag{2.24}$$

due to Killing Eq. (2.8). As a result, geodesics of a free particle in Kerr geometry will be characterized by two constants

$$E = k^\beta g_{\alpha\beta} \frac{\mathrm{d}x^\alpha}{\mathrm{d}\tau} \,, \qquad -L = m^\beta g_{\alpha\beta} \frac{\mathrm{d}x^\alpha}{\mathrm{d}\tau} \,, \tag{2.25}$$

where τ is the affine parameter associated with the geodesic. These quantities can be interpreted as the energy and angular momentum (per mass) of the particle, respectively. Due to the circular form of the BL metric, the metric components of the coordinates (t, φ) define a product decomposition, providing the separation of the previous equations,

$$\begin{aligned} \dot{t} \equiv \frac{\mathrm{d}t}{\mathrm{d}\tau} &= \frac{1}{\Delta}\left[(r^2 + a^2 + \frac{2Ma^2}{r})E - \frac{2Ma}{r}L\right] , \\ \dot{\varphi} \equiv \frac{\mathrm{d}\varphi}{\mathrm{d}\tau} &= \frac{1}{\Delta}\left[\frac{2Ma}{r}E + \left(1 - \frac{2M}{r}\right)L\right] , \end{aligned} \tag{2.26}$$

specified for the equatorial plane $\theta = \pi/2$. The final equation for the geodesic is provided by the line element (2.19), which becomes also a first order ODE, after the substitution of $\dot{t}$ and $\dot{\varphi}$.

Consider now a zero angular momentum observer (ZAMO) infalling radially, with $L = 0$, then we can get the angular velocity Ω, as measured at infinity

$$\Omega = \frac{\dot{\varphi}}{\dot{t}} = -\frac{g_{t\varphi}}{g_{\varphi\varphi}} = \frac{2aM}{r^3 + a^2(2M + r)} . \tag{2.27}$$

Asymptotically we obtain $\Omega \to 0$, but for a finite distance, observers are forced to co-rotate with the BH. Particularly, at the event horizon, $r = r_+$, one finds that

$$\Omega_H = \frac{a}{2Mr_+} = \frac{J}{2M\left(M^2 + \sqrt{M^4 - J^2}\right)} . \tag{2.28}$$

A special linear combination of Killing vector fields,

$$\boldsymbol{\xi} = \boldsymbol{k} + \Omega_H \boldsymbol{m} , \tag{2.29}$$

is also a Killing vector field, but this one is particularly important because it is also a null vector normal to the event horizon, defining it as a Killing horizon of $\boldsymbol{\xi}$. Due to the BL chart singularity, the normal vector to radial surfaces, $\boldsymbol{n}$, is the zero vector at $r = r_+$, but using ingoing EF coordinates we obtain

$$\boldsymbol{n}_{|r=r_+} = (g^{rv}\partial_v + g^{rr}\partial_r + g^{r\chi}\partial_\chi)_{|r=r_+} = -\frac{2Mr_+}{(\rho^2)_{|r=r_+}}\left(\partial_v + \frac{a}{2Mr_+}\partial_\chi\right) \propto \boldsymbol{\xi} . \tag{2.30}$$

Since null geodesics on the outer horizon follow curves generated by the Killing vector ξ, the integral curves of this vector obey $\xi^\alpha \partial_\alpha(\varphi - \Omega_H t) = 0$, resulting in $\varphi = \Omega_H t + const.$

Therefore, we say that the BH is "rotating" with angular velocity Ω_H.

2.5 Ergoregion and the Penrose process

One of the main characteristic that distinguishes Kerr BHs from other spherical solutions is the existence of an *ergoregion*. In this region the Killing vector $\boldsymbol{k}$ becomes spacelike, $\boldsymbol{k}^2 = g_{tt} < 0$, which is bounded by the hypersurface

$$r_{\text{ergo}}(\theta) = M + \sqrt{M^2 - a^2\cos^2\theta}\,. \tag{2.31}$$

This region lies outside the event horizon if $a \neq 0$, then being defined as $r_+ < r < r_{\text{ergo}}(\theta)$. Notice that a static observer moves in a timelike curve with (r, θ, φ) constant, *i.e.* with tangent vector proportional to $\boldsymbol{k}$, therefore such observer cannot exist inside the ergoregion because the time Killing vector becomes spacelike, otherwise it would violate causality. We can see that $\boldsymbol{u}^2 = g_{\alpha\beta}u^\alpha u^\beta = g_{tt}(u^t)^2 + 2g_{t\varphi}u^t u^\varphi + g_{\varphi\varphi}(u^\varphi)^2 > 0$ only occurs when $g_{t\varphi}u^\varphi > 0$, as all other terms are positive. Inside the ergoregion, $g_{t\varphi} > 0$, therefore all observers are forced to rotate in the same direction as the BH [15].

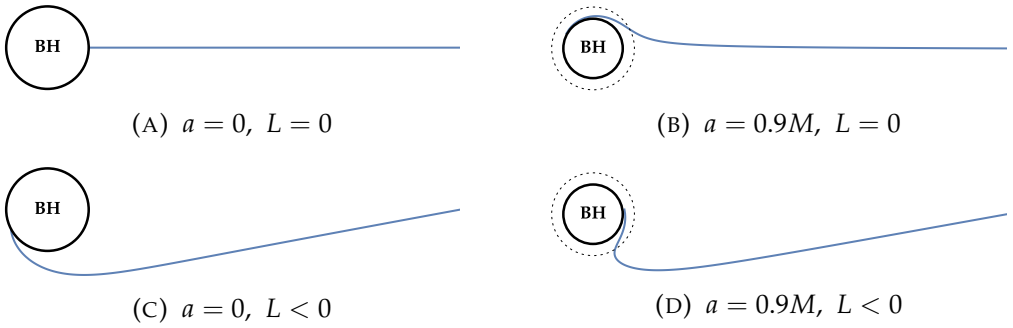

FIGURE 2.2: Illustration of the Schwarzschild (A,C) and Kerr (B,D) null equatorial infalling geodesics given by Eqs. (2.26), for $r(0) = 20M$, with emphasis on $L \neq 0$. Even starting with opposite angular momentum, the Kerr geodesic (D) is forced to co-rotate with the BH once crossed the ergoregion (dotted).

Despite BHs being always thought as "perfect absorbers" due to the existence of a casual boundary, the ergoregion allows energy extraction from the BH, through the Penrose process, an intrinsic feature of rotating BHs. Much like spontaneous pair creation and amplification at discontinuities are related but distinct effects, the Penrose process allows for a better understating of the phenomena of superradiance in GR.

Considering a particle with rest mass μ and four-momentum $p^\alpha = \mu u^\alpha$, we may identify the constant of motion

$$E = \boldsymbol{k} \cdot \boldsymbol{p} = \mu(g_{tt}u^t + g_{t\varphi}u^\varphi) \, . \tag{2.32}$$

as it's energy measured by a stationary observer at infinity, due to relations (2.25). As shown above, the Killing vector is asymptotically timelike but is spacelike inside the ergoregion, thus $g_{tt} < 0$. For a future-directed geodesic, $p^t = \mu u^t > 0$, the energy beyond the ergosurface needs not to be positive. Suppose, that by some means such particle manages to decay inside the ergoregion into two other particles, with momenta $\boldsymbol{p_1}$ and $\boldsymbol{p_2}$. Contracting with $\boldsymbol{k}$, implies that $E = E_1 + E_2$. Supposing that the first of the particles has negative energy, $E_1 < 0$, then

$$E_2 = E + |E_1| > E \, . \tag{2.33}$$

It can be shown that the particle with negative energy (bounded) must fall into the BH while the other may escape the ergoregion, with greater energy than the particle sent in. Energy is conserved by making the BH absorb the particle with negative energy, therefore resulting in a net energy extraction [11].

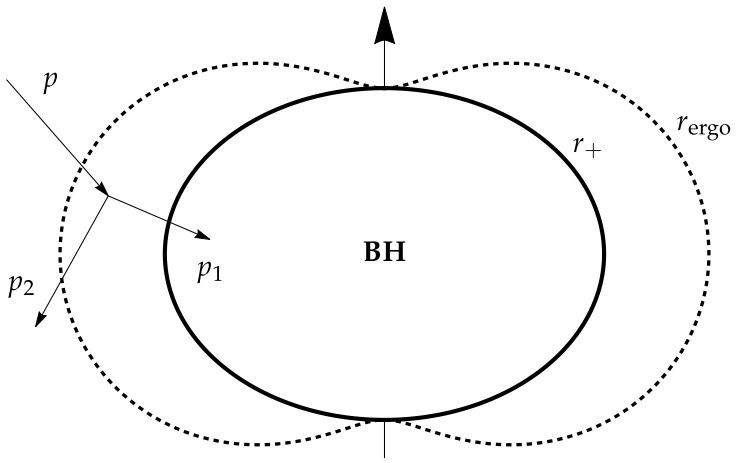

FIGURE 2.3: Illustration of the Penrose process, with ergoregion (dotted) and event horizon surfaces parameterized in Kerr-Schild cartesian coordinates.

To understand the limits of the Penrose process, we use the fact that a stationary observer near the horizon must follow orbits of ξ, given by Eq. (2.29). Although a particle may have negative energy as measured by an asymptotic observer, a stationary observer

following geodesics at horizon must locally measure positive energies when the particle crosses the horizon, which implies that $\boldsymbol{\xi} \cdot \boldsymbol{p_1} \geq 0$. The BH will have a variation of mass $\delta M = E_1$ and angular momentum $\delta J = L_1$, where $L_1 = -\boldsymbol{m} \cdot \boldsymbol{p_1}$ is the particle's angular momentum. As a result,

$$\delta J \leq \frac{2M\left(M^2 + \sqrt{M^4 - J^2}\right)}{J} \delta M \,, \tag{2.34}$$

which is equivalent to $\delta\left(M^2 + \sqrt{M^4 - J^2}\right) \geq 0$. This quantity is usually refereed as the "area" of the event horizon, $4\pi(r_+^2 + a^2) = 8\pi\left(M^2 + \sqrt{M^4 - J^2}\right)$. Energy extraction from the Penrose process is limited by the requirement that the horizon area must always increase, which is a special case of the second law of BH mechanics [27].

We can tie the superradiance process with this particle counterpart using a simple and general argument. Asymptotically, we may think of waves as a collective of quantum (photons, gravitons, ...), each carrying $\hbar\omega$ of energy and $\hbar m$ of angular momentum [28], where m labels a mode with definite angular momentum. Therefore, when a given quanta is absorbed, the variation of the BH mass and angular momentum is given by

$$\delta J = \frac{m}{\omega} \delta M \,. \tag{2.35}$$

The condition for superradiance (1.1) appears explicitly in the second law of BH mechanics (2.34), which guarantees that $\delta M(1 - \Omega_H m/\omega) > 0$, *i.e.* confirming energy extraction from the BH when superradiance occurs, while the lack of superradiance increases the mass of the BH.

Chapter 3

Teukolsky's master equation

3.1 Newman-Penrose formalism

The study of gravitational and electromagnetic perturbations in a BH background was performed long before Kerr found his solution, for other spacetimes such as Schwarzschild's. Despite its simplicity, the procedure involved was already algebraically tedious. In the Kerr case, the metric was far more complicated, making the problem almost untreatable.

Fortunately, the NP formalism [14] provides an alternative method of studying perturbations. This formalism results from a natural introduction of spinor techniques in GR, after the choice of a null complex tetrad basis,

$$\boldsymbol{e}_a = (e_a)^\mu \frac{\partial}{\partial x^\mu} \qquad (a = 1,2,3,4)\,, \tag{3.1}$$

where all quantities will be projected, *i.e.* for the Weyl tensor we define

$$C_{abcd} = (e_a)^\alpha\,(e_b)^\beta\,(e_c)^\gamma\,(e_d)^\delta\,C_{\alpha\beta\gamma\delta}\,. \tag{3.2}$$

Penrose believed that the light-cone was the essential element of the spacetime, thus it was of importance to find null directions. The basis consisted in two real vectors, $\mathbf{l}$ and $\mathbf{n}$, and two complex conjugate vectors $\mathbf{m}$ and $\bar{\mathbf{m}}$. Besides satisfying

$$\mathbf{l}^2 = \mathbf{n}^2 = \mathbf{m}^2 = \bar{\mathbf{m}}^2 = 0\,, \tag{3.3}$$

orthogonality conditions of NP formalism require

$$\mathfrak{l}\cdot\mathfrak{m}=\mathfrak{l}\cdot\bar{\mathfrak{m}}=\mathfrak{n}\cdot\mathfrak{m}=\mathfrak{n}\cdot\bar{\mathfrak{m}}=0\,. \tag{3.4}$$

Still we are left with the ambiguity raised by multiplication of scalar functions to each vector, therefore it is customary to impose normalization conditions to the basis,

$$\mathfrak{l}\cdot\mathfrak{n}=1\,,\qquad \mathfrak{m}\cdot\bar{\mathfrak{m}}=-1\,. \tag{3.5}$$

This formalism is a special case of tetrad calculus, where we can identify the new basis as $(\mathfrak{l},\mathfrak{n},\mathfrak{m},\bar{\mathfrak{m}})$. The "metric" for manipulating tetrad indices, η_{ab}, is defined by all restrictions provided above,

$$g^{\mu\nu}=\eta^{ab}(e_a)^\mu(e_b)^\nu=\mathfrak{l}^\mu\mathfrak{n}^\nu+\mathfrak{n}^\mu\mathfrak{l}^\nu-\mathfrak{m}^\mu\bar{\mathfrak{m}}^\nu-\bar{\mathfrak{m}}^\mu\mathfrak{m}^\nu\,. \tag{3.6}$$

Additionally these vectors define new directional derivatives. We will depart shortly from standard notation, by redefining these derivatives as

$$\mathbb{D}=\nabla_{\mathfrak{l}}\,,\qquad \mathbb{\Delta}=\nabla_{\mathfrak{n}}\,,\qquad \mathbb{\delta}=\nabla_{\mathfrak{m}}\,,\qquad \bar{\mathbb{\delta}}=\nabla_{\bar{\mathfrak{m}}}\,. \tag{3.7}$$

More details and definitions on the tetrad formalism can be found in Appendix A.

3.1.1 Kinnersley tetrad

The Riemann tensor may have up to twenty non-vanishing components. We know that ten of these are present in the symmetric Ricci tensor, that is intrinsically connected to matter and energy. The other components are pure gravitational degrees of freedom and are encoded in the Weyl tensor. It becomes the most useful object when the Ricci tensor vanishes, such as for vacuum solutions and source-free gravitational waves. In order to remove the Ricci tensor degrees of freedom, the tensor must be constructed as trace-free,

$$\eta^{ad}C_{abcd}=C_{1bc2}+C_{1bc2}-C_{3bc4}-C_{4bc3}=0\,. \tag{3.8}$$

Together with the other symmetries inherited from the Riemann tensor, for instance the first Bianchi identity, $C_{a[bcd]}=0$, it is possible to show that some of these NP components vanish while others remain related, leaving us with ten degrees of freedom. As a result,

in the NP formalism the Weyl tensor can be represented by five complex scalars, usually chosen as

$$\begin{aligned}
\psi_0 &= -C_{1313} = -C_{\alpha\beta\gamma\delta}\, \mathfrak{l}^\alpha \mathfrak{m}^\beta \mathfrak{l}^\gamma \mathfrak{m}^\delta \,, \qquad \psi_1 = -C_{1213} = -C_{\alpha\beta\gamma\delta}\, \mathfrak{l}^\alpha \mathfrak{n}^\beta \mathfrak{l}^\gamma \mathfrak{m}^\delta \,, \\
\psi_2 &= -C_{1342} = -C_{\alpha\beta\gamma\delta}\, \mathfrak{l}^\alpha \mathfrak{m}^\beta \bar{\mathfrak{m}}^\gamma \mathfrak{n}^\delta \,, \qquad \psi_3 = -C_{1242} = -C_{\alpha\beta\gamma\delta}\, \mathfrak{l}^\alpha \mathfrak{n}^\beta \bar{\mathfrak{m}}^\gamma \mathfrak{n}^\delta \,, \\
\psi_4 &= -C_{2424} = -C_{\alpha\beta\gamma\delta}\, \mathfrak{n}^\alpha \bar{\mathfrak{m}}^\beta \mathfrak{n}^\gamma \bar{\mathfrak{m}}^\delta \,.
\end{aligned} \tag{3.9}$$

The complex conjugates can be obtained by doing the replacement $3 \rightleftarrows 4$, by exchanging $\mathfrak{m}$ with $\bar{\mathfrak{m}}$ and vice-versa. The Weyl tensor has a unique decomposition in terms of a linear combination of NP scalars and tensorial product of two-forms. This decomposition has the general form,

$$\begin{aligned}
\frac{1}{4} C_{\mu\nu\rho\sigma} = &- \psi_0\, V_{\mu\nu} V_{\rho\sigma} - \psi_1 \left(V_{\mu\nu} W_{\rho\sigma} + W_{\mu\nu} V_{\rho\sigma}\right) \\
&- \psi_2 \left(U_{\mu\nu} V_{\rho\sigma} + V_{\mu\nu} U_{\rho\sigma} + W_{\mu\nu} W_{\rho\sigma}\right) \\
&- \psi_3 \left(U_{\mu\nu} W_{\rho\sigma} + W_{\mu\nu} U_{\rho\sigma}\right) - \psi_4\, U_{\mu\nu} U_{\rho\sigma} + \text{ c.c.}
\end{aligned} \tag{3.10}$$

where $U_{\mu\nu} = \mathfrak{l}_{[\mu}\mathfrak{m}_{\nu]}$, $V_{\mu\nu} = \bar{\mathfrak{m}}_{[\mu}\mathfrak{n}_{\nu]}$, $W_{\mu\nu} = \mathfrak{l}_{[\mu}\mathfrak{n}_{\nu]} - \mathfrak{m}_{[\mu}\bar{\mathfrak{m}}_{\nu]}$. It is clear that the values that these five complex scalars take is completely dependent on the choice of tetrad frame.

BH solutions are "type D" spacetimes according to Petrov's classification, which was a major restriction necessary to the discovery of Kerr's metric. For these spacetimes it is possible to find two different doubly-degenerate principal directions of the Weyl tensor, which we choose to be the real vectors of the tetrad, $\mathfrak{l}$ and $\mathfrak{n}$ [29]. These yield

$$C_{\mu\alpha\beta[\nu}\mathfrak{l}_{\rho]}\mathfrak{l}^\alpha\mathfrak{l}^\beta = 0 \,, \qquad C_{\mu\alpha\beta[\nu}\mathfrak{n}_{\rho]}\mathfrak{n}^\alpha\mathfrak{n}^\beta = 0 \,. \tag{3.11}$$

In NP formalism terms, this implies, respectively,

$$\psi_0 = \psi_1 = 0 \,, \qquad \psi_3 = \psi_4 = 0 \,. \tag{3.12}$$

Finding the principal directions may not be trivial, but we can apply successive local transformations of the six-parameter Lorentz group in order to rotate the tetrad vectors. This procedure allows for the simplification of the Weyl tensor by vanishing NP scalars, "locking" the orientation of the tetrad frame. The Weyl scalar ψ_2 becomes invariant under boosts in the principal directions, usually refereed as "type III" rotations [29]. These keep the light-cone structure intact by maintaining the direction of $\mathfrak{l}$ and $\mathfrak{n}$ unchanged (up to

multiplication of scalar functions), being useful to change between ingoing and outgoing frames [30]. Kinnersly solved the type D vacuum field equations [31], finding a suitable tetrad

$$\begin{aligned}\boldsymbol{\mathfrak{l}} &= \left(\frac{r^2+a^2}{\Delta},\, 1,\, 0,\, \frac{a}{\Delta}\right)\,,\\ \boldsymbol{\mathfrak{n}} &= \frac{1}{2\rho^2}\left(r^2+a^2,\, -\Delta,\, 0,\, a\right)\,,\\ \boldsymbol{\mathfrak{m}} &= \frac{1}{\sqrt{2}\bar{\rho}^2}\left(ia\sin\theta,\, 0,\, 1,\, i\csc\theta\right)\,,\end{aligned} \tag{3.13}$$

where $\bar{\rho} = r + ia\cos\theta$ and $\rho^2 \equiv |\bar{\rho}|^2 = \bar{\rho}\bar{\rho}^*$.

The NP formalism provides a full set of first-order coupled differential equations, relating the NP scalars components of the Weyl and Maxwell tensors. These equations result from the second Bianchi identity, $C_{\mu\nu[\rho\sigma;\lambda]} = 0$, and the Maxwell equations. In order to write these equations explicitly we need to define the *spin coefficients* using the connection $\gamma_{abc} = (e_a)^\mu (e_b)_{\mu;\nu} (e_c)^\nu$, which replaces the Christopher symbols in this formalism.

To study GWs, instead of perturbing the background metric, the NP formalism provides a natural way of performing perturbations by modification of the tetrad, $\boldsymbol{\mathfrak{l}} = \boldsymbol{\mathfrak{l}}^B + \boldsymbol{\mathfrak{l}}^P$, $\boldsymbol{\mathfrak{n}} = \boldsymbol{\mathfrak{n}}^B + \boldsymbol{\mathfrak{n}}^P$, etc., and also the NP scalars, $\psi_a = \psi_a{}^B + \psi_a{}^P$, maintaining only first-order terms [13]. The formalism reveals decoupled equations for $\psi_0{}^P$ and $\psi_4{}^P$, which implies that these dynamic variables are the only independent degrees of freedom of the GWs.

3.1.2 Maxwell equations

We focus with more detail on EM perturbations with a fixed background because they involve a simpler procedure and then we will tie with the same master equation that also describes GW perturbations.

In the NP formalism, all Maxwell equations, $F_{[\mu\nu;\rho]} = 0$ and Eq. (2.5), reduce to

$$F_{[ab|c]} = 0\,, \qquad \eta^{bc} F_{ab|c} = 0 \tag{3.14}$$

(see Appendix A). The Maxwell tensor $F_{\mu\nu}$ has a total of six components which encodes the vector quantities of the electric and the magnetic fields. We may reduce the equation

using three complex NP scalars,

$$\begin{aligned}\phi_0 &= F_{13} = F_{\alpha\beta}\,\mathfrak{l}^\alpha \mathfrak{m}^\beta\,,\\ \phi_1 &= \tfrac{1}{2}(F_{12}+F_{43}) = \tfrac{1}{2}F_{\alpha\beta}\,(\mathfrak{l}^\alpha \mathfrak{n}^\beta + \bar{\mathfrak{m}}^\alpha \mathfrak{m}^\beta)\,,\\ \phi_2 &= F_{42} = F_{\alpha\beta}\,\bar{\mathfrak{m}}^\alpha \mathfrak{n}^\beta\,.\end{aligned} \tag{3.15}$$

Considering all possible combinations of NP indices in (3.14), we gather eight equations, double the amount of necessary relations. This occurs because the conjugates ϕ_0^*, ϕ_1^*, ϕ_2^* are coupled in these equations. Eliminating every term of the form $F_{23|a}$ or $F_{14|b}$,

$$\phi_{2|1} = \phi_{1|4}\,, \tag{3.16a}$$

$$\phi_{1|2} = \phi_{2|3}\,, \tag{3.16b}$$

$$\phi_{1|1} = \phi_{0|4}\,, \tag{3.16c}$$

$$\phi_{0|2} = \phi_{1|3}\,. \tag{3.16d}$$

We may expand explicitly the left-hand side of Eq. (3.16a),

$$\begin{aligned}\phi_{2|1} &= \phi_{2,1} - \eta^{ab}(\gamma_{a41}F_{b2} + \gamma_{a21}F_{4b})\\ &= \phi_{2,1} - (\gamma_{241}F_{12} + \gamma_{121}F_{42}) + (\gamma_{341}F_{42} + \gamma_{421}F_{43})\\ &= \phi_{2,1} + 2F_{42}\left(\frac{\gamma_{341}+\gamma_{211}}{2}\right) + 2\gamma_{421}\left(\frac{F_{12}+F_{43}}{2}\right)\\ &= \mathbb{D}\phi_2 + 2\varepsilon\phi_2 - 2\pi\phi_1\,,\end{aligned} \tag{3.17}$$

where we used the antisymmetry of the spin connection, $\gamma_{abc} = -\gamma_{bac}$. The right-hand side yields

$$\begin{aligned}\phi_{1|4} &= \phi_{1,4} - \tfrac{1}{2}\eta^{ab}(\gamma_{a14}F_{b2} + \gamma_{a24}F_{1b} + \gamma_{a44}F_{b3} + \gamma_{a34}F_{4b})\\ &= \phi_{1,4} - \tfrac{1}{2}(\gamma_{144}F_{23} + \gamma_{134}F_{42} + \gamma_{214}F_{12} + \gamma_{234}F_{41})\\ &\qquad + \tfrac{1}{2}(\gamma_{314}F_{42} + \gamma_{414}F_{42} + \gamma_{324}F_{14} + \gamma_{424}F_{13})\\ &= \phi_{2,1} - \gamma_{244}F_{13} + \gamma_{314}F_{42}\\ &= \bar{\delta}\phi_1 - \lambda\phi_0 + \tau\phi_2\,.\end{aligned} \tag{3.18}$$

The spin coefficients $\varepsilon, \pi, \lambda, \tau$, along with other NP definitions are found in Appendix B.1. If we repeat the same expansion for the other Maxwell equations, we gather the set

$$\mathbb{D}\phi_2 - \bar{\mathbb{\delta}}\phi_1 = -\lambda\phi_0 + 2\pi\phi_1 + (\varrho - 2\varepsilon)\phi_2 \,, \tag{3.19a}$$

$$\mathbb{\Delta}\phi_1 - \mathbb{\delta}\phi_2 = \nu\phi_0 - 2\mu\phi_1 + (2\beta - \tau)\phi_2 \,, \tag{3.19b}$$

$$\mathbb{D}\phi_1 - \bar{\mathbb{\delta}}\phi_0 = (\pi - 2\alpha)\phi_0 + 2\varrho\phi_1 - \kappa\phi_2 \,, \tag{3.19c}$$

$$\mathbb{\Delta}\phi_0 - \mathbb{\delta}\phi_1 = (2\gamma - \mu)\phi_0 - 2\tau\phi_1 + \sigma\phi_2 \,. \tag{3.19d}$$

The Kinnersley tetrad guarantees that $\kappa = \sigma = \lambda = \nu = 0$, decoupling all equations above. After substitution of all spin coefficients,

$$\left(\mathbb{D} + \frac{1}{\bar{\rho}^*}\right)\phi_2 = \left(\bar{\mathbb{\delta}} + \frac{2ia\sin\theta}{\sqrt{2}(\bar{\rho}^*)^2}\right)\phi_2 \,, \tag{3.20a}$$

$$\left(\mathbb{\Delta} - \frac{\Delta}{\rho^2\bar{\rho}^*}\right)\phi_1 = \left[\mathbb{\delta} + \frac{1}{\sqrt{2}\bar{\rho}}\left(\cot\theta - \frac{ia\sin\theta}{\bar{\rho}^*}\right)\right]\phi_2 \,, \tag{3.20b}$$

$$\left(\mathbb{D} + \frac{2}{\bar{\rho}^*}\right)\phi_1 = \left[\bar{\mathbb{\delta}} + \frac{1}{\sqrt{2}\bar{\rho}^*}\left(\cot\theta - \frac{ia\sin\theta}{\bar{\rho}^*}\right)\right]\phi_0 \,, \tag{3.20c}$$

$$\left[\mathbb{\Delta} + \frac{\Delta}{2\rho^2}\left(\frac{1}{\bar{\rho}^*} - \frac{2(r-M)}{\Delta}\right)\right]\phi_0 = \left(\mathbb{\delta} + \frac{2ia\sin\theta}{\sqrt{2}\bar{\rho}\bar{\rho}^*}\right)\phi_1 \,. \tag{3.20d}$$

An important consequence of the symmetries of the Kerr spacetime allows for a wave decomposition of the form $\phi_0, \phi_1, \phi_2 \sim e^{-i\omega t + im\varphi}$. Therefore, the four differential operators group into radial $(\mathbb{D}, \mathbb{\Delta})$ and angular $(\mathbb{\delta}, \bar{\mathbb{\delta}})$. The procedure for separation of the Maxwell equations can be further simplified by introducing new operators

$$\begin{aligned} \mathcal{D}_n &= \partial_r - \frac{iK}{\Delta} + 2n\frac{r-M}{\Delta} \,, & \mathcal{D}_n^\dagger &= \partial_r + \frac{iK}{\Delta} + 2n\frac{r-M}{\Delta} \,, \\ \mathcal{L}_n &= \partial_\theta - Q + n\cot\theta \,, & \mathcal{L}_n^\dagger &= \partial_\theta + Q + n\cot\theta \,, \end{aligned} \tag{3.21}$$

where we define the functions $K = (r^2 + a^2)\omega - ma$, $Q = a\omega\sin\theta - m\csc\theta$. In this definition, n is any integer. These operators are related to the tetrad by

$$\mathbb{D} = \mathcal{D}_0 \,, \qquad \mathbb{\Delta} = -\frac{\Delta}{2\rho^2}\mathcal{D}_0^\dagger \,, \qquad \mathbb{\delta} = \frac{1}{\sqrt{2}\bar{\rho}}\mathcal{L}_0^\dagger \,, \qquad \bar{\mathbb{\delta}} = \frac{1}{\sqrt{2}\bar{\rho}^*}\mathcal{L}_0 \,, \tag{3.22}$$

as a result of the substitutions $\partial_t \to -i\omega$, $\partial_\varphi \to im$. We may use the fact that $\mathcal{D}_n$ and $\mathcal{L}_n$ act mostly as radial and angular derivatives, respectively, to deduce the properties

$$\mathcal{D}_n \Delta = \Delta \mathcal{D}_{n+1} \,, \tag{3.23a}$$

$$\mathcal{L}_n \sin\theta = \sin\theta \, \mathcal{L}_{n+1} \,, \tag{3.23b}$$

$$\left(\mathcal{D}_n + \frac{q}{\bar{\rho}^*}\right) \frac{1}{(\bar{\rho}^*)^p} = \frac{1}{(\bar{\rho}^*)^p} \left(\mathcal{D}_n + \frac{q-p}{\bar{\rho}^*}\right) \,, \tag{3.23c}$$

$$\left(\mathcal{L}_n + \frac{iqa\sin\theta}{\bar{\rho}^*}\right) \frac{1}{(\bar{\rho}^*)^p} = \frac{1}{(\bar{\rho}^*)^p} \left(\mathcal{L}_n + \frac{i(q-p)a\sin\theta}{\bar{\rho}^*}\right) \,, \tag{3.23d}$$

$$\left(\mathcal{D}_n + \frac{q}{\bar{\rho}^*}\right) \left(\mathcal{L}_n + \frac{iqa\sin\theta}{\bar{\rho}^*}\right) = \left(\mathcal{L}_n + \frac{iqa\sin\theta}{\bar{\rho}^*}\right) \left(\mathcal{D}_n + \frac{q}{\bar{\rho}^*}\right) \,, \tag{3.23e}$$

for any integers p, q, n, holding also for $\mathcal{D}_n^\dagger$ and $\mathcal{L}_n^\dagger$.

In order to achieve the separable form, we still need to perform a replacement of the Maxwell NP scalars by new dynamical variables

$$\Phi_0 = \phi_0 \,, \qquad \Phi_1 = \sqrt{2}\bar{\rho}^* \phi_1 \,, \qquad \Phi_2 = 2(\bar{\rho}^*)^2 \phi_2 \,, \tag{3.24}$$

and using properties (3.23c) and (3.23d), we go from Eqs. (3.20) to

$$\left(\mathcal{D}_0 - \frac{1}{\bar{\rho}^*}\right) \Phi_2 = \left(\mathcal{L}_0 + \frac{ia\sin\theta}{\bar{\rho}^*}\right) \Phi_1 \,, \tag{3.25a}$$

$$\Delta \left(\mathcal{D}_0^\dagger + \frac{1}{\bar{\rho}^*}\right) \Phi_1 = -\left(\mathcal{L}_1^\dagger - \frac{ia\sin\theta}{\bar{\rho}^*}\right) \Phi_2 \,, \tag{3.25b}$$

$$\left(\mathcal{D}_0 + \frac{1}{\bar{\rho}^*}\right) \Phi_1 = \left(\mathcal{L}_1 - \frac{ia\sin\theta}{\bar{\rho}^*}\right) \Phi_0 \,, \tag{3.25c}$$

$$\Delta \left(\mathcal{D}_1^\dagger - \frac{1}{\bar{\rho}^*}\right) \Phi_0 = -\left(\mathcal{L}_0^\dagger + \frac{ia\sin\theta}{\bar{\rho}^*}\right) \Phi_1 \,. \tag{3.25d}$$

Now we may use the commutation relation (3.23e) together with (3.23a) to separate the equations for Φ_0 and Φ_2. In order to obtain the first equation, we must first apply the operator $(\mathcal{L}_0^\dagger + ia\sin\theta/\bar{\rho}^*)$ to Eq. (3.25c) and then use the commutation relation to substitute Eq. (3.25d). Similarly, applying $(\mathcal{L}_0 + ia\sin\theta/\bar{\rho}^*)$ to Eq. (3.25b) we obtain the final equation. This yield

$$\left[\Delta \mathcal{D}_1 \mathcal{D}_1^\dagger + \mathcal{L}_0^\dagger \mathcal{L}_1 + 2i\omega(r + ia\cos\theta)\right] \Phi_0 = 0 \,, \tag{3.26}$$

$$\left[\Delta \mathcal{D}_0^\dagger \mathcal{D}_0 + \mathcal{L}_0 \mathcal{L}_1^\dagger - 2i\omega(r + ia\cos\theta)\right] \Phi_2 = 0 \,. \tag{3.27}$$

Still, there is another way of combining equations, *i.e.* Eq. (3.25b) with (3.25d) and the remaining two form the set

$$\mathcal{L}_0\mathcal{L}_1\Phi_0 = \mathcal{D}_0\mathcal{D}_0\Phi_2 \,, \tag{3.28}$$

$$\mathcal{L}_0^\dagger\mathcal{L}_1^\dagger\Phi_2 = \Delta\mathcal{D}_0^\dagger\mathcal{D}_0^\dagger\Delta\Phi_0 \,. \tag{3.29}$$

Thus, we went from four first-order differential equations relating three NP scalars to four second-order differential equations, two of each decoupled, eliminating the need for the scalar ϕ_1. The last two equations imply that each of the complex NP scalars contains all the information necessary to describe an EM wave (two polarizations). One may think that we only need one of each group of equations to solve all perturbations, but no closed form solution has yet been found. Thus the problem has to be tackled using approximations or numerical methods, recurring to all last four equations (3.26–3.29), as we will see below.

Due to the nature of the operators $\mathcal{D}_n$ and $\mathcal{L}_n$, we may separate the equations for $\Phi_0 \sim R_{+1}(r)S_{+1}(\theta)$ and $\Phi_2 \sim R_{-1}(r)S_{-1}(\theta)$ into two pairs of equations,

$$\left(\Delta\mathcal{D}_0\mathcal{D}_0^\dagger + 2i\omega r\right)\Delta R_{+1} = \lambda\!\!\!^{-}\Delta R_{+1} \,, \tag{3.30a}$$

$$\left(\mathcal{L}_0^\dagger\mathcal{L}_1 - 2a\omega\cos\theta\right)S_{+1} = -\lambda\!\!\!^{-}S_{+1} \,, \tag{3.30b}$$

and

$$\left(\Delta\mathcal{D}_0^\dagger\mathcal{D}_0 - 2i\omega r\right)R_{-1} = \lambda\!\!\!^{-}R_{-1} \,, \tag{3.31a}$$

$$\left(\mathcal{L}_0\mathcal{L}_1^\dagger + 2a\omega\cos\theta\right)S_{-1} = -\lambda\!\!\!^{-}S_{-1} \,, \tag{3.31b}$$

where $\lambda\!\!\!^{-}$ is a separation constant. We use the property (3.23a) in to obtain Eq. (3.30a). The constant $\lambda\!\!\!^{-}$ must be real, as the angular differential operators $\mathcal{L}_n$ are also real. Notice that we do not distinguish the separation constants of both equations. Performing the transformation $\theta \to \pi - \theta$, the angular operators transforms as $\mathcal{L}_0^\dagger\mathcal{L}_1 \to \mathcal{L}_0\mathcal{L}_1^\dagger$. Then if $S_{+1}(\theta)$ is a solution for Eq. (3.30b) for a given separation constant $\lambda\!\!\!^{-}$, this implies that $\tilde{S}_{-1}(\theta) = S_{+1}(\pi - \theta)$ is a solution for Eq. (3.31b) for the same constant. In other words, the separation constant must be the same for both equations. Also, solutions R_{-1} and ΔR_{+1} obey the same complex conjugate equations due to $\mathcal{D}_n^\dagger = (\mathcal{D}_n)^*$.

The second-order equations relating Φ_0 and Φ_2 can be separated in the same fashion. Naturally, the separation constant will differ from the eigenvalue Eqs. (3.30) and

(3.31). Using the same substitutions made previously, we divide each equation by the corresponding ansatz to obtain

$$\frac{\mathcal{L}_0\mathcal{L}_1 S_{+1}}{S_{-1}} = \frac{\Delta\mathcal{D}_0\mathcal{D}_0 R_{-1}}{\Delta R_{+1}} = \mathcal{B}\,, \tag{3.32}$$

$$\frac{\mathcal{L}_0^\dagger\mathcal{L}_1^\dagger S_{-1}}{S_{+1}} = \frac{\Delta\mathcal{D}_0^\dagger\mathcal{D}_0^\dagger\Delta R_{+1}}{R_{-1}} = \mathcal{B}\,. \tag{3.33}$$

The separation constant $\mathcal{B}$ is real and equal for both equations. This claim rests on the same arguments as for the eigenvalue $\lambda\!\!\!^{-}$. We also make the angular functions S_{-1}, S_{+1} equally normalized. We may observe the latter by assuming two different separation constants $\mathcal{B}_1$, $\mathcal{B}_2$. Then, we have

$$\begin{aligned}(\mathcal{B}_1)^2\int_0^\pi \mathrm{d}\theta\sin\theta\,(S_{-1})^2 &= \int_0^\pi \mathrm{d}\theta\sin\theta\,(\mathcal{L}_0\mathcal{L}_1 S_{+1})(\mathcal{L}_0\mathcal{L}_1 S_{+1})\\ &= \int_0^\pi \mathrm{d}\theta\sin\theta\,(\mathcal{L}_0^\dagger\mathcal{L}_1^\dagger\mathcal{L}_0\mathcal{L}_1 S_{+1})S_{+1}\\ &= \mathcal{B}_1\mathcal{B}_2\int_0^\pi \mathrm{d}\theta\sin\theta\,(S_{+1})^2\,,\end{aligned} \tag{3.34}$$

where we used integration by parts twice. Thus $(\mathcal{B}_1)^2 = \mathcal{B}_1\mathcal{B}_2 = \mathcal{B}^2$. We can compute the coefficient by computing the operation

$$\begin{aligned}\mathcal{L}_0^\dagger\mathcal{L}_1^\dagger\mathcal{L}_0\mathcal{L}_1 &= \mathcal{L}_0^\dagger(\mathcal{L}_0\mathcal{L}_1^\dagger - 4a\omega\cos\theta)\mathcal{L}_1\\ &= \mathcal{L}_0\mathcal{L}_1^\dagger(-\lambda\!\!\!^{-} + 2a\omega\cos\theta) - 4a\omega\cos\theta\,\mathcal{L}_0^\dagger\mathcal{L}_1 + 4a\omega\sin\theta\,\mathcal{L}_1\\ &= -\lambda\!\!\!^{-}\,\mathcal{L}_0\mathcal{L}_1^\dagger + 2a\omega\left[\cos\theta\,\mathcal{L}_0\mathcal{L}_1^\dagger - \sin\theta(\mathcal{L}_1 + \mathcal{L}_1^\dagger)\right]\\ &\qquad - 4a\omega\cos\theta\,\mathcal{L}_0^\dagger\mathcal{L}_1 + 4a\omega\sin\theta\,\mathcal{L}_1\\ &= (-\lambda\!\!\!^{-} + 2a\omega\cos\theta)\mathcal{L}_0\mathcal{L}_1^\dagger + 4a\omega Q\sin\theta\\ &= (-\lambda\!\!\!^{-} + 2a\omega\cos\theta)(-\lambda\!\!\!^{-} - 2a\omega\cos\theta) + 4a\omega(-a\omega\sin^2\theta + m)\\ &= \lambda\!\!\!^{-2} - 4a^2\omega^2 + 4a\omega m = \mathcal{B}^2\,,\end{aligned} \tag{3.35}$$

applied on the angular function S_{+1}. The commutation relations between the angular operators can be found directly or by noticing that $[\boldsymbol{e}_a, \boldsymbol{e}_b] = \eta^{cd}(\gamma_{cba} - \gamma_{cab})\boldsymbol{e}_d$. Then using Eq. (3.30b) it is possible to eliminate the second-order angular operators. To obtain $\mathcal{B}^2$, the same procedure could be done for S_{-1} or the the radial functions.

It will be more profitable to study Eqs. (3.26) and (3.27) as a special case of the Teukolsky master equation [12] which describes all the linearized perturbations around the Kerr BH. The generality of this equation is the primary reason for the focus on the EM case.

The treatment for GWs differs in the perturbation formalism only in algebraic complexity, resulting in the same master equation. With the Teukolsky master equation we can proceed considering general perturbations, but there are several numerical and analytical details that make EM waves and GWs differ later on [32].

The general equation reads

$$\begin{aligned}&\frac{1}{\Delta^s}\frac{\partial}{\partial r}\left(\Delta^{s+1}\frac{\partial \Upsilon_s}{\partial r}\right)+\frac{1}{\sin\theta}\frac{\partial}{\partial\theta}\left(\sin\theta\frac{\partial\Upsilon_s}{\partial\theta}\right)-\left[\frac{(r^2+a^2)^2}{\Delta}-a^2\sin^2\theta\right]\frac{\partial^2\Upsilon_s}{\partial t^2}\\&-\frac{4Mar}{\Delta}\frac{\partial^2\Upsilon_s}{\partial t\partial\varphi}-\left(\frac{a^2}{\Delta}-\frac{1}{\sin^2\theta}\right)\frac{\partial^2\Upsilon_s}{\partial\varphi^2}+2s\left[\frac{M(r^2-a^2)}{\Delta}-r-ia\cos\theta\right]\frac{\partial\Upsilon_s}{\partial t}\\&+2s\left[\frac{a(r-M)}{\Delta}+\frac{i\cos\theta}{\sin^2\theta}\right]\frac{\partial\Upsilon_s}{\partial\varphi}-(s^2\cot^2\theta-s)\Upsilon_s=0\,,\end{aligned}\tag{3.36}$$

where s is the field *spin weight* and each field quantity Υ_s is related to the NP scalars as shown in the Table 3.1. Depending on the spin weight, the equation may describe massless scalar ($s=0$) or Dirac fields ($s=\pm\frac{1}{2}$), as well as electromagnetic ($s=\pm1$) or gravitational waves ($s=\pm2$). Substituting the spin-weight for the EM waves we obtain Eqs. (3.26) and (3.27).

s	Υ_s
$+1$	$\Phi_0=\phi_0$
-1	$\Phi_2=2(\bar{\rho}^*)^2\phi_2$
$+2$	$\Psi_0=\psi_0$
-2	$\Psi_4=4(\bar{\rho}^*)^4\psi_4$

TABLE 3.1: Newman-Penrose fields that obey the Teukolsky master equation for different spin-weights [29]

Obviously, Teukolsky's equation is explicitly independent of t and φ, thus Υ_s accepts a decomposition in $e^{-i\omega t+im\varphi}$, which we already assumed in the EM case to separate the equations. Stationarity and axisymmetry of the spacetime geometry guarantees this form. The azimuthal wave number m must be an integer, due to periodic boundary conditions on the BL coordinate φ. We may separate all perturbations in a completely general mode decomposition

$$\Upsilon_s=\int \mathrm{d}\omega\ \sum_{\ell,m} e^{-i\omega t+im\varphi}\,{}_sS_{\ell m}(\theta)\,{}_sR_{\ell m}(r)\,.\tag{3.37}$$

The integer ℓ plays a role in labelling all possible solutions for the eigenvalue problem of both radial and angular equations,

$$\frac{1}{\Delta^s}\frac{\mathrm{d}}{\mathrm{d}r}\left(\Delta^{s+1}\frac{\mathrm{d}\,{}_sR_{\ell m}}{\mathrm{d}r}\right)+\left[\frac{K^2-2is(r-M)K}{\Delta}+4is\omega r-{}_s\mathcal{F}_{\ell m}\right]{}_sR_{\ell m}=0\,, \tag{3.38}$$

$$\frac{1}{\sin\theta}\frac{\mathrm{d}}{\mathrm{d}\theta}\left(\sin\theta\frac{\mathrm{d}\,{}_sS_{\ell m}}{\mathrm{d}\theta}\right)+\left[a^2\omega^2\cos^2\theta-2sa\omega\cos\theta-\frac{(m+s\cos\theta)^2}{\sin^2\theta}+s+{}_s\mathcal{A}_{\ell m}\right]{}_sS_{\ell m}=0\,. \tag{3.39}$$

The radial and angular eigenvalues are related to the separation constant on Eqs. (3.30) and (3.31) through

$${}_s\mathcal{F}_{\ell m}={}_s\mathcal{A}_{\ell m}-2ma\omega+a^2\omega^2\underset{(s=\pm1)}{=}\lambda-s(s+1)\,. \tag{3.40}$$

Due to the form of the angular equation, the eigenvalues ${}_s\mathcal{F}_{\ell m}$, ${}_s\mathcal{A}_{\ell m}$ as well as the function ${}_sS_{\ell m}(\theta)$ depends also on the coupling $a\omega$. Clearly, the same does not hold for the radial function ${}_sR_{\ell m}(r)$.

3.2 Spin-Weighted Spheroidal Harmonics

To shed some light into the explicit form of ${}_s\mathcal{A}_{\ell m}$, we will need to dive into the eigenvalue problem for the angular equation. We may transform Eq. (3.39) into a more familiar form using the change of coordinate $z=\cos\theta$ and renaming the dimensionless parameter $c=a\omega$, obtaining

$$\frac{\mathrm{d}}{\mathrm{d}z}\left[(1-z^2)\frac{\mathrm{d}\,{}_sS_{\ell m}}{\mathrm{d}z}\right]+\left[(cz)^2-2csz-\frac{(m+sz)^2}{1-z^2}+s+{}_s\mathcal{A}_{\ell m}\right]{}_sS_{\ell m}=0\,. \tag{3.41}$$

We may also use freely ${}_sS_{\ell m}(\cos\theta)\equiv{}_sS_{\ell m}(\theta)$. We will consider c real as we are analyzing superradiance of EM waves in vacuum, although we could generalize the spin-weighted spheroidal harmonic (SWSH) equation to imaginary c values to describe waves in a particular medium.

Spherically symmetric problems allow for a decomposition using spherical harmonics $Y_{\ell m}(\theta,\varphi)$ of angular dependent functions with finite boundary conditions. These have innumerable applications in physics such as the hydrogen atom or the description of

anisotropies in the cosmic microwave background. By setting $s = 0$ and $c = 0$ (spherical), then it is clear that the solutions for Eq. (3.41) are given by the associated Legendre polynomials, $P_\ell^m(z)$. Therefore, ${}_sS_{\ell m}$ is a generalization of a spherical harmonic [33], with

$$ {}_0S_{\ell m}(\theta,\varphi) \underset{(c=0)}{=} Y_{\ell m}(\theta,\varphi)\,, \qquad {}_0\mathcal{A}_{\ell m} \underset{(c=0)}{=} \ell(\ell+1)\,, \tag{3.42} $$

where ${}_sS_{\ell m}(\theta,\varphi) \equiv e^{im\varphi}{}_sS_{\ell m}(\theta)$. The values of ℓ are non-negative integers, with the restriction of $\ell \geq |m|$. We require that spin-weighted spheroidal harmonics (SWSHs) are similarly normalized to unity and also a complete set of orthogonal functions, for any spin-weight and coupling c,

$$ \int_0^\pi \mathrm{d}\theta \sin\theta\, {}_sS_{\ell m}(\theta)\, {}_sS_{\ell' m'}(\theta) = \int_{-1}^{1} \mathrm{d}z\, {}_sS_{\ell m}(z) {}_sS_{\ell' m}(z) = \frac{1}{2\pi}\delta_{\ell\ell'}\,. \tag{3.43} $$

Perturbations of any type in Schwarzschild spacetime are written using spin-weighted *spherical* harmonics, ${}_sY_{\ell m}(\theta,\varphi)$, which are still spherical harmonics ($c = 0$). Due to the shared symmetries with spherical harmonics it is possible to find a closed form for $s \neq 0$ harmonics. We can raise and lower spin-weight with the use of the operators commonly denoted as $\bar{\eth}$ and $\eth$ (see Appendix C), respectively, applied on $Y_{\ell m}$,

$$ \begin{aligned} (\bar{\eth})^s Y_{\ell m} &= \sqrt{\frac{(\ell+s)!}{(\ell-s)!}}\, {}_sY_{\ell m}\,, \\ (-1)^s(\eth)^s Y_{\ell m} &= \sqrt{\frac{(\ell+s)!}{(\ell-s)!}}\, {}_{-s}Y_{\ell m}\,, \end{aligned} \tag{3.44} $$

limited by $|s| \leq \ell$. Eqs. (3.32) and (3.33) are closely related to former, as applications of the operators $\mathcal{L}_s^\dagger$ and $\mathcal{L}_s$ generalize $\bar{\eth}$ and $\eth$, respectively.

Thus, for the non-spherical symmetry we could in principle obtain all SWSHs if we knew the closed form for ${}_0S_{\ell m}$ and its eigenvalues. The problem lies in the fact that no such decomposition of elementary function has been found. This require us to follow numerical and approximate methods to find the values of ${}_sS_{\ell m}$.

The major advances on the study of the eigenvalues of the SWSHs was performed by Leaver in 1985 [34, 35]. Working out the asymptotical and critical behavior of the equation, we observe the equation diverges at the poles, $z = \pm 1$, where the it takes the form $(1 \mp z)\, {}_sS_{\ell m}{}'(z) \sim \mp\frac{1}{4}(m \pm s)^2\, {}_sS_{\ell m}(z)$. In order to guarantee that a SWSH is everywhere

analytical, Leaver proposed the series expansion at $z = -1$,

$$ {}_sS_{\ell m}(z) = e^{cz}(1+z)^{k_-}(1-z)^{k_+}\sum_{p=0}^{\infty} a_p(1+z)^p \,, \tag{3.45} $$

where $k_\pm = \frac{1}{2}|m \pm s|$. The exponential in the ansatz accounts for the large z behavior of the equation. Substituting in the angular equation, we obtain a three-term recurrence relation between the expansion coefficients a_p and the boundary condition at $z = -1$,

$$ \alpha_p a_{p+1} + \beta_p a_p + \gamma_p a_{p-1} = 0 \,, \qquad \alpha_0 a_1 + \beta_0 a_0 = 0 \,, \tag{3.46} $$

where

$$ \begin{aligned} \alpha_p &= -2(1+p)(1+2k_+ + p) \,, \\ \beta_p &= (k_- + k_+ + p - s)(1 + k_- + k_+ + p + s) \\ &\qquad - 2c(1 + 2k_- + 2p + s) - c^2 - {}_s\mathcal{A}_{\ell m} \,, \\ \gamma_p &= 2c(k_- + k_+ + p + s) \,. \end{aligned} \tag{3.47} $$

We then find an equation for the eigenvalue ${}_s\mathcal{A}_{\ell m}$ with explicit dependence on m, s and c, by combining the previous relations into a continued fraction,

$$ \beta_0 = \frac{\alpha_0\gamma_1}{\beta_1 -}\frac{\alpha_1\gamma_2}{\beta_2 -}\frac{\alpha_2\gamma_3}{\beta_3 -}\cdots \left(\equiv \frac{\alpha_0\gamma_1}{\beta_1 - \frac{\alpha_1\gamma_2}{\beta_2 - \frac{\alpha_2\gamma_3}{\beta_3 - \ldots}}} \right) \,. \tag{3.48} $$

We can also consider the r-th inversion of Eq. (3.48),

$$ \beta_r - \frac{\alpha_{r-1}\gamma_r}{\beta_{r-1} -}\frac{\alpha_{r-2}\gamma_{r-1}}{\beta_{r-2} -}\cdots\frac{\alpha_1\gamma_2}{\beta_1 -}\frac{\alpha_0\gamma_1}{\beta_0} = \frac{\alpha_r\gamma_{r+1}}{\beta_{r+1} -}\frac{\alpha_{r+1}\gamma_{r+2}}{\beta_{r+2} -}\cdots \,. \tag{3.49} $$

These equations involve an infinite fraction that depends explicitly on c, m, s, which raises suspicion that we may have an infinite spectrum. This is in a close parallel to the spherical case, where we have a infinite number of harmonics, although no proof has been found. If we notice that $\gamma_p \propto c$, then the zero order expansion of the eigenvalue expansion in $c \ll 1$ corresponds to $\beta_r = 0$. In the spherical geometry, this corresponds to truncating the series at r, as $\gamma_p = 0$ for any p. Thus, the eigenvalue root depends explicitly on the integer r,

entailing the discretization of the spectra

$$ {}_s\mathcal{A}_{\ell m} = \ell(\ell+1) - s(s+1) + \mathcal{O}(a\omega) \,, \tag{3.50} $$

where we identified $\ell = r + k_+ + k_-$. Since $r \geq 0$, then we must have $\ell \geq \max\{|m|, |s|\}$, *i.e.* the leading contribution for the multipole expansion is the dipole for EM waves and the quadrupole for GWs. Changing r for ℓ corresponds simply to a relabeling of the eigenfunctions in order to match the values of the spectra with know cases ($c = 0$).

It will be useful to expand ${}_s\mathcal{A}_{\ell m}$ in high order terms in order to obtain the series coefficients for the eigenvalue (see Appendix D). Up to sixth order, only the zero-order term depends on the sign of the spin weight [36, 37], in agreement with Eq. (3.40). In the general angular equation, inversion of spin corresponds to inversion of poles, *i.e.* stays invariant under the transformation $(s, z) \to (-s, -z)$. Under this transformation, the eigenvalue must obey $s + {}_s\mathcal{A}_{\ell m} = -s + {}_{-s}\mathcal{A}_{\ell m}$, thus it is beneficial to define

$$ {}_s\mathcal{A}_{\ell m} = {}_s\mathcal{E}_{\ell m} - s(s+1) \,, \tag{3.51} $$

to also exploit the symmetry of spin inversion in numerical computations. This way, we can simply write that $\lambda = {}_{\pm1}\mathcal{E}_{\ell m}$.

3.3 Analytic radial approximations

Like the angular equation, in general it is not possible to solve the radial Eq. (3.38) by known analytical methods. The only apparent line of attack would be to numerical solve the equation, but it will be important to find the asymptotic form of ${}_sR_{\ell m}$ at infinity as well as its near-horizon behavior. For both methods it will prove beneficial to change the variables into dimentionaless quantities [38],

$$ x = \frac{r - r_+}{r_+} \,, \qquad \tau = \frac{r_+ - r_-}{r_+} \,, \qquad \varpi = (2 - \tau)(\bar{\omega} - m\bar{\Omega}_H) \,, \tag{3.52} $$

where every barred frequency is normalized relative to the BH horizon, $\bar{\omega} \equiv \omega r_+$. Due to (2.23), we have that $0 \leq \tau \leq 1$. Using this coordinate, $x \to 0$ represents the BH horizon.

The radial equation now reads

$$\frac{1}{[x(x+\tau)]^s}\frac{\mathrm{d}}{\mathrm{d}x}\left([x(x+\tau)]^{s+1}\frac{\mathrm{d}\,{}_sR_{\ell m}}{\mathrm{d}x}\right)+ \\ +\left[\frac{\mathcal{K}^2-is(2x+\tau)\mathcal{K}}{x(x+\tau)}+4is(1+x)\bar{\omega}-{}_s\mathcal{F}_{\ell m}\right]{}_sR_{\ell m}=0\,, \tag{3.53}$$

where we normalize $\mathcal{K}=K/r_+=\varpi+x(x+2)\bar{\omega}$. In this method, it will be sufficient to use a spherical approximation for the harmonics eigenvalues, ${}_s\mathcal{F}_{\ell m}=\ell(\ell+1)-s(s+1)+\mathcal{O}(a\omega)$, for small enough frequencies.

The near-horizon approximation corresponds to considering only small distances compared to the perturbations characteristic wavelength, $r-r_+\ll\omega^{-1}$ ($\bar{\omega}x\ll 1$). Because superradiant scattering occurs when $\omega\lesssim\Omega_H$, we also neglect terms $\mathcal{O}(\varpi x)$. In this limit, $\mathcal{K}\simeq\varpi$. The resultant equation remains singular at the horizons $x=0$ and $x=-\tau$. Thus, making the substitution ${}_sR_{\ell m}(x)\simeq x^{\alpha}(x+\tau)^{\beta}F(x)$, the function $F(x)$ is analytical if $\alpha+\beta=-s$ and also if $\alpha=-\frac{1}{2}s\pm\left(\frac{1}{2}s+i\varpi/\tau\right)$. Boundary conditions at the horizon requires that a physical observer measures a negative radial group velocity of the signal. In order words, we require the wave to travel into the black hole and never outwards. Since $x^{\pm i\varpi/\tau}\simeq e^{\pm i\kappa r_*}$, where $\kappa\equiv\omega-m\Omega_H$, then the ingoing solution requires $\alpha=-s-i\varpi/\tau$. The near-horizon solution gives

$${}_sR_{\ell m}(x)\simeq A\,x^{-s-i\varpi/\tau}(x+\tau)^{i\varpi/\tau}\,{}_2F_1\left(-\ell,\,\ell+1,\,1-s-\frac{2i\varpi}{\tau};\,-\frac{x}{\tau}\right)\,, \tag{3.54}$$

where $F(x)={}_2F_1(a,b,c;x)$ is the hypergeometric function.

Asymptotically, we consider $x\gg\tau$, where $\mathcal{K}\sim x^2\bar{\omega}$. The resultant equation, allows to substitute a power law ${}_sR_{\ell m}(x)\sim x^{\alpha}e^{-i\bar{\omega}x}M(x)$. In order for $M(x)$ to be analytic everywhere, then we must have $\alpha^2+(2s+1)\alpha={}_s\mathcal{F}_{\ell m}$. We are left with Kummer's differential equation for $M(x)$, where $\alpha=\ell-s$ or $\alpha=-1-\ell-s$. The general solution is the combination

$${}_sR_{\ell m}(x)\sim C\,e^{-i\bar{\omega}x}x^{\ell-s}\,{}_1F_1(1+\ell-s,\,2\ell+2;\,-2i\bar{\omega}x) \\ +D\,e^{-i\bar{\omega}x}x^{-1-\ell-s}\,{}_1F_1(-\ell-s,\,-2\ell;\,-2i\bar{\omega}x)\,, \tag{3.55}$$

where ${}_1F_1(a,b;x)$ are Olver's confluent hypergeometric functions and C, D are integration constants.

Altought useful, these solutions do not provide enough physical insight. Another way

of obtaining the same assympotic behavior is by transforming the radial equation into a Schrodinger-like potential problem

$$\left[\frac{\mathrm{d}^2}{\mathrm{d}r_*^2} + V_{\mathrm{eff}}\right] {}_sU_{\ell m} = 0\,, \tag{3.56}$$

where ${}_sU_{\ell m} = \sqrt{\Delta^s(r^2+a^2)}\,{}_sR_{\ell m}$ and the tortoise coordinate r_* was defined in Eq. (2.21). We write the potential as a function of the radial coordiante [13],

$$V_{\mathrm{eff}} = \frac{K^2 - 2is(r-M)K + \Delta(4is\omega r - {}_s\mathcal{F}_{\ell m})}{(r^2+a^2)^2} - G^2 - \frac{\mathrm{d}G}{\mathrm{d}r_*} \tag{3.57}$$

where $G = s(r-M)/(r^2+a^2) + r\Delta/(r^2+a^2)^2$. Even tought r_* is related to the radial coordinate through an non-invertable relation, we use this coordinate to remove all the Δ singularities from the diferential equation.

Taking $r \to \infty$ ($r_* \to \infty$), the potential becomes

$$V_{\mathrm{eff}} \sim \omega^2 + \frac{2is\omega}{r}\,, \tag{3.58}$$

with assympotic solution ${}_sU_{\ell m} \sim r^{\pm s} e^{\mp i\omega r_*}$. The combination of both solutions corresponds to

$${}_sR_{\ell m}(r) \sim A_{\mathrm{in}}\,\frac{e^{-i\omega r_*}}{r} + A_{\mathrm{out}}\,\frac{e^{i\omega r_*}}{r^{2s+1}}\,. \tag{3.59}$$

The ingoing and outgoing wave coeficients can be related to the integration coeficients B, C by expanding the hypergeometric function in (3.55) at infinity,

$$\begin{aligned} A_{\mathrm{in}} &= \left[C(-2i\bar{\omega})^{-\ell+s-1}\frac{\Gamma(2\ell+2)}{\Gamma(\ell+s+1)} + D(-2i\bar{\omega})^{\ell+s}\frac{\Gamma(-2\ell)}{\Gamma(-\ell+s)}\right] r_+\,, \\ A_{\mathrm{out}} &= \left[C(2i\bar{\omega})^{-\ell-s-1}\frac{\Gamma(2\ell+2)}{\Gamma(\ell-s+1)} + D(2i\bar{\omega})^{\ell-s}\frac{\Gamma(-2\ell)}{\Gamma(-\ell-s)}\right] (r_+)^{2s+1}\,. \end{aligned} \tag{3.60}$$

We may notice the ratio of gamma functions with negative integer valued arguments, which can be misinterpreted as a divergence due to existing poles of $\Gamma(z)$. This is a mere artifact of the asymptotic expantion for general confluent hypergeometric arguments. A way to circumvent this problem is to consider Euler's reflection formula for any value of

ℓ and then take the limit to the integer set,

$$\lim_{\ell\in\mathbb{Z}} \frac{\Gamma(-2\ell)}{\Gamma(-\ell\pm s)} = \frac{\Gamma(\ell\mp s+1)}{\Gamma(2\ell+1)} \lim_{\ell\in\mathbb{Z}} \frac{\sin(\ell\pi)\cos(\mp s\pi)}{\sin(2\ell\pi)} = \frac{(-1)^{\ell+s}}{2}\frac{(\ell\mp s)!}{(2\ell)!} \,. \tag{3.61}$$

At the event horizon $r = r_+$, where $r_* \to -\infty$ and $\Delta = 0$. The effective radial potential is simplified to a constant

$$V_{\text{eff}} \simeq \left(\kappa - is\frac{r_+ - M}{2Mr_+}\right)^2 \,. \tag{3.62}$$

Due to the logarithmic behavior of r_* at the horizon, the solution takes the form ${}_sU_{\ell m} \sim e^{\pm i\kappa r_*}(r-r_+)^{\pm s/2} \sim \Delta^{\pm s/2}\, e^{\pm i\kappa r_*}$. The boundary conditions at $r = r_+$ state that the horizon solution must only have the ingoing solution

$${}_sR_{\ell m} \simeq A_{\text{hole}}\, \Delta^{-s}\, e^{-i\kappa r_*} \,. \tag{3.63}$$

Expanding solution (3.54), the integration constants relate through $A_{\text{hole}} = (r_+)^{-s}A$.

With both approximations it is possible to extend the solutions of small frequency waves to overlapping regions and perform a matching of coefficients [6, 7], which can be used to find how much of the wave is reflected/amplified. The near region $r - r_+ \ll \omega^{-1}$ and the asymptotic region $r - r_+ \gg r_+$ overlap when $\omega r_+ \ll 1$ ($\bar{\omega} \ll 1$). The overlapping region becomes larger as ωr_+ becomes smaller. We proceed by expanding the far region solution (3.55) at the horizon, $x = 0$, where the lowest order terms are simply

$${}_sR_{\ell m} \simeq C\, x^{\ell-s} + D\, x^{-1-\ell-s} \,. \tag{3.64}$$

On the other hand, expanding the near region solution (3.55) at infinity we get

$$\begin{aligned} {}_sR_{\ell m} \sim\; & A\,\tau^{-\ell}\frac{\Gamma(2\ell+1)}{\Gamma(\ell+1)}\frac{\Gamma(1-s-2i\varpi/\tau)}{\Gamma(\ell+1-s-2i\varpi/\tau)}x^{\ell-s} \\ & + A\,\tau^{\ell+1}\frac{\Gamma(-2\ell-1)}{\Gamma(-\ell)}\frac{\Gamma(1-s-2i\varpi/\tau)}{\Gamma(-\ell-s-2i\varpi/\tau)}x^{-\ell-1-s} \,. \end{aligned} \tag{3.65}$$

The matching is possible because the solutions when expanded in regions in the limit of their validity are given in terms of two monomials of $x^{\ell-s}$ and $x^{-1-\ell-s}$. A combination of

these results yields

$$\frac{D}{C} = \frac{(-1)^{\ell+1}}{2} \frac{(\ell!)^2}{(2\ell)!(2\ell+1)!} \frac{\Gamma(\ell+1-s-2i\varpi/\tau)}{\Gamma(-\ell-s-2i\varpi/\tau)} \tau^{2\ell+1} , \tag{3.66}$$

where we used the same identification as in Eq. (3.61) for the Γ functions with negative arguments. With this result it is possible to find the ratio between the incoming and the outgoing energy from the BH.

3.4 Amplification factor ${}_sZ_{\ell m}$

Potential barrier problems are heavilly associated with reflection and absortion of radiation. Central potentials have waves scattered diferently for each mode (ω, ℓ, m), depending on the incident angle of the wave. The stress-energy tensor allows to define conserved currents, which can be used to compute the flow of energy and angular momentum. In particular, we will be interested in calculating the asymptotic energy flow going inward and outward of the BH.

Different Killing vectors have distinct currents, due to different possible projections of the stress-energy tensor. These currents are conserved due to $\nabla_\mu T^{\mu\nu} = 0$ and the Killing Eq. (2.8). The energy flux is defined as [11]

$$\mathrm{d}E = T^{\mu}{}_{\nu}\, k^{\nu}\, \mathrm{d}\Sigma_{\mu} \tag{3.67}$$

where $\mathrm{d}\Sigma_\mu$ is defined as the 3-surface element. An asymptotically flat geometry such as the Kerr metric has infinity r-constant hypersurface with induced 3-metric $\boldsymbol{h} = h_{\alpha\beta}\, \mathrm{d}y^\alpha \mathrm{d}y^\beta$, where $h_{\alpha\beta} = g_{\alpha\beta}$ for $y^\alpha \in (t, \theta, \varphi)$. In BL coordinates, the normal to the surface is the outgoing radial vector $\boldsymbol{n} = (\mathrm{d}r)^\sharp$, while the other vectors form the tangent basis. By computing the highest order term when $r \to \infty$, the surface element is asymptotically spherically symmetric, given by

$$\mathrm{d}\Sigma_\mu = n_\mu \sqrt{\det \boldsymbol{h}}\, \mathrm{d}t\, \mathrm{d}\theta\, \mathrm{d}\varphi \sim n_\mu\, r^2 \sin\theta\, \mathrm{d}t\, \mathrm{d}\theta\, \mathrm{d}\varphi\, . \tag{3.68}$$

We are obviously interested in obtaining an expression relating the flow of energy at infinity and the Maxwell NP scalar. Thus, will be convenient to describe the stress-energy tensor using symmetric tetrad combinations and NP scalars and their conjugates. Much like the Weyl and the Maxwell tensor, this composition is uniquelly defined by Eqs. (2.7)

and (3.15),

$$\begin{aligned} 2T_{\mu\nu} = {} & \phi_0^* \phi_0 \, \mathfrak{n}_\mu \mathfrak{n}_\nu + \phi_2^* \phi_2 \, \mathfrak{l}_\mu \mathfrak{l}_\nu + 2\phi_1^* \phi_1 \left[\mathfrak{l}_{(\mu} \mathfrak{n}_{\nu)} + \mathfrak{m}_{(\mu} \bar{\mathfrak{m}}_{\nu)} \right] \\ & - 4\phi_0^* \phi_1 \, \mathfrak{n}_\mu \mathfrak{m}_\nu - 4\phi_1^* \phi_2 \, \mathfrak{l}_\mu \mathfrak{m}_\nu + 2\phi_0^* \phi_2 \, \mathfrak{m}_\mu \mathfrak{m}_\nu + \text{c.c.} \end{aligned} \tag{3.69}$$

Energy flow is thus computed by taking the series expansion of

$$r^2 \, T^r{}_t = -r^2 \frac{\Delta}{\rho^2} \, T_{rt} = -r^2 \left(\frac{1}{4} |\phi_0|^2 - |\phi_2|^2 \right) + \mathcal{O}\left(\frac{1}{r} \right) , \tag{3.70}$$

recalling definition (3.24) when considering the asymptotic form of ${}_sR_{\ell m}$ in Eq. (3.59). We can clearly identify the ingoing and outgoing flows as

$$\frac{\mathrm{d}^2 E_{\text{in}}}{\mathrm{d}t \mathrm{d}\Omega} = \lim_{r\to\infty} \frac{r^2}{4} |\phi_0|^2 , \qquad \frac{\mathrm{d}^2 E_{\text{out}}}{\mathrm{d}t \mathrm{d}\Omega} = \lim_{r\to\infty} r^2 |\phi_2|^2 , \tag{3.71}$$

In order to obtain the full conservation law we must find the absorbed radiation by the BH. We turn now to the horizon null hypersurface, for which the normal vector n in BL coordinates is the zero vector, due to $g^{rr} = 0$. Similarly, the stress-energy tensor in this tetrad basis is ill-defined since $\mathfrak{l}$ is singular at the horizon, where $\Delta = 0$. The Kinnersley tetrad keeps its properties, by applying a boost in the null directions [11, 15, 30, 39]

$$\tilde{\mathfrak{l}} = \frac{\Delta}{2(r^2 + a^2)} \mathfrak{l} , \qquad \tilde{\mathfrak{n}} = \frac{2(r^2 + a^2)}{\Delta} \mathfrak{n} , \tag{3.72}$$

while removing the singularity at the horizon. The NP field quantities are now given by $\tilde{\Upsilon}_s = [\Delta / 2(r^2 + a^2)]^s \, \Upsilon_s$. In addition, we shall use the ingoing EF coordinates, defined in Eq. (2.20), as the chart is the indicated to consider inward future directed waves, because $(\mathfrak{l} \cdot \partial_v)$ is a positive constant,

$$\tilde{\mathfrak{l}} = \left(1, \frac{\Delta}{2(r^2 + a^2)}, 0, \frac{a}{r^2 + a^2} \right) , \qquad \tilde{\mathfrak{n}} = \left(0, -\frac{r^2 + a^2}{\rho^2}, 0, 0 \right) . \tag{3.73}$$

If we set $r = r_+$, we obtain that $\tilde{\mathfrak{l}} = \boldsymbol{\xi}$. This implies that $\tilde{\mathfrak{l}}$ is a normal vector to the event horizon, just like $(\mathrm{d}r)^\sharp$, but they are opposite to each other as $g^{rv} < 0$.

The radial 3-surface element cannot be of the form in Eq. (3.68), since the induced metric at the horizon is now singular, $\sqrt{\det \boldsymbol{h}} = \Delta \rho^2 \sin\theta = 0$. Special considerations must be taken when taking the induced metric of a null hypersurface. We usually choose $\boldsymbol{k} = \partial_v$ as one of the surface tangent vectors, due to $\boldsymbol{\xi} \cdot \boldsymbol{k} = 0$. Then we compute the

induced metric σ of a 2-surface space spanned by the vectors ∂_θ and ∂_χ [40]. The general 3-surface element for a null horizon, normal to the inward radial direction, is given by

$$\mathrm{d}\Sigma_\mu = \tilde{\mathrm{l}}_\mu \left(\sqrt{\det\sigma}\,\mathrm{d}\theta\,\mathrm{d}\chi\right)\mathrm{d}v = \tilde{\mathrm{l}}_\mu\, 2Mr_+ \sin\theta\,\mathrm{d}\theta\,\mathrm{d}\varphi\,\mathrm{d}t\,, \tag{3.74}$$

where $\det\sigma = g_{\theta\theta}\,g_{\chi\chi} - (g_{\theta\chi})^2$. In the last equality we used the fact that the jacobian $\partial(v,\chi)/\partial(t,\varphi) = 1$. The resultant energy flux going inside the BH is then computed by

$$\frac{\mathrm{d}^2E_{\rm hole}}{\mathrm{d}t\mathrm{d}\Omega} = 2Mr_+T_{\mu\nu}\tilde{\mathrm{l}}^\mu k^\nu \qquad (r=r_+)\,. \tag{3.75}$$

Generalizing Eq. (3.67), we may define the the flow of angular momentum using the axisymmetic Killing vector, $\mathrm{d}L = -T^\mu{}_\nu\, m^\nu\,\mathrm{d}\Sigma_\mu$, and combining previous results to write

$$\frac{\mathrm{d}^2E_{\rm hole}}{\mathrm{d}t\mathrm{d}\Omega} - \Omega_H\frac{\mathrm{d}^2L_{\rm hole}}{\mathrm{d}t\mathrm{d}\Omega} = 2Mr_+T_{\mu\nu}\,\tilde{\mathrm{l}}^\mu\tilde{\mathrm{l}}^\nu \qquad (r=r_+)\,. \tag{3.76}$$

The computation of the flow of the energy into the BH requires finding the ratio between the energy and angular momentum carried by waves. For a scalar wave $\Phi \sim e^{-i\omega t+im\varphi}$, we can easily find the ratio by computing $\mathrm{d}L/\mathrm{d}E = -T^r{}_\varphi/T^r{}_t = -\partial_\varphi\Phi/\partial_t\Phi = m/\omega$, using the standard scalar energy-stress tensor [28]. Another simpler argument was made in (2.35), obtaining the same result. Since this ratio holds for any type of perturbation [30],

$$\frac{\mathrm{d}^2E_{\rm hole}}{\mathrm{d}t\mathrm{d}\Omega} = \frac{2Mr_+\omega}{\omega - m\Omega_H}\tilde{\phi}_0\tilde{\phi}_0^* = \frac{\omega}{8Mr_+\kappa}|\Delta\phi_0|^2 \qquad (r=r_+)\,. \tag{3.77}$$

Double projection of the future-directed inward vector $\tilde{\mathrm{l}}$ onto the energy-stress tensor gives us $|\tilde{\phi}_0|^2$, due to the decomposition (3.69). At the horizon, the boosted NP scalar can be written as $\tilde{\phi}_0 = (\Delta\phi_0)/(4Mr_+)$, where $\Delta\phi_0$ is regular at the horizon by construction and also by checking with the boundary solution (3.63).

Now, we are prepared to define the amplification factor as

$${}_sZ_{\ell m} = \frac{\mathrm{d}E_{\rm out}/\mathrm{d}t}{\mathrm{d}E_{\rm in}/\mathrm{d}t} - 1\,, \tag{3.78}$$

where we integrated over the solid angle. The factor is defined as the overall gain/loss effect for each mode (ω,ℓ,m), therefore it measures how much of the wave was *globally* reflected (${}_sZ_{\ell m} = 0$), absorbed (${}_sZ_{\ell m} < 0$) or amplified (${}_sZ_{\ell m} > 0$). Assuming a single

mode decomposition and remebering that $\phi_2 = \Phi_2/(2\bar{\rho}^2) \sim {}_{-1}R_{\ell m}/(2r^2)$, we show that

$$ {}_{\pm1}Z_{\ell m} + 1 = \left| \frac{\lim_{r\to\infty}(\frac{1}{r}\,{}_{-1}R_{\ell m})}{\lim_{r\to\infty}(r\,{}_{+1}R_{\ell m})} \right|^2 = \left| \frac{A_{\rm out}(s=-1)}{A_{\rm in}(s=+1)} \right|^2 \equiv \left| \frac{\mathcal{Z}_{\rm out}}{\mathcal{Y}_{\rm in}} \right|^2 , \tag{3.79} $$

Naturally, in order to give use to the D/C ratio from the matching of coefficients, we need to obtain the ratio $A_{\rm out}/A_{\rm in}$ for the same spin weight. We redefine these constants in Table 3.2. Using Eq. (3.32), we can relate the *ingoing* integration constants from both

	$\omega r \gg 1$	$\omega r \ll 1$
${}_1R_{\ell m}$	$\mathcal{Y}_{\rm in}\,\dfrac{e^{-i\omega r_*}}{r} + \mathcal{Y}_{\rm out}\,\dfrac{e^{i\omega r_*}}{r^3}$	$\mathcal{Y}_{\rm hole}\,\Delta^{-1}e^{-i\kappa r_*}$
${}_{-1}R_{\ell m}$	$\mathcal{Z}_{\rm in}\,\dfrac{e^{-i\omega r_*}}{r} + \mathcal{Z}_{\rm out}\,r\,e^{i\omega r_*}$	$\mathcal{Z}_{\rm hole}\,\Delta\,e^{-i\kappa r_*}$

TABLE 3.2: Radial function solutions (ϕ_0 and ϕ_2) for near-horizon and far-horizon approximations

ϕ_0 and ϕ_2. In the large r limit, this equation is simplified into $(\partial_r - i\omega)(\partial_r - i\omega)\,{}_{-1}R_{\ell m} \sim \mathcal{B}\,({}_{+1}R_{\ell m})$, and considering terms only up to $\mathcal{O}(\frac{1}{r})$ we substitute $\mathcal{Y}_{\rm in}$ [30],

$$ {}_{\pm1}Z_{\ell m} + 1 = \frac{\mathcal{B}^2}{16\omega^4}\left|\frac{\mathcal{Z}_{\rm out}}{\mathcal{Z}_{\rm in}}\right|^2 , \tag{3.80} $$

where now the expression is only using $s=-1$ coefficients. Still, the amplification should not depend on the sign of spin-weight, *i.e.* the amplification should be the same for all EM waves, the same holding true for GW perturbations. The *in-out* ratio is given by

$$ \begin{aligned} \frac{\mathcal{B}^2}{16\omega^4}\left|\frac{\mathcal{Z}_{\rm out}}{\mathcal{Z}_{\rm in}}\right|^2 &= \frac{\mathcal{B}^2}{\ell^2(\ell+1)^2}\left|\frac{1+\frac{(-1)^{\ell+1}}{2}\frac{D}{C}\frac{\Gamma(\ell)\Gamma(\ell+2)}{\Gamma(2\ell+1)\Gamma(2\ell+2)}(2i\bar{\omega})^{2\ell+1}}{1-\frac{(-1)^{\ell+1}}{2}\frac{D}{C}\frac{\Gamma(\ell)\Gamma(\ell+2)}{\Gamma(2\ell+1)\Gamma(2\ell+2)}(2i\bar{\omega})^{2\ell+1}}\right|^2 \\ &\simeq 1 - (2\bar{\omega})^{2\ell+1}\frac{\Gamma(\ell)\Gamma(\ell+2)}{\Gamma(2\ell+1)\Gamma(2\ell+2)}\,\mathrm{Re}\left\{2i\,\frac{D}{C}\right\} , \end{aligned} \tag{3.81} $$

where we approximated the relative normalization $\mathcal{B} = \lambda\!\!\!^{-} + \mathcal{O}(a\omega) = \ell(\ell+1) + \mathcal{O}(a\omega)$, by considering a small deviation from spherical symmetry.

The D/C ratio has a non-trivial expression in terms of Γ functions of non-integers arguments. The factorial property of Γ allows the approximation ($y = -2i\varpi/\tau$)

$$ \frac{\Gamma(\ell+1-s+y)}{\Gamma(-\ell-s+y)} = \prod_{n=-\ell-s}^{\ell-s}(n+y) \underset{(s=\pm1)}{\simeq} (-1)^{\ell+1}\frac{\ell+1}{\ell}\,y\prod_{n=1}^{\ell}(n^2-y^2)\,. \tag{3.82} $$

Combining all results, the amplification factor for EM perturbations yields

$$ {}_{\pm1}Z_{\ell m} \simeq -4\bar{\omega}(\bar{\omega} - m\bar{\Omega}_H)\,(2-\tau)(2\bar{\omega}\tau)^{2\ell}\left[\frac{(\ell-1)!(\ell+1)!}{(2\ell)!(2\ell+1)!}\right]^2 \prod_{n=1}^{\ell}\left(n^2 + \frac{4\varpi^2}{\tau^2}\right) . \quad (3.83) $$

A very similar expression can be obtained for GW perturbations (see e.g. [38]). The validity of this result is mainly based on the overlapping of the far-region and near-region solutions. When the BH is extremal, $\tau = 0$, the factor is regular and proportional to ${}_{\pm1}Z_{\ell m} \propto -(4\varpi\bar{\omega})^{2\ell+1}$, while the amplification occurs mostly when $\ell = m = 1$, due to the dampening of the quickly growing factorials in the denominator of ${}_{\pm1}Z_{\ell m}$.

We know that the EM fields must be real quantities, therefore physical waves must also include negative valued ω in the mode decomposition (3.37). The amplification factor explicity demonstrates that superradiance occurs when

$$ \omega(\omega - m\Omega_H) < 0 . \quad (3.84) $$

For $\omega > 0$, amplification occurs for $m > 0$ modes, in the region (1.1), while for $\omega < 0$, only modes with $m < 0$ can be amplified. The circular symmetry of the spacetime garantees that superradiance phenomena is invariant under the change of $(\omega, m) \to (-\omega, -m)$. In other other words,

$$ {}_sZ_{\ell,-m}(-\omega) = {}_sZ_{\ell m}(\omega) , \quad (3.85) $$

which is clear from the EM case in (3.83).

Chapter 4

Numerical methods

In this chapter will will develop the necessary method to compute the gain/loss factor, using Mathematica™. We will go beyond the spherical approximation and calculate the SWSHs eigenvalues for any BH angular momentum. With the eigenvalue defined for a particular mode, we will compute the asymptotic radial coefficients, which in turn are used to compute the amplification factor in three different ways.

4.1 Angular Eigenvalues

The need for obtaining the angular eigenvalues ${}_s\mathcal{E}_{\ell m}$ rests on the dependency to solve the radial equation numerically with no spherical approximation. Additionally, the relative normalization constant $\mathcal{B}$, which depends explicitly on the eigenvalue, will be rather important in one of the methods used to calculate the gain/loss factor ${}_sZ_{\ell m}$ for each mode (ω, ℓ, m). There is no reason to differentiate the eigenvalue for given BH angular momentum and a particular frequency, since the relevant parameter for the eigenvalues is $c = a\omega$. Focusing on superradiant modes and on the lowest multipoles we only will need eigenvalues for small values of c, e.g. $0 < c < 3$. Even for extremal BHs, the typical frequency value for the leading superradiant mode is $\bar{\omega} \sim 1/2$, so this margin is sufficient even for observing the effects in non-superradiant modes. Due to the circular symmetry, ${}_s\mathcal{E}_{\ell,-m}(c) = {}_s\mathcal{E}_{\ell m}(-c)$, instead of computing for negative values of c, we will consider all integer azimuthal numbers $|m| \leq \ell$.

4.1.1 Leaver method

The first method implemented was Leaver's [34]. This method consists is using the three-term recursion relation obtained for SWSHs and correspondent continued fraction (3.48) and its inversions. Since the problem is now numerical, we have to stop the continued fraction at some particular $p = N$. By substitution of the parameters s and m and c, we are left with an equation with N roots for ${}_s\mathcal{E}_{\ell m}$. A root-finding algorithm is a method that allows to approximate roots of some equation $f(x) = 0$, by suggestion of a connected region were f has different signs at the boundary. The method "FindRoot" in Mathematica™ allows to distinguish the roots of an equation by finding the closest to a particular input value. Firstly, we use the the expansion coefficients for $c \ll 1$ (Appendix D) to suggest a value of the eigenvalue ${}_s\mathcal{E}_{\ell m}$ that is close to $\ell(\ell+1)$. We improved on this method by starting the curve at $c = 0$, and then obtaining the eigenvalue numerically for small increments in c and then using the last eigenvalue solution as the initial guess for the next increment. This is particularly useful to generate and save a complete table of eigenvalues for take given range and then use interpolation methods to guess eigenvalues for intermediate c values.

For both methods the obtained curves are well behaved for $\ell = 1$, but for bigger ℓ we start to observe some discontinuities, especially when we increase the range of c. For a

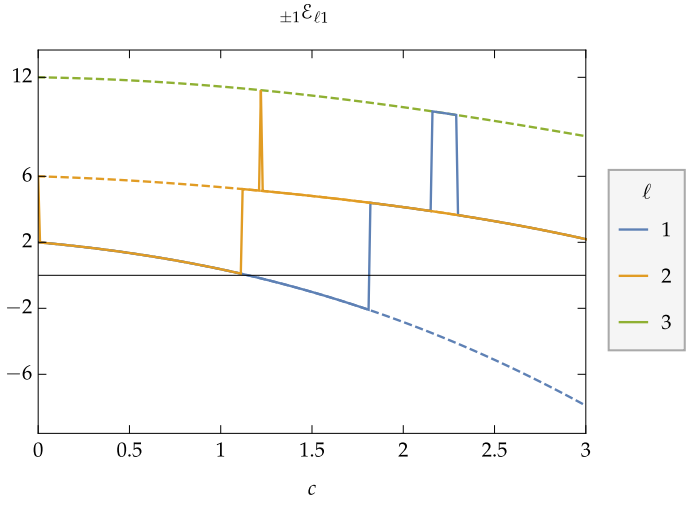

FIGURE 4.1: Showcasing discontinuities in the values of ${}_{\pm1}\mathcal{E}_{\ell1}$ for $m = 1, 2$ when using an incorrect implementation of the Leaver method. Real values of the eigenvalues are shown as dashed lines ($m = 1, 2, 3$) of the same color.

fixed s and m, we have an infinite number of curves labeled by ℓ and in some cases the root finding algorithm selects roots from adjacent curves, either from the branch $\ell - 1$, $\ell + 1$

or even distant values. These solutions cannot ever intersect, otherwise the eigenvalue would be degenerate and the SWSHs would not be a orthogonal basis of functions. The issue rests on the lack of accuracy when identifying of the ℓ-th root. We lose accuracy when trying to obtain roots on levels further down in the continued fraction. We solve the problem by considering the inversion (3.49), choosing $r = \ell + \max\{|m|, |s|\}$, as the main information in the value taken by the ℓ-th root is in the β_r coefficient, with the continuous fractions providing higher order contributions in c.

Once the eigenvalue root is known, one can find any number of the series expansions coefficients a_p, for a particular eigenfunction (3.45), by using the three-coefficient recursion relation (3.46).

4.1.2 Spectral method

Due to initial problems with the Leaver method, we decided to use the spectral method [41], since the spheroidal Eq. (3.39) can be seen as a perturbed version of the spherical case, $c = 0$. We may rewrite the equation using three operators depending on their order in c,

$$(\mathcal{H}^{(0)} + \mathcal{H}^{(1)} + \mathcal{H}^{(2)})_s S_{\ell m} = -_s\mathcal{E}_{\ell m}\ {}_s S_{\ell m} \tag{4.1}$$

The zeroth order operator, $\mathcal{H}^{(0)}$, defines the eigenvalue problem for the spin-weighted spherical harmonics, which will provide the complete non-perturbed basis, $\mathcal{H}^{(0)}\,{}_sY_{\ell m} = -\ell(\ell+1)\,{}_sY_{\ell m}$. The other two operators are quickly identified from the angular equation as $\mathcal{H}^{(1)} = -2sc\cos\theta$ and $\mathcal{H}^{(2)} = c^2\cos^2\theta$. Simple perturbation theory [32] states that

$$\begin{aligned} {}_s\mathcal{E}_{\ell m} &= \ell(\ell+1) - \int \mathrm{d}\Omega\,({}_sY_{\ell m})^*\,\mathcal{H}^{(1)}\,{}_sY_{\ell m} + \mathcal{O}(c^2)\,, \\ {}_sS_{\ell m} &= {}_sY_{\ell m} - \sum_{j\neq\ell} \frac{\int \mathrm{d}\Omega\,({}_sY_{jm})^*\,\mathcal{H}^{(1)}\,{}_sY_{\ell m}}{j(j+1)-\ell(\ell+1)}\,{}_sY_{jm} + \mathcal{O}(c^2)\,. \end{aligned} \tag{4.2}$$

We may include $\mathcal{H}^{(2)}$ by using a higher order expansion, which can be found in any Quantum Mechanics textbook. The integrals $\int \mathrm{d}\Omega\,({}_sY_{jm})^*\,\mathcal{H}^{(1)}\,{}_sY_{\ell m}$ and $\int \mathrm{d}\Omega\,({}_sY_{jm})^*\,\mathcal{H}^{(2)}\,{}_sY_{\ell m}$ may be computed using Clebsch-Gordon coefficients decomposition generalized for spin-weighted harmonics (C.11). These operators can be written in terms of general matrix

elements in the basis of spin-weighted spherical harmonics [42],

$$\begin{aligned} h^{(1)}_{j\ell} &= \int \mathrm{d}\Omega\, \cos\theta\, ({}_sY_{jm})^*\, {}_sY_{\ell m} = \sqrt{\frac{2\ell+1}{2j+1}}\langle \ell, m; 1, 0|j, m\rangle \langle \ell, -s; 1, 0|j, -s\rangle\ , \\ h^{(2)}_{j\ell} &= \int \mathrm{d}\Omega\, \cos^2\theta\, ({}_sY_{jm})^*\, {}_sY_{\ell m} = \frac{\delta_{j\ell}}{3} + \frac{2}{3}\sqrt{\frac{2\ell+1}{2j+1}}\langle \ell, m; 2, 0|j, m\rangle \langle \ell, -s; 2, 0|j, -s\rangle\ , \end{aligned} \tag{4.3}$$

remembering that $\cos\theta$ and $\cos^2\theta$ can be rewritten using ${}_0Y_{10}(\theta,\varphi)$ and ${}_0Y_{20}(\theta,\varphi)$. The first integral is proportional to the Leaver series coefficient f_1 defined in Appendix D.

Perturbation theory shows that the SWSHs can be expanded in terms of spherical harmonics. This should not be a surprising fact as any angular function $f(\theta,\varphi)$ with a particular spin-weight can be represented using a decomposition using spin-weighted spherical harmonics. Having this idea in mind, we write

$${}_sS_{\ell m}(c;\theta,\varphi) = \sum_j b^{(\ell)}_j\, {}_sY_{jm}(\theta,\varphi) \qquad \Big(\ell, j \geq \max\{|s|,|m|\}\Big)\ . \tag{4.4}$$

Replacing the expansion in Eq. (4.1), we can take advantage of the orthogonality of the harmonics, $\int \mathrm{d}\Omega\, ({}_sY_{jm})^*\, {}_sY_{\ell m} = \delta_{\ell j}$, by multiplying the the equation by $({}_sY_{\ell m})^*$ and integrating the solid angle. The angular equation is replaced by an eigenvalue matrix equation $\sum_j a_{ij}\, b^{(\ell)}_j = -{}_s\mathcal{E}_{\ell m}\, b^{(\ell)}_i$, such that

$$a_{ij} = \begin{cases} c^2\, h^{(2)}_{ii} - 2sc\, h^{(1)}_{ii} - i(i+1) & i = j \\ c^2\, h^{(2)}_{ij} - 2sc\, h^{(1)}_{ij} & |i-j| = 1 \\ c^2\, h^{(2)}_{ij} & |i-j| = 2 \\ 0 & \text{otherwise} \end{cases} \qquad \Big(i, j \geq \max\{|s|,|m|\}\Big)\ , \tag{4.5}$$

where the the eigenvalues of this matrix are $-{}_s\mathcal{E}_{\ell m}$ and the correspondent eigenvector is given by $b^{(\ell)}_j$.

Like the Leaver method, we will have to truncate the matrix at some finite size. From Eq. (4.5), we know that the zeroth order contribution to the ℓ-th eigenvalue will be the element $a_{\ell\ell}$. We opted to implement a $N \times N$ centered submatrix such that $i, j \geq \ell_{\min} \equiv \max\{|s|,|m|\}$ and truncating the matrix at $N > \ell + 1 - \ell_{\min}$, in order to include the $a_{\ell\ell}$ terms in the approximation. In reality, we must implement a variable $N \equiv N(c)$, so that it increases the size of the taken submatrix in order to include extra corrections for larger values of c. The size of the submatrix also increases linearly with ℓ. The best way to

approximate ${}_s\mathcal{E}_{\ell m}$ would be to not construct the submatrix including all values of $\ell_{\min}$ but instead to center the submatrix at $a_{\ell\ell}$ and increase its size to fine-tune the eigenvalue. Since we will take very large ℓ values, we will use the first method for simplicity.

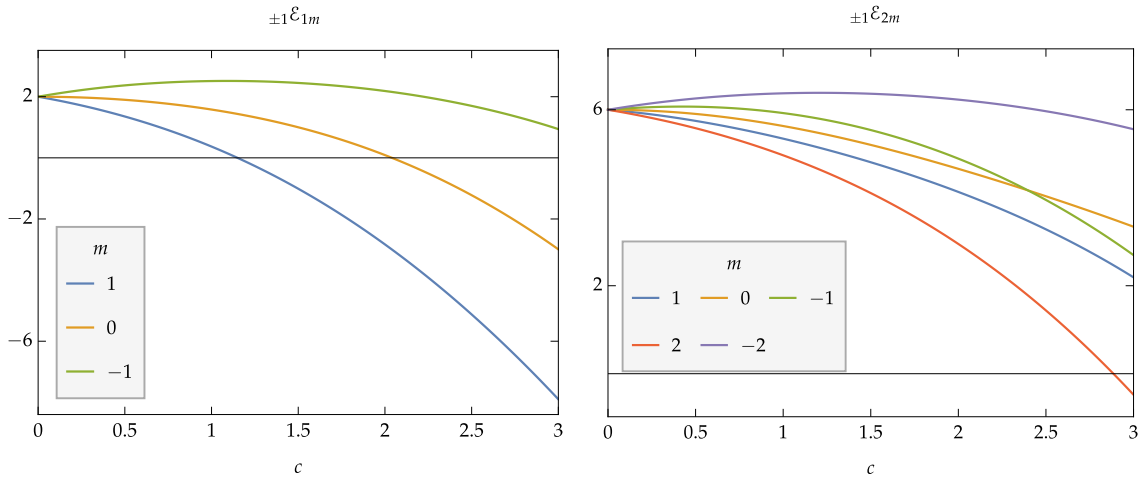

FIGURE 4.2: Eigenvalues for $\ell = 1$ (left) and $\ell = 2$ (right) for typical values of c, using the spectral method.

Optimized numerical methods allow for fast computation of the eigenvalues and eigenvectors of a band-diagonal matrix. The "Eigensystem" method found in Mathematica™ returns an array of eigenvalues and their correspondent normalized eigenvectors, guaranteeing Eq. (3.43). Since the result is a positively sorted list of $-{}_s\mathcal{E}_{\ell m}$, with $0 \leq \ell - \ell_{\min} \leq N - 1$, of which we need to select the negative of the $(N - \ell + \ell_{\min})$-th element. We show EM eigenvalues form lower ℓ values in Figure 4.2. This procedure also returns correct

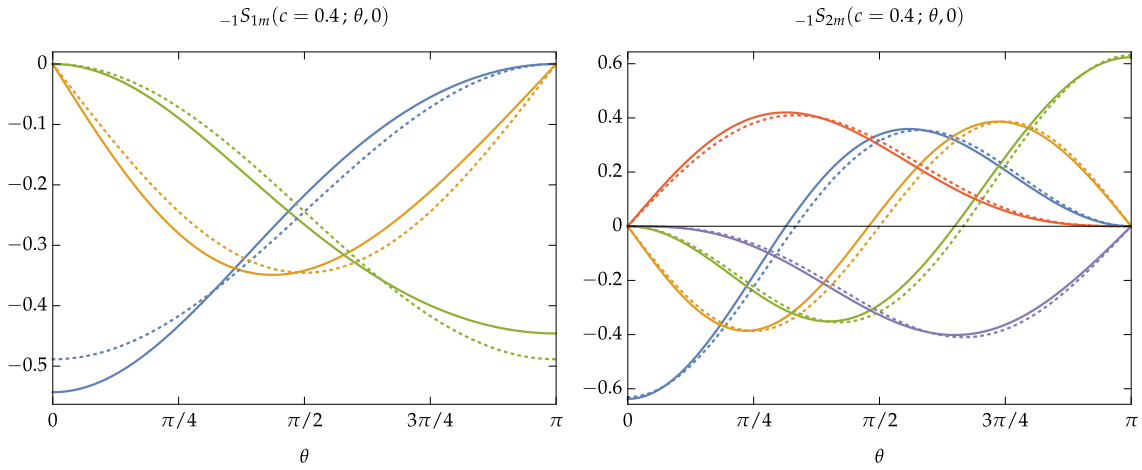

FIGURE 4.3: Plots of all spin-weighted spheroidal harmonics ${}_{-1}S_{\ell m}(\theta, 0)$ with $\ell = 1$ (left) and $\ell = 2$ (right) for $s = -1$ and $c = 0.4$. This plot shares the same legend coloring as the above (Figure 4.2). Dotted curves represent the values of the ${}_{-1}Y_{\ell m}$, when $c \to 0$.

eigenvectors for approximating the eigenfunction using (4.4). In order to ensure that the SWSHs have the same phase convections of their spherical counterparts, we must ensure that the correspondent eigenvector has $b_\ell^{(\ell)} > 0$, by mapping the obtained vector components as $b_j^{(\ell)} \mapsto \mathrm{sgn}(b_\ell^{(\ell)})\, b_j^{(\ell)}$. This process is computationally more stressful, since it requires computing and combining N different spherical harmonics with the same s and m. In the superradiance range, the values of c can be small $\left(< \frac{1}{2}|m|\right)$, therefore the SWSHs may not differ greatly from ${}_sY_{\ell m}(\theta, \varphi)$, with smaller deviations as ℓ increases (e.g. see Figure 4.3). In this regime, we may the use pure spin-weighted spherical harmonics as approximations, as they do not change the qualitative behaviour of the ${}_sS_{\ell m}(\theta, \varphi)$.

4.2 Amplification factor

Finding non-approximate forms to the amplification factor ${}_{\pm1}Z_{\ell m}$ requires the numerical solving of the radial Eq. (3.53), which is already in an adimensional form. We computed the angular eigenvalues beforehand, which depend on the mode (ℓ, m) as well as the coupling $c = a\omega$. Additionally the equation depends on the BH parameters (M, J) and ω explicitly, but it is possible to normalize all variables so that we only need to specify $(\mathcal{J}, \ell, m, \bar{\omega})$, where $\mathcal{J} = a/M = J/M^2$. We choose to work with barred frequencies because $\bar{\Omega}_H = \mathcal{J}/2$, which makes it easier to numerically select superradiant modes.

We need to obtain numerical interpolations for ${}_{\pm1}R_{\ell m}$, by integrating the solution outwards from the horizon, at $x = 0$, up to a sufficiently large $x_\infty \gg |\bar{\omega}|^{-1}$. The solutions for $s = \pm 1$ contain the all the EM field information, but they have different asymptotic behaviors. For ϕ_0, Eq. (3.59) tells us that the ingoing coefficient tends to overshadow the outgoing coefficient, while the opposite occurs for ϕ_2. This way seems natural to try to solve both equations, where we can obtain $\mathcal{Y}_{\mathrm{in}}$ and $\mathcal{Z}_{\mathrm{out}}$ separately (Table 3.2).

Knowing the irregularities of the solution at the horizon, we propose the ansatz

$$ {}_{\pm1}R_{\ell m} = (r_+)^{\mp1}\, x^{\mp1 - i\bar{\omega}/\tau} f_\pm(x)\,, \tag{4.6} $$

where $f(x)$ is a new function that obeys a regular second-order differential equation. Thus we need to set two initial conditions at the horizon, $f_\pm(0)$ and $f_\pm'(0)$. We expect to $|f_\pm(x)|$ to become approximately constant at large x, because this form is written in way a that also matches the behavior of the radial function at infinity, ${}_{\pm1}R_{\ell m} \sim r^{\mp1}$.

Comparing Eq. (4.6) with the asymptotic form at large x as well as near the horizon form, we obtain

$$\begin{aligned} r_+\tau\,\frac{\mathcal{Y}_{\rm in}}{\mathcal{Y}_{\rm hole}} &= \frac{f_+(x_\infty)}{f_+(0)}\exp\left[-i\bar{\omega}x_\infty - i\bar{\omega}(2-\tau)\log(x_\infty) - i\frac{\varpi}{\tau}\log(x_\infty)\right]\,, \\ \frac{1}{r_+\tau}\,\frac{\mathcal{Z}_{\rm out}}{\mathcal{Z}_{\rm hole}} &= \frac{f_-(x_\infty)}{f_-(0)}\exp\left[+i\bar{\omega}x_\infty + i\bar{\omega}(2-\tau)\log(x_\infty) - i\frac{\varpi}{\tau}\log(x_\infty)\right]\,. \end{aligned} \tag{4.7}$$

If both solutions are normalized such that $f_\pm(0) = 1$, then we have to deal with the relative normalization of $\mathcal{Z}_{\rm hole}/\mathcal{Y}_{\rm hole}$ [30]. We can obtain such ratio in terms of known parameters by considering Eq. (3.32) at $x \simeq 0$,

$$(r_+\tau)^2\,\frac{\mathcal{Z}_{\rm hole}}{\mathcal{Y}_{\rm hole}} = -\frac{\mathcal{B}\tau^2}{2\varpi(i\tau+2\varpi)}\,. \tag{4.8}$$

Therefore to compute the amplification factor we use ($f_\pm(0)=1$)

$${}_{\pm1}Z_{\ell m} = \frac{\mathcal{B}^2\tau^4}{4\varpi^2(\tau^2+4\varpi^2)}\left|\frac{f_-(x_\infty)}{f_+(x_\infty)}\right|^2 - 1\,. \tag{4.9}$$

Another way of dealing with the relative normalization would be to select different initial conditions at the horizon $x = 0$. We could cancel the relative normalization of $\mathcal{Z}_{\rm hole}/\mathcal{Y}_{\rm hole}$ if we set any normalization that results in $f_-(0)/f_+(0) = -\mathcal{B}\tau^2/[2\varpi(i\tau + 2\varpi)]$, eliminating the dependence on $\mathcal{B}$, τ, ϖ in Eq. (4.9).

The differential equation obtained from substituting (4.6) into Eq. (3.53) is identically zero for $x = 0$. Therefore, no matter what initial conditions set for $f_\pm{}'$, the system would not evolve due to stiffness, which makes the step size of the integrator effectively zero. The usual solution for stiff differential equations is to start the solver at a small distance from the horizon $\epsilon > 0$. We adjust the initial conditions by substituting the series expansion of $f_\pm(x) = \sum_{n=0}^{N_H} a_n x^n$ in the radial equation, discarding terms higher than $\mathcal{O}(x^{N_H})$ and obtaining the coefficients $a_n \propto a_0$, $1 \leq n \leq N_H$, like is done in [38]. Therefore we may set the initial conditions as

$$f_\pm(\epsilon) = f_\pm(0)\sum_{n=0}^{N_H}\left(\frac{a_n}{a_0}\right)\epsilon^n\,, \qquad f_\pm{}'(\epsilon) = f_\pm(0)\sum_{n=1}^{N_H}\left(\frac{a_n}{a_0}\right)\epsilon^n\,, \tag{4.10}$$

where $f_\pm(0) = 1$ are the original horizon conditions considered. We found $\epsilon = 10^{-12}$, $N_H = 6$ and $x_\infty = 200\times 2\pi/|\bar{\omega}|$ working perfectly for the "NDSolve" integrator. Effectively we will have $|f_\pm{}'(\epsilon)| \simeq \epsilon$, but this contribution is sufficient to remove stiffness from

the system and has important contributions in the case of extremal BHs ($\mathcal{J} \to 1$).

This previous method requires us to call the integrator twice which is not very effective numerically. Exploring the conservation of the Wronskian (conserved current) of Eq. (3.56), we can obtain [30]

$$\frac{\mathrm{d}E_{\mathrm{in}}}{\mathrm{d}t} - \frac{\mathrm{d}E_{\mathrm{out}}}{\mathrm{d}t} = \frac{\mathrm{d}E_{\mathrm{hole}}}{\mathrm{d}t} \,, \tag{4.11}$$

which simply states total energy conservation. Therefore we can rewrite Eq. (3.78) using only the *hole-in* ratio, thus we are able to get the amplification factor with just with the $s = +1$ solution,

$$_{\pm 1}Z_{\ell m} = -\frac{\bar{\omega}\tau^2}{\varpi}\left|\frac{f_+(0)}{f_+(x_\infty)}\right|^2 \,. \tag{4.12}$$

If we use the *out-hole* ratio in the amplification factor we only need to solve for $s = -1$,

$$_{\pm 1}Z_{\ell m} = -\left(1 + \frac{\mathcal{B}^2\tau^2}{4\bar{\omega}\varpi(\tau^2 + 4\varpi^2)}\left|\frac{f_-(x_\infty)}{f_-(0)}\right|^2\right)^{-1} \,. \tag{4.13}$$

For the mode $\ell = m = 1$ at $\mathcal{J} = 0.9999$, we obtain the maximum amplification of about 4.36% for a frequency of about $\omega M \simeq 0.436$. Modes in the region (3.84) have always $_{\pm 1}Z_{\ell m} > 0$, but the amplification factor decreases quickly as ℓ increases (Figure 4.6). For frequencies where $|\omega| > |m\Omega_H|$, we obtain that the value of $_{\pm 1}Z_{\ell m} \to -1$. This in no

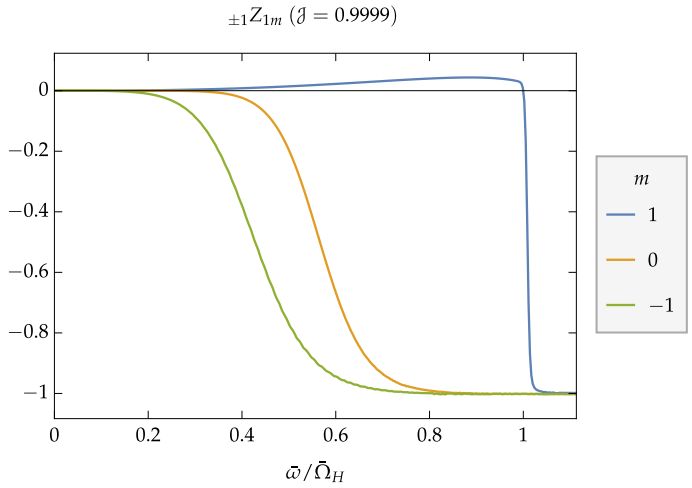

FIGURE 4.4: Amplification factor of an extremal BH ($\mathcal{J} = 0.9999$) for modes with $\ell = 1$. In this figure, superradiance occurs only for $m = 1$ as predicted.

surprising fact because as ω increases so does the ingoing wave energy. Therefore when

crossing the superradiant threshold the wave possesses enough energy to cross the V_{eff} barrier, being absorbed by the BH.

Thus we have three ways of computing ${}_{\pm1}Z_{\ell m}$, but only two of them are independent. We rename these different forms in Eqs. (4.12), (4.13), (4.9) as $Z^{(1)}$, $Z^{(2)}$, $Z^{(3)}$, respectively. We can rearrange the RHS of the expressions so that we have

$$Z^{(3)} = Z^{(1)}\left[1 + \frac{1}{Z^{(2)}}\right] - 1\,. \tag{4.14}$$

It is expected that if the amplification factors based only on a single solution for ϕ_0 or ϕ_2 are approximately equal, then the same would be true when considering $Z^{(3)}$, which uses both solutions. However, from a closer look at Figure 4.5 we can see that this is not true, especially for higher values of ℓ. Somehow it appears that we are not able to compute the

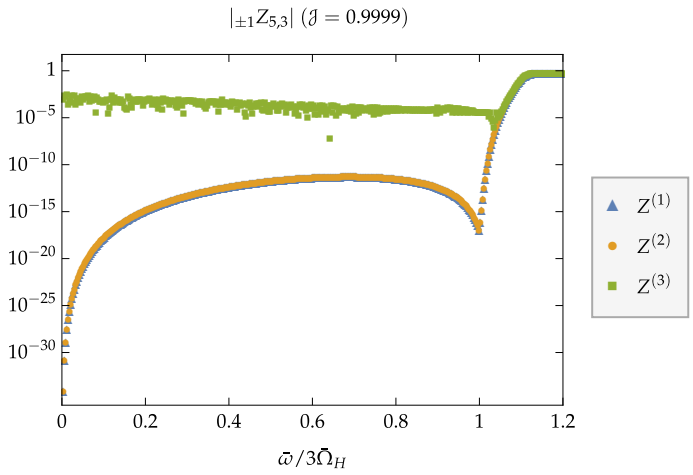

FIGURE 4.5: Log plot demonstrating error propagation for ${}_{\pm1}Z_{53}$ when computing the factor using both numerical solutions for the radial part of ϕ_0 and ϕ_2.

ratio of $\mathcal{Y}_{\text{in}}$ and $\mathcal{Z}_{\text{out}}$ with enough accuracy, probably because the large values that $f_{\pm}(x_\infty)$ take do not hold the necessary precision to compute their ratio accurately.

To better understand this, let us choose a superradiant frequency. For larger values of ℓ (with small m) the gain/loss factor is practically zero. Still we have huge differences in the order of magnitude of the amplification factor when comparing results from using only one solution and using both. Since two different equations are numerically solved, there will always be a discrepancy due to the independent numerical solutions, $Z^{(2)} = Z^{(1)}(1+\eta)$, with η very small. The problem is that this error is propagated in absolute value, $Z^{(3)} \simeq Z^{(1)} - \eta$. For example, when $(\mathcal{J}, \ell, m, \bar{\omega}) = (0.9999, 5, 3, 0.1)$ we have $\eta \simeq -0.003$ and $Z^{(1)} \sim 10^{-20}$, which implies that when using both solutions we have a discrepancy

of a factor of 10^{17}. Therefore we cannot use the expression $Z^{(3)}$ to accurately compute the amplification factor, when we have $\eta \gg Z^{(1)}, Z^{(2)}$.

We further to increase the numerical precision in this problem by considering higher order terms in the asymptotic expansion of Eq. (3.59). Separately, we will substitute both asymptotic series in Eq. (3.53), one for the ingoing part and another for the outgoing [15]. Together they have the form

$$ {}_{-1}R_{\ell m}(r) = e^{-i\bar{\omega}x}\, x^{-1-i(2-\tau)\bar{\omega}} \sum_{n=0}^{N_\infty} I_n\, x^{-n} + e^{-i\bar{\omega}x} x^{1+i(2-\tau)\bar{\omega}} \sum_{n=0}^{N_\infty} O_n\, x^{-n}\,, \tag{4.15} $$

where we identify $I_0\, r_+ = \mathcal{Z}_{\rm in}/\mathcal{Z}_{\rm hole}$ and $O_0/r_+ = \mathcal{Z}_{\rm out}/\mathcal{Z}_{\rm hole}$. Although we have chosen the $s = -1$ solution, the same procedure can be done for $s = +1$, because when using a higher order expansion, both ingoing and outgoing coefficients are present.

Firstly, we directly substitute the series into Eq. (3.53), neglecting terms above $\mathcal{O}(x^{-N_\infty})$ and grouping the exponentials terms, in order to obtain $I_n \propto I_0$, $O_n \propto O_0$ ($1 \leq n \leq N_\infty$), exactly like the series used above to define boundary conditions at the horizon. Secondly, substitution of the numerical ansatz (4.6) in the LHS of the previous equation, together with its derivative, we have a system of two linear equations, which in the limit of large-x limit allows to determine

$$ \frac{1}{r_+}\frac{\mathcal{Z}_{\rm in}}{\mathcal{Z}_{\rm hole}} = I_0\Big(f_-(x_\infty),\, f_-'(x_\infty)\Big)\,, \qquad r_+\frac{\mathcal{Z}_{\rm out}}{\mathcal{Z}_{\rm hole}} = O_0\Big(f_-(x_\infty),\, f_-'(x_\infty)\Big)\,. \tag{4.16} $$

Lastly, we may use the previous expression (4.11) to compute ${}_{\pm1}Z_{\ell m}$ using only one of the coefficient, instead of using Eq. (3.80). This new method solves some of the precision problems from the initial implementation when using both ϕ_0 and ϕ_2, for a smaller $x_\infty = 80 \times 2\pi/|\bar{\omega}|$ and $N_\infty = 10$, with the same $\epsilon = 10^{-12}$.

A similar method is implemented in [15], which is very similar with the obtained results. These are very similar to those of Teukolsky [32]. By identifying the source of the problem as the error propagation in expression (4.9), we are now aware that we must use definitions of ${}_{\pm1}Z_{\ell m}$ that have either *in* or *out* coefficient. Therefore we are able to obtain result with more precision and less noise compared to data originated from other methods (e.g. compare with [15]).

In Figure 4.6, we have the logarithm-scaled plot of the amplification factor for different superradiant modes. We can infer that ${}_{\pm1}Z_{\ell m}$ decreases in order of magnitude as ℓ increases. Therefore the mode with the highest amplification factor is $\ell = m = 1$, we

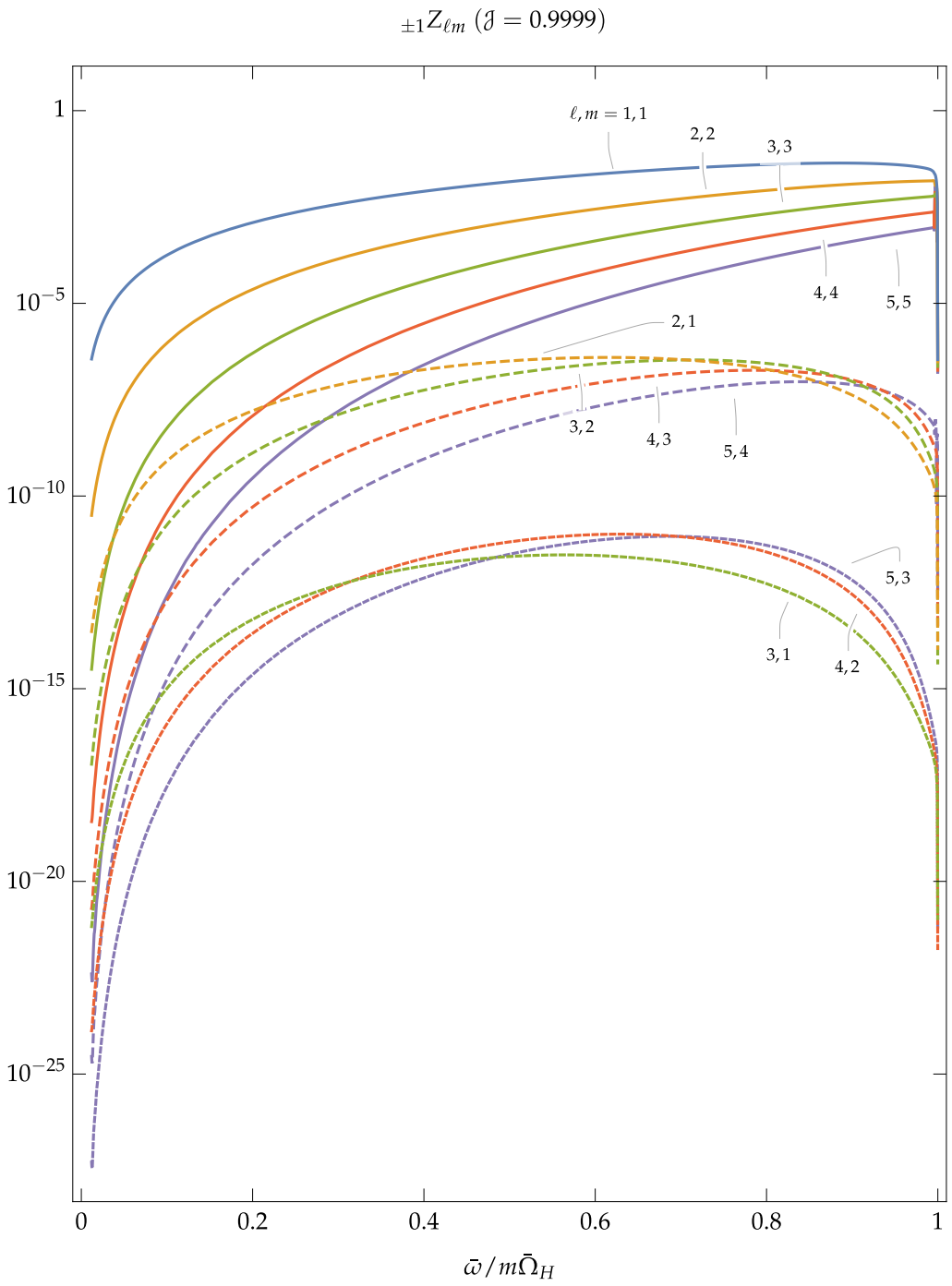

FIGURE 4.6: Log plot of $_{\pm 1}Z_{\ell m}$ as a function of $\bar{\omega}/m\bar{\omega}_H$ [32]. Each color represents the same value of ℓ, while different dashing corresponds to grouping the modes as $|\ell - m| = 0, 1, 2$.

is plotted in detail in Figure 4.4. This particular plot reveals information which most relevent when considering a wave which is a superposition of harmonic modes.

Chapter 5

Superradiant scattering of plane waves

The result of EM and gravitational radiation amplification was a surprising prediction of Einstein's theory of gravitation in the Kerr geometry. A method for direct or indirect observation of this process would provide a probe of rotating BHs and thus it would constitute an important test of GR in regions of extreme gravity. We have studied so far under which conditions an EM multipole mode (ω, ℓ, m) can undergo superradiant scattering. We know that each mode will be independently amplified/attenuated as shown above. The challenge is to observationally infer the occurrence of superradiance for a realistic EM wave, which is generically a superposition of superradiant and non-superradiant modes. This chapter will follow closely results worked out in [38].

Having shown that superradiance occurs for small frequencies we need to find astrophysical sources that emit EM waves. Binary systems of rotating neutron stars and BHs may exhibit the necessary conditions for superradiant scattering. These objects, also known as pulsars, possess a strong magnetic field with magnetic dipole moment typically misaligned with the rotation axis. Obviously the magnetic field configuration of a neutron star can be very complicated but its main properties are best described by the *oblique-rotator* model [43], which considers only the leading order in the multipolar expansion, *i.e.* a magnetic dipole moment

$$\mathbf{m}_P = \frac{m_P}{2}\left[e^{-i\omega t}\sin\alpha_S(\hat{\mathbf{x}} \pm i\hat{\mathbf{y}}) + \cos\alpha_S\,\hat{\mathbf{z}}\right] + \text{ c.c. }, \tag{5.1}$$

where ω is the frequency of rotation. The upper (lower) sign corresponds to a neutron

star co-rotating (counter-rotating) with the BH. The moment $\mathbf{m}_P$ makes an angle α_S with the rotation axis, resulting in the precession of the pulsars' magnetic axis, which produces a periodic focused beam of EM radiation. This periodicity is so precise that makes pulsars ideal for measuring time differences in GR tests. Some neutron stars have a millisecond rotation period producing radiation of a few kHz, which is in range of the superradiant frequencies of a typical stellar mass BH.

We will focus on scattering of incident plane waves, which means we will consider a source that is far away from the BH. More specifically, we consider incident plane waves from a magnetic dipole source whose electric and magnetic radiation fields, which are found in standard textbooks [44], are given by

$$\begin{aligned}\mathbf{E} &= \frac{\mu_0}{8\pi}\frac{e^{i\omega|\mathbf{r}-\mathbf{r}_S|}}{|\mathbf{r}-\mathbf{r}_S|}\left(\frac{\mathbf{r}-\mathbf{r}_S}{|\mathbf{r}-\mathbf{r}_S|}\times\frac{\mathrm{d}^2\mathbf{m}_P}{\mathrm{d}t^2}\right) + \text{ c.c.} \\ &\simeq -\frac{\mu_0}{8\pi}\frac{e^{i\omega L}}{L}e^{i\mathbf{k}\cdot\mathbf{r}}\left(\hat{\mathbf{r}}_S\times\frac{\mathrm{d}^2\mathbf{m}_P}{\mathrm{d}t^2}\right) + \text{ c.c.}\,,\end{aligned} \tag{5.2}$$

where $\mathbf{k} = -\omega\hat{\mathbf{r}}_S$ and $L = |\mathbf{r}_S|$ is the distance between the source and the BH. This approximation is valid when $r = |\mathbf{r}|$ is large compared with the radiation wavelength and the physical dimension of the dipole. Additionally, in the last step we require that $r \ll L$. With the similar procedure the magnetic field can be obtain using $\mathbf{B} \simeq -\hat{\mathbf{r}}_S \times \mathbf{E}$. Thus, when sufficiently far away from the dipole the radiation can be seen as plane waves propagating in the direction of $(-\hat{\mathbf{r}}_S) = (\sin\theta_0\cos\varphi_0, \sin\theta_0\sin\varphi_0, \cos\theta_0)$.

5.1 Harmonics decomposition

By projecting the complex representation of $\mathbf{E}$ using the perpendicular directions $\mathbf{e}_{\hat{\theta}_0}$ and $\mathbf{e}_{\hat{\varphi}_0}$, we can obtain the two EM field polarizations,

$$\epsilon_\theta = \frac{\mu_0\, m_P\, \omega^2 \sin\alpha_S}{8\pi}\frac{e^{i\omega L}}{L}e^{\pm i\varphi_0}\cos\varphi_0\,, \qquad \epsilon_\varphi = \pm i\,\frac{\mu_0\, m_P\, \omega^2 \sin\alpha_S}{8\pi}\frac{e^{i\omega L}}{L}e^{\pm i\varphi_0}\,, \tag{5.3}$$

To use results from previous chapters it is convenient to write the EM degrees of freedom using the NP formalism. There is no need for computing both NP scalars, since we know that the result will be very similar. Asymptotically we have $\mathfrak{m} \sim \partial_\theta + i\csc\theta\,\partial_\varphi$, thus we may show that $\phi_0 = (\mathbf{E}+i\mathbf{B})\cdot(\mathbf{e}_{\hat{\theta}} + i\mathbf{e}_{\hat{\varphi}})/\sqrt{2}$ and $2\phi_2 = (\mathbf{E}+i\mathbf{B})\cdot(\mathbf{e}_{\hat{\theta}} - i\mathbf{e}_{\hat{\varphi}})/\sqrt{2}$. Together with the dipole field approximation, this expansion is valid for $r_+ \ll r \ll L$. Following the work done in Chapter 4, we will keep using ϕ_2 as our primary scalar as it

is the indicated for studying outgoing radiation. Thus, we may write

$$\phi_2{}^{(\text{plane})} = -\frac{2\pi i}{3}\left(\epsilon_R\, e^{-i\omega t + i\mathbf{k}\cdot\mathbf{r}} + \epsilon_L^*\, e^{i\omega t - i\mathbf{k}\cdot\mathbf{r}}\right) \sum_{m=-1}^{+1} {}_{-1}Y_{1,m}(\theta_0,\varphi_0)^*\, {}_{-1}Y_{1,m}(\theta,\varphi)\,, \tag{5.4}$$

where $\hat{\mathbf{k}} \equiv (\theta_0, \varphi_0)$ and $\hat{\mathbf{r}} \equiv (\theta, \varphi)$ are the directions of incidence and observation, respectively. This result can be easily obtained by explicitly expanding the harmonics sum. The left and right polarizations are defined as

$$\begin{aligned} \epsilon_R &= \frac{\epsilon_\theta - i\epsilon_\varphi}{\sqrt{2}} = \mp\frac{\mu_0\, m_P\, \omega^2 \sin\alpha_S}{2\sqrt{6\pi}}\frac{e^{i\omega L}}{L}\, {}_{-1}Y_{1,\pm1}(\theta_0,\varphi_0)\,, \\ \epsilon_L^* &= \frac{\epsilon_\theta^* - i\epsilon_\varphi^*}{\sqrt{2}} = \pm\frac{\mu_0\, m_P\, \omega^2 \sin\alpha_S}{2\sqrt{6\pi}}\frac{e^{-i\omega L}}{L}\, {}_{-1}Y_{1,\mp1}(\theta_0,\varphi_0)\,. \end{aligned} \tag{5.5}$$

It may seem that ϕ_2 for a plane wave is approximately describe using only $\ell = 1$ harmonics, but we must not forget the angular dependence in

$$e^{i\mathbf{k}\cdot\mathbf{r}} = 4\pi \sum_{\ell,m} i^\ell j_\ell(\omega r)\, Y_{\ell m}(\theta_0,\varphi_0)^*\, Y_{\ell m}(\theta,\varphi)\,, \tag{5.6}$$

whose decomposition in terms of $s = 0$ spherical harmonics is well-known [44], where $j_\ell(z)$ corresponds to the spherical Bessel function of the first kind. Substituting this expansion into Eq. (5.4) we obtain a superposition of different spin-weight harmonics and after grouping $\hat{\mathbf{k}}$ and $\hat{\mathbf{r}}$ terms these can be expanded using Clebsh-Gordon coefficients.

$$\begin{aligned} \phi_2{}^{(\text{plane})} &= -2\pi\,\epsilon_R\, e^{-i\omega t} \sum_{\ell,m}\left(\sum_{n=\ell-1}^{\ell+1} i^{n+1}\, j_n(\omega r)\, \frac{2n+1}{2\ell+1}\, |\langle n,0;1,1|\ell,1\rangle|^2\right) {}_{-1}Y_{\ell m}(\hat{\mathbf{k}})^*\, {}_{-1}Y_{\ell m}(\hat{\mathbf{r}}) \\ &\quad + (\,\epsilon_R \to \epsilon_L^*,\, \omega \to -\omega\,) \\ &\sim +2\pi\,\epsilon_R\, e^{-i\omega t} \sum_{\ell,m}\left(-\frac{1}{2\omega}\frac{e^{i\omega r}}{r} + (-1)^\ell\, \frac{\ell(\ell+1)}{8\omega^3}\frac{e^{-i\omega r}}{r^3}\right) {}_{-1}Y_{\ell m}(\hat{\mathbf{k}})^*\, {}_{-1}Y_{\ell m}(\hat{\mathbf{r}}) \\ &\quad + (\,\epsilon_R \to \epsilon_L^*,\, \omega \to -\omega\,)\,. \end{aligned} \tag{5.7}$$

The expression for ϕ_0 is very similar, changing the coefficients of $e^{\pm i\omega r}$ accordingly so they obey Eqs. (3.32) and (3.33) when $r \gg r_+$, replacing ${}_{-1}Y_{\ell m}(\hat{\mathbf{r}}) \to {}_{+1}Y_{\ell m}(\hat{\mathbf{r}})$.

We have shown that even a simple plane wave is a superposition of modes with positive and negative frequencies modulated by the left and right polarizations, respectively,

which are proportional to ${}_{-1}Y_{1,\pm1}(\theta_0, \varphi_0)$. According to condition (3.84), modes with either $\omega > 0$, $m > 0$ or $\omega < 0$, $m < 0$ can be amplified. The position of the source modulates the incident wave changing its mode composition. Therefore if the plane wave source co-rotates with the BH, when $\theta_0 \to 0$ the positive frequencies dominate because $\epsilon_L^* \to 0$, coinciding with the region were $m > 0$ harmonics predominate. Analogously, when $\theta_0 \to \pi$ negative frequencies dominate as $\epsilon_R \to 0$. On the other hand, when considering counter-rotation and the incidence at one of the poles, harmonics with $m\omega > 0$ have null coefficients so those modes are never amplified. More specifically, when we have exactly $\theta_0 = 0$ ($\theta_0 = \pi$) the modes $m = 1$ ($m = -1$) are the only non-zero contributions of the EM wave if and only if the source co-rotates with the BH, while other m modes vanish. This has been used in [38] to show that a plane wave can be overall amplified by a spinning black hole when it is incident along the BH rotation axis and the source co-rotates with the latter. For a pulsar orbiting a Kerr BH, this results in a modulation of the pulsar's total luminosity.

5.2 Scattering theory

We understand that we have limited observational capabilities and only have access to given a direction of observation for this hypothetical binary system. If it were possible to map the entire scattered wave with enough detail we could in principle extract and compare each mode with the ones of the emitted wave. For this analysis we would only need to know the global gain/loss factor, given by ${}_{\pm1}Z_{\ell m}$. Therefore we will resort to scattering theory of waves to study the angular effects of superradiance.

Intuitively, it is understood that only a small part of the incident wave will be scattered by the BH. The scattered part together with the indent wave produce a characteristic interference pattern. In order to differentiate the scattered wave we need to remove the background incident plane wave. Scattering theory assumes that we may write

$$\phi_2 - \phi_2{}^{(\text{plane})} = f(\theta, \varphi)\frac{e^{i\omega(r_*-t)}}{r} + (\omega \to -\omega,\, f \to g)\,, \tag{5.8}$$

where ϕ_2 is written similarly with coefficients $\mathcal{Z}_{\text{out}}$ and $\mathcal{Z}_{\text{in}}$ obtained numerically in Chapter 4.

Up to this point we used the approximation of plane wave first introduced in (5.4), which can only be used in flat space. The fact is that this approximation does not take

into account the long-range behaviour of Kerr's gravitational field, which decays as $\mathcal{O}(\frac{1}{r})$ as obtained in (3.58). We know that from the asymptotic form of the radial function that this can be bypassed by a logarithmic phase-correction in the exponential, substituting $r \to r_*$. The ingoing part of ϕ_2 is naturally the same as $\phi_2{}^{(\text{plane})}$, so that the scattered wave only has an outgoing part, given by

$$f(\theta,\varphi) = -\frac{\pi\,\epsilon_R}{\omega}\sum_{\ell,m}\left[(-1)^{\ell+1}\frac{\ell(\ell+1)}{4\omega^2}\frac{\mathcal{Z}_{\text{out}}}{\mathcal{Z}_{\text{in}}} - 1\right]{}_{-1}Y_{\ell m}(\hat{\mathbf{k}})^*\,{}_{-1}Y_{\ell m}(\hat{\mathbf{r}})\,. \tag{5.9}$$

A similar expression is obtained for $g(\theta,\varphi)$ proportional to ϵ_L^*.

The long-range effect of the background is independent of the BH rotation (also in Schwarzschild), *i.e.* we must not mistake the spherical approximation with long-range effects of the effective gravitational potential. The plane wave decomposition in (5.4) discards, to a first approximation, the effects of the BH rotation, therefore using spherical rather than spheroidal harmonics. We nevertheless expect this to be a good first approximation for the small c values relevant for the lowest multipoles in the superradiant frequency regime. We can also recall that the mode factor in Eq. (5.9) is very similar to the expression (3.80), derived in Chapter 3. We see that for $a\omega \to 0$,

$$\frac{\mathcal{B}}{4\omega^2}\frac{\mathcal{Z}_{\text{out}}}{\mathcal{Z}_{\text{in}}} \simeq \frac{\ell(\ell+1)}{4\omega^2}\frac{\mathcal{Z}_{\text{out}}}{\mathcal{Z}_{\text{in}}}\,, \tag{5.10}$$

remembering that $\mathcal{B} = \left[({}_{\pm1}\mathcal{E}_{\ell m})^2 - 4a^2\omega^2 + 4ma\omega\right]^{1/2}$. An argument could be made that the latter expression for the coefficient is the correct one instead of the one in Eq. (5.9), but this approximation is good enough when considering superradiant frequencies $|\omega| \simeq 0.4\Omega_H$ for a typical stellar mass extremal BH (see Figure 4.3).

5.3 Phase-shifts

If wo assume co-rotation of the source with incidence along the axis at $\theta_0 = \varphi_0 = 0$ we will only need to compute $f(\theta,\varphi)$, since $\epsilon_L^* = 0$. This assumption eases the need to compute modes other than $m = 1$. Therefore, truncating the harmonic expansion (5.9) at some $\ell = \ell_{\text{max}}$ implies that scattering with incidence on axis reduces the number of necessary harmonics in $\ell_{\text{max}}(\ell_{\text{max}}+1)$.

Proceeding with the sum over multipoles, using the numerically obtained results for the ratio $\mathcal{Z}_{\text{out}}/\mathcal{Z}_{\text{out}}$ as described in the previous chapter, it appears that the partial wave

sum is divergent near $\theta = 0$, since the value of increasing $f(0,0)$ seams to increase more with each contribution (see Figure 5.1). This problem is due to the long-range effect of the

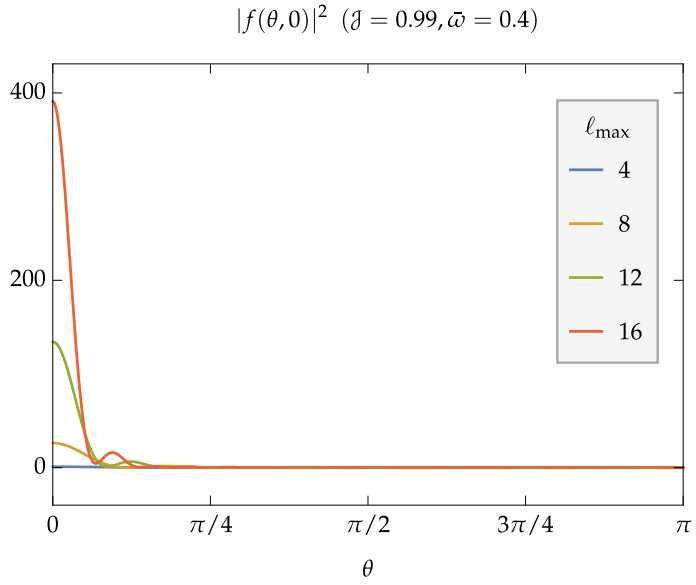

FIGURE 5.1: Plot of the scattering function $|f(\theta,0)|^2$ truncated at different $\ell_{\max}$, for values of $\mathcal{J} = 0.99$ and $\bar{\omega} = 0.4$, showing divergence in $\theta = \theta_0 = 0$.

gravitational potential of BHs. Central potentials falling as $1/r$ (check (3.58)) do not have an effect on the global amplitude of the wave but the scattered wave has phase-shifts in each of the mode coefficients, producing a divergence at $(\theta, \varphi) = (\theta_0, \varphi_0)$. This problem was also studied in classical Coloumb scattering, where $f(\theta,0)$ is known to diverge at $\theta = \theta_0$. This result appears strange at first, but we must remember that, being a complete space of functions, the harmonics obey $\sum_{\ell m} {}_{-1}Y_{\ell m}(\hat{\mathbf{k}})^* {}_{-1}Y_{\ell m}(\hat{\mathbf{r}}) = \delta(\cos\theta - \cos\theta_0)\delta(\varphi - \varphi_0)$.

In order to regularize the sum for $f(\theta,\varphi)$, it is convenient to separate it in two terms,

$$f(\theta,\varphi) = f_{\rm N}(\theta,\varphi) + f_{\rm D}(\theta,\varphi)\,, \tag{5.11}$$

$f_{\rm N}(\theta,\varphi)$ carries all the scattering information about the Newtonian effects of the long-range $1/r$ (Coulomb) potential. It can be written as

$$f_{\rm N}(\theta,\varphi) = -\frac{\pi\,\epsilon_R}{\omega}\sum_{\ell,m}\left(e^{2i\delta_{\rm N}} - 1\right) {}_{-1}Y_{\ell m}(\hat{\mathbf{k}})^* {}_{-1}Y_{\ell m}(\hat{\mathbf{r}})\,, \tag{5.12}$$

where the phase-shifts are [45]

$$e^{2i\delta_{\rm N}} = \frac{\Gamma(\ell+1-2iM\omega)}{\Gamma(\ell+1+2iM\omega)}\,. \tag{5.13}$$

Assuming an incidence $\theta_0 = 0$, summing the series leads to a similar result as the Rutherford elastic scattering in a Coulomb potential, $|f_{\rm N}(\theta,0)|^2 \sim 1/\sin^4(\theta/2) \sim 1/\theta^4$, which appears to explain the divergence at $\theta = 0$.

On the other hand, the $f_{\rm D}(\theta,\varphi)$ encloses all the information regarding the main scattering effects, including superradiance. From Eq. (5.11), simple algebra states that

$$f_{\rm D}(\theta,\varphi) = -\frac{\pi\,\epsilon_R}{\omega}\sum_{\ell,m}\left[\frac{\mathcal{B}}{\ell(\ell+1)}\sqrt{{}_{\pm1}Z_{\ell m}+1}\,e^{2i\delta_\ell} - e^{2i\delta_{\rm N}}\right]{}_{-1}Y_{\ell m}(\hat{\mathbf{k}})^*\,{}_{-1}Y_{\ell m}(\hat{\mathbf{r}})\,, \tag{5.14}$$

where we define

$$2\delta_\ell = \arg\left[(-1)^{\ell+1}\,\frac{\mathcal{Z}_{\rm out}}{\mathcal{Z}_{\rm in}}\right]\,. \tag{5.15}$$

For this sum to converge two things must occur. First, absolute value (5.10) must go to 1. Numerically, we find that in the limit of $\ell/\omega \to \infty$ mode amplitudes are not significantly affected by the BH, ${}_{\pm1}Z_{\ell m} \to 0$ (check Figure 4.6). Also, from Eq. (3.35) we know that for $c = a\omega$ constant, increasing ℓ leads to the eigenvalue $\mathcal{B} \sim {}_{\pm1}\mathcal{E}_{\ell m} \sim \ell(\ell+1)$, which cancels the factor in (5.14).

Secondly, the numerically computed phases using (5.15) must converge to the Newtonian phase-shifts (5.13), $\delta_\ell \to \delta_N$. Results appear to indicate that these phases, like δ_N, are independent of m. Also they appear to have the same asymptotic form, apart from a constant offset δ_0. We attribute this difference to an ambiguity in the definition of the tortoise coordinate, given by

$$r_* = r + \frac{2Mr_+}{r_+-r_-}\log\left(\frac{r-r_+}{r_+}\right) - \frac{2Mr_-}{r_+-r_-}\log\left(\frac{r-r_-}{r_-}\right) + \text{ const. }\,, \tag{5.16}$$

which is needed to extract the complex asymptotic coefficients of (3.59). It is expect for this integration constant to be dependent only on a and M, which implies that for constant $\bar{\omega}$ the value of δ_0 depends only on $\mathcal{J}$. We fit numerically the value of δ_0 independently for each case. From Figure 5.2 we verify that these phases indeed share the same asymptotic behaviour when $\ell \gg 1$. On the other hand, larger deviations from the δ_N occur for values of ℓ close to 1 where effect BH spin are predominant. Taking the $\mathcal{J} \to 0$ limit quickly takes the values of δ_ℓ closer to δ_N.

The correspondent partial wave sums for the phases presented above are shown in Figure 5.3. The truncation of the series (5.14) at $\ell = \ell_{\rm max}$ leads to interference oscillations

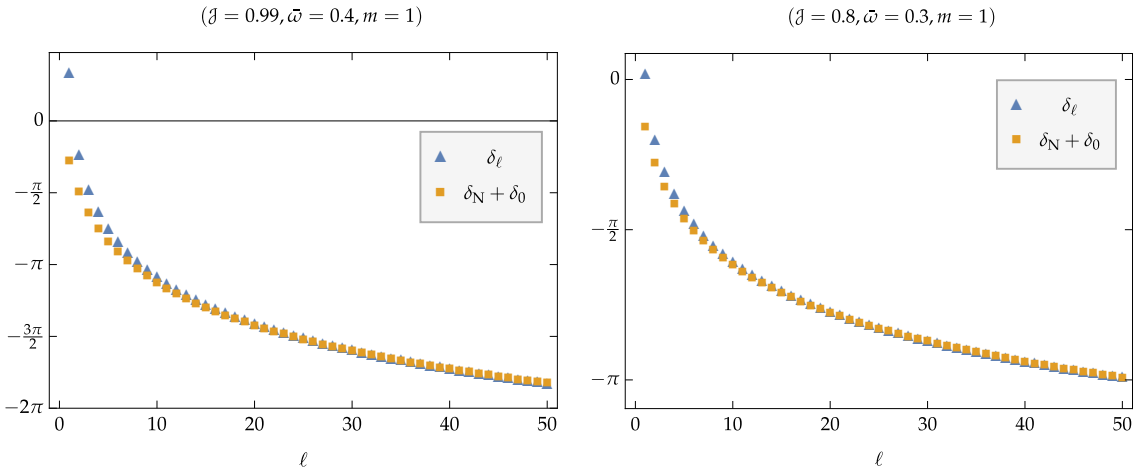

FIGURE 5.2: Plots of the phase-shifts δ_ℓ compared with the newtonian shifts δ_N summed with a given adjustment constant δ_0 (fitted), for two given BH configurations and modes.

of characteristic length $2\pi/\ell_{\text{max}}$. Comparing with Figure 5.1 it seams that the partial wave expansion for $|f_{\text{D}}(\theta,0)|^2$ is now converging in the range $32 \leq \ell_{\text{max}} \leq 48$. We expected that the computation of $f_D(\theta,\varphi)$ would give us a clean channel to identify superradiance phenomena in scattering of plane waves, but Figure 5.3 shows that performing the mode sum from $\ell = 16$ through $\ell = 24$, which we know to have effectively ${}_{\pm1}Z_{\ell 1} = 0$ ($< 10^{-85}$), still has a great impact on the value of $|f_D(\theta,0)|^2$. Even tough these modes are fully reflected, effects of amplification/absorption are masked by the mode interference introduced by the phase-shifts in each mode. Thus we must find other ways of isolating these effects from relevant superradiant modes with lower ℓ values.

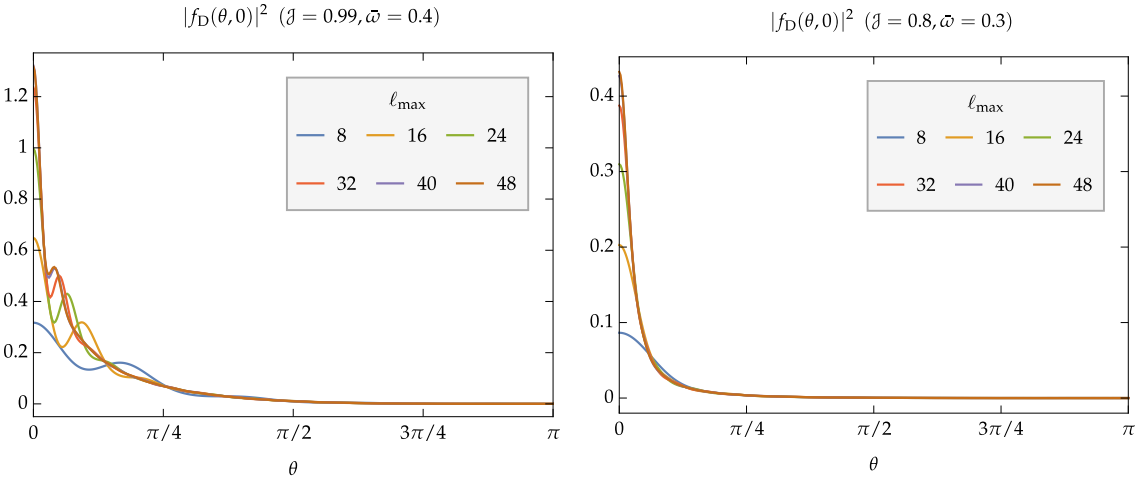

FIGURE 5.3: Plots of the regularized partial wave sum, $|f_D(\theta,0)|^2$, for the same configurations of Figure 5.2.

Chapter 6

Discussion and future work

In this work we sought to understand the effect of superradiance scattering of EM waves in the Kerr spacetime. The objective was to demonstrate if superradiance occurred in the case of scattering of an EM wave radiated from a physically realistic source by a rotating BH. General waves are a superpositions of modes (ω, ℓ, m), for which we know superradiance occurs when $\omega(\omega - m\Omega_H) < 0$. In this region the modes are either reflected or amplified, with the maximum amplification in the case of EM waves being of approximately 4.4%. This occurs when the BH is extremal, $a \to M$ and on the lowest multipole $\ell = 1$, with the percentage dropping quickly to zero as ℓ increases. Modes with large $|\omega|$ are quickly absorbed by the BH since they can "cross" the centrifugal barrier in the effective potential, reaching the event horizon. To compute these amplification factors we need: (i) to compute the angular eigenvalues that enter the radial equation; (ii) to obtain the coefficients $\mathcal{Z}_{\text{in}}$ and $\mathcal{Z}_{\text{out}}$, by solving the radial equation. In second step we devised a way of not rewriting the radial equation using the tortoise coordinate r_*, removing the singularities by considering a clever ansatz, without sacrificing precision or computational speed. We showed that it is possible to find the amplification factor of each mode either using only $|\mathcal{Z}_{\text{in}}|^2$ or $|\mathcal{Z}_{\text{out}}|^2$, or a combination of both coefficients. In this work we discuss why it is more advantageous to write the gain/loss factor using only one of the previous coefficients. Although the routine is defined for EM perturbations, it can be quickly updated to accommodate GW perturbations for future work studies. The resultant complex coefficients also play an integral part in the computation of phase-shifts, which are present for each mode. Particularly, for a plane wave with superradiant frequency we know that most of the multipole modes are deflected with no change in the

amplitude. This effect is characteristic of long-ranged potentials that fall as $1/r$. When observing the BH from a particular direction, the effect of these phase-shifts will dominate and conceal the effects of superradiance. In principle we could remove these interference effects, integrating over all the solid angle if we could gather information about the EM wave scattering in all directions, leaving only global amplification/absorption effects, but we do not know if that will be ever possible. Therefore we need to find a way to isolate the lower superradiant modes. A possible idea would be use a source orbiting the BH, with possibility for variation of distance to the BH and incidence angle, due to the chaotic orbits of the Kerr geometry.

In summary, in this thesis we have developed a computational routine that numerically yields the outcome of scattering of any EM wave mode in the Kerr spacetime, including both amplification/absorption factors and phase-shifts. This code can be used to determine the scattered wave corresponding to any realistic incident wave if its mode decomposition is known, as we illustrated for the case of a plane wave produced by a distant precessing magnetic dipole. The tools developed in this work will thus play a key role in future studies of superradiant scattering off astrophysical black holes, which may potentially yield an important probe of general relativity in the strong gravity regime.

Appendix A

Tetrad techniques

A.1 Noncoordinate representation

The standard way of expressing quantities in GR was to use a local coordinate basis. This corresponds to use

$$\frac{\partial}{\partial x^\mu} \qquad (x^\mu = t, r, \theta, \varphi) \tag{A.1}$$

as our vector basis. One-form basis can be defined the usual way. The tetrad formalism allows for an alternative choice of a *noncoordinate* basis, by introducing a set of linear independent four-vectors [10, 29],

$$\boldsymbol{e}_a = (e_a)^\mu \frac{\partial}{\partial x^\mu} \qquad (a = 1, 2, 3, 4)\ . \tag{A.2}$$

We will use Greek alphabet $(\alpha, \beta, \gamma, \dots)$ for the coordinate components and the Latin alphabet $(a, b, c, \dots)$ for the tetrad components. The tetrad fields also defined directional derivatives, for example for any scalar field f

$$f_{,a} = \boldsymbol{e}_a(f) = (e_a)^\mu \frac{\partial f}{\partial x^\mu} = (e_a)^\mu f_{,\mu}\ . \tag{A.3}$$

However, this formalism must not be mistaken with as change of coordinates, $y = \phi(x)$, such that $(e_a)^\mu = \partial x^\mu / \partial y^a$, since those coordinates may not exist. A tetrad frame is a pointwise rotation of the coordinate frame, *i.e.* the concept is related to passive transformations rather that active (diffeomorphisms).

Given any tensor field $F_{\mu\nu}$, we can obtain its tetrad components by projecting it onto the tetrad frame,

$$F_{ab} = (e_a)^\mu (e_b)^\nu F_{\mu\nu} \,. \tag{A.4}$$

We may invert this expression, by defining the inverse tetrad, $(e^a)_\mu$, such that

$$(e_a)^\mu (e^b)_\mu = (e_a)^\mu (e^b)^\nu g_{\mu\nu} = \delta_a{}^b \,, \tag{A.5}$$

hence invariant quantities remain unchanged,

$$\boldsymbol{A}^2 = A^\mu A_\mu = A^a (e_a)^\mu \, A_b (e^b)_\mu = A^a A_a \,. \tag{A.6}$$

We can then substitute the manifold metric for the tetrad "metric"

$$\eta_{ab} = \boldsymbol{e}_a \cdot \boldsymbol{e}_b = g_{\mu\nu} (e_a)^\mu (e_b)^\nu \,, \tag{A.7}$$

which can be used for raising/lowering tetrad indices,

$$A^a = \eta^{ab} A_b \,, \tag{A.8}$$

and to contract tetrad components, such as $\eta_{ab} A^a A^b = \boldsymbol{A}^2$. This implies that we may return to the original metric using

$$g^{\mu\nu} = \eta^{ab} (e_a)^\mu (e_b)^\nu \,. \tag{A.9}$$

By analyzing the underlying symmetries of spacetime, one may choose a basis makes the components of η_{ab} constant, which is particularly important for the NP formalism. Going forward, we will assume that this is the case.

A.2 Spin connection

The analogy with the coordinate basics breaks when applying the a directional derivative of a tetrad components,

$$A_{a,b} = (e_b)^\nu \partial_\nu A_a = (e_b)^\nu \nabla_\nu \left[(e_a)^\mu A_\mu \right] = (e_a)^\mu (e_b)^\nu A_{\mu;\nu} + (e_c)^\mu (e_a)_{\mu;\nu} (e_b)^\nu A^c \,, \tag{A.10}$$

due to extra terms resultant of the tetrad derivatives. Tetrad decompositions, A^a, are scalars and must not be mistaken as vector fields such as $(e_a)^\mu$ or A^μ. These extra terms can be written using the spin connection

$$\gamma_{cab} = (e_c)^\mu (e_a)_{\mu;\nu} (e_b)^\nu \,, \tag{A.11}$$

which is antisymmetric in the first two indices,

$$\gamma_{cab} = -\gamma_{acb} \,, \tag{A.12}$$

due to the metric compatibility of the covariant derivative, $\nabla_\mu g_{\nu\rho} = 0$. Nonetheless, this only holds if η_{ab} is constant, otherwise we would have $\gamma_{abc} + \gamma_{bac} = \eta_{ab,c}$

The other term is called the *intrinsic* derivative of A_a in the direction of e_b, being defined as the projection of the tensor $A_{\mu;\nu}$ in the tetrad frame,

$$A_{a|b} = (e_a)^\mu (e_b)^\nu A_{\mu;\nu} \tag{A.13}$$

If we have a higher rank tensor, $F_{\mu\nu}$, we can generalize the intrinsic derivative inverting Eq. (A.10) and generalizing for multiple indices with the use of the spin connection,

$$F_{ab|c} = F_{ab,c} - \eta^{nm}(F_{nb}\gamma_{mac} + F_{an}\gamma_{mbc}) \,. \tag{A.14}$$

Obviously, the spin connection replaces the Christoper symbols, $\Gamma^\rho_{\mu\nu}$, in the tetrad formalism, although they are fundamentally different. We will avoid the computation of the Christoper symbols because every equation involving a covariant derivative will become an intrinsic derivative in NP formalism due to tetrad projections. This will become useful during calculations as we generally need $\frac{1}{2}d^2(d+1)$ computations to fully define the latter, while the spin connection has $\frac{1}{2}d^2(d-1)$ independent components. For $d = 4$, the use of the spin connection implies 16 components less to work with.

Appendix B

Additional Newman-Penrose definitions and computations

In this appendix we will present important computations of NP formalism in Kerr background (2.19), using the Kinnersley tetrad defined in (3.13). We will find useful in the one-form conversion from the Kinnersley vectors, $(\boldsymbol{e}_a)^\flat = (e_a)_\mu \mathrm{d}x^\mu$,

$$\begin{aligned}
\boldsymbol{\mathfrak{l}}^\flat =& \frac{1}{\Delta}\Big(\Delta, -\rho^2, 0, -a\Delta\sin^2\theta\Big)\,, \\
\boldsymbol{\mathfrak{n}}^\flat =& \frac{1}{2\rho^2}\Big(\Delta, \rho^2, 0, -a\Delta\sin^2\theta\Big)\,, \\
\boldsymbol{\mathfrak{m}}^\flat =& \frac{1}{\sqrt{2}\bar{\rho}}\Big(ia\sin\theta, 0, -\rho^2, -i(r^2+a^2)\sin\theta\Big)\,,
\end{aligned} \tag{B.1}$$

where $\Delta = r^2 - 2Mr + a^2$, $\bar{\rho} = r + ia\cos\theta$, $\rho^2 = \bar{\rho}\bar{\rho}^*$.

B.1 Spin coefficients

The spin connection is defined as the covariant derivative of the tetrad field projected onto the tetrad frame. For example, we write $\gamma_{412} = \bar{\mathfrak{m}}^\mu \mathfrak{l}_{\mu;\nu}\mathfrak{n}^\nu = \bar{\mathfrak{m}}^\mu \mathfrak{n}^\nu \nabla_\nu \mathfrak{l}_\mu = \bar{\mathfrak{m}}^\mu \mathbb{\Delta} \mathfrak{l}_\mu$. It has 24 components due to the antisymmetry of the first tetrad indices. These can be

encapsulated using 12 complex variables [29],

$$\begin{aligned}
\kappa &= \gamma_{311}\,, & \varrho &= \gamma_{314}\,, & \varepsilon &= \tfrac{1}{2}(\gamma_{211}+\gamma_{341})\,,\\
\sigma &= \gamma_{313}\,, & \mu &= \gamma_{243}\,, & \gamma &= \tfrac{1}{2}(\gamma_{212}+\gamma_{342})\,,\\
\lambda &= \gamma_{244}\,, & \tau &= \gamma_{312}\,, & \alpha &= \tfrac{1}{2}(\gamma_{214}+\gamma_{344})\,,\\
\nu &= \gamma_{242}\,, & \pi &= \gamma_{241}\,, & \beta &= \tfrac{1}{2}(\gamma_{213}+\gamma_{343})\,.
\end{aligned} \tag{B.2}$$

The computation of these coefficients can be done without computation of the Christopher symbols associated with the covariant derivative. This is cleverly avoided by observing that for any torsion-free connection, $(e_b)_{[\mu;\nu]} = (e_b)_{[\mu,\nu]}$. Therefore we define

$$\lambda_{abc} = (e_a)^\mu (e_c)^\nu \left[(e_b)_{\mu,\nu} - (e_b)_{\nu,\mu}\right]\,. \tag{B.3}$$

The computation of the various spin coefficients can be easily performed noticing that $\lambda_{abc} = \gamma_{abc} - \gamma_{cba}$, which can be inverted to

$$\gamma_{abc} = \frac{1}{2}\left(\lambda_{abc} + \lambda_{cab} - \lambda_{bca}\right)\,. \tag{B.4}$$

All relevant non-vanishing λ-symbols can be computed by simple coordinate derivatives on the one-form basis,

$$\begin{aligned}
\lambda_{122} &= -\frac{1}{\rho^4}\left[(r-M)\rho^2 - r\Delta\right]\,, & \lambda_{314} &= -\frac{2ia\cos\theta}{\rho^2}\,,\\
\lambda_{132} &= \frac{i\sqrt{2}ar\sin\theta}{\rho^2\bar{\rho}}\,, & \lambda_{324} &= -\frac{ia\Delta\cos\theta}{\rho^4}\,,\\
\lambda_{213} &= -\frac{\sqrt{2}a^2\cos\theta\sin\theta}{\rho^2\bar{\rho}}\,, & \lambda_{334} &= \frac{(ia+r\cos\theta)\csc\theta}{\sqrt{2}\bar{\rho}^2}\,,\\
\lambda_{243} &= -\frac{\Delta}{2\rho^2\bar{\rho}}\,, & \lambda_{341} &= -\frac{1}{\bar{\rho}}\,.
\end{aligned} \tag{B.5}$$

All other necessary symbols may be found by the symmetry $\lambda_{abc} = -\lambda_{cba}$ or by complex conjugation ($3 \rightleftarrows 4$). For example, for computing the spin coefficient μ, we need to use

the relation $\lambda_{432} = -\lambda_{234} = -(\lambda_{243})^*$. Assembling all symbols, we obtain

$$\begin{gathered}
\kappa = \sigma = \lambda = \nu = 0\,, \\
\varrho = -\frac{1}{\bar{\rho}}\,, \qquad \mu = -\frac{\Delta}{2\rho^2\bar{\rho}^*}\,, \qquad \tau = -\frac{ia\sin\theta}{\sqrt{2}\rho^2}\,, \qquad \pi = \frac{ia\sin\theta}{\sqrt{2}(\bar{\rho}^*)^2}\,, \\
\varepsilon = 0\,, \qquad \gamma = \mu + \frac{r-M}{2\rho^2}\,, \qquad \alpha = \pi - \beta^*\,, \qquad \beta = \frac{\cot\theta}{2\sqrt{2}\bar{\rho}}\,.
\end{gathered} \tag{B.6}$$

Appendix C

Spin-weighted spherical harmonics

Spin-weight spherical harmonics [42, 46, 47] are a generalization of the standard spherical harmonics found in many well know physical problems such as the hydrogen atom. They define a set of eigenfunctions which solves the equation

$$\frac{1}{\sin\theta}\frac{\mathrm{d}}{\mathrm{d}\theta}\left(\sin\theta\frac{\mathrm{d}\,{}_sY_{\ell m}}{\mathrm{d}\theta}\right)+\left[s-\frac{(m+s\cos\theta)^2}{\sin^2\theta}\right]{}_sY_{\ell m}=-\lambda\,{}_sY_{\ell m}\,, \tag{C.1}$$

with eigenvalues $\lambda=\ell(\ell+1)-s(s+1)$.

These harmonics are complex functions defined on the S^2. If take a point in a sphere (θ,φ), we can define a right-handed basis at each point, $\boldsymbol{e}_\theta=\partial_\theta$ and $\boldsymbol{e}_\varphi=1/\sin\theta\,\partial_\varphi$, where $\boldsymbol{e}_\theta\cdot\boldsymbol{e}_\theta=\boldsymbol{e}_\varphi\cdot\boldsymbol{e}_\varphi=1$ and $\boldsymbol{e}_\theta\cdot\boldsymbol{e}_\varphi=0$. A given function f defined on S^2 is said to have spin-weight s if under the rotation of an angle α of the tangent vectors to the sphere,

$$\boldsymbol{e}_\theta\to\cos\alpha\,\boldsymbol{e}_\theta-\sin\alpha\,\boldsymbol{e}_\varphi\,,\qquad \boldsymbol{e}_\theta\to\sin\alpha\,\boldsymbol{e}_\theta+\cos\alpha\,\boldsymbol{e}_\varphi\,, \tag{C.2}$$

implies that the function transforms as

$$f(\theta,\varphi)\to e^{is\alpha}f(\theta,\varphi)\,. \tag{C.3}$$

In the case of spherical symmetry, $a=0$, we may write the Kinnersly angular vector as $\mathfrak{m}=(\boldsymbol{e}_\theta+i\,\boldsymbol{e}_\varphi)/(\sqrt{2}r^2)$. Under the same transformation, we have $\mathfrak{m}\to e^{i\alpha}\mathfrak{m}$. From definition (3.15), since we contract the Maxwell tensor with $\bar{\mathfrak{m}}$ once to obtain ϕ_2, we know that $\phi_2\to e^{-i\alpha}\phi_2$, thus is has spin-weight -1. On the other hand, for gravitational waves the NP scalars ψ_0 and ψ_4 are double contractions $\mathfrak{m}$ and $\bar{\mathfrak{m}}$ on the Weyl tensor, respectively. Therefore they are $s=2$ and $s=-2$ quantities, respectively.

All spin-weight spherical harmonics can be obtained using raising and lowering operators on the scalar spherical harmonics. In particular we have that ${}_0Y_{\ell m} = Y_{\ell m}$. These operators are defined as

$$\begin{aligned} \eth f &= -(\sin\theta)^s \left\{ \partial_\theta + \frac{i}{\sin\theta}\partial_\varphi \right\} \left[(\sin\theta)^{-s} f \right] = -\left(\partial_\theta + \frac{i}{\sin\theta}\partial_\varphi - s\cot\theta \right) f \,, \\ \bar{\eth} f &= -(\sin\theta)^{-s} \left\{ \partial_\theta - \frac{i}{\sin\theta}\partial_\varphi \right\} \left[(\sin\theta)^{s} f \right] = -\left(\partial_\theta - \frac{i}{\sin\theta}\partial_\varphi + s\cot\theta \right) f \,. \end{aligned} \tag{C.4}$$

Is clear from the definition of the operators, that for a function f is a function with spin-weight s, then $\eth f$ has spin-weight $s+1$ while $\bar{\eth} f$ has spin-weight $s-1$, due to an extra $e^{\pm i\alpha}$ factor under the transformation (C.2).

Expanding $\eth\bar{\eth}$ we can found the property that for any function f with definite spin-weight, we have

$$\frac{1}{2}(\bar{\eth}\eth - \eth\bar{\eth}) f = s f. \tag{C.5}$$

This last equation can also be shown using the properties

$$\begin{aligned} \eth\, {}_sY_{\ell m} &= +\sqrt{\ell(\ell+1) - s(s+1)}\ {}_{s+1}Y_{\ell m} \,, \\ \bar{\eth}\, {}_sY_{\ell m} &= -\sqrt{\ell(\ell+1) - s(s+1)}\ {}_{s-1}Y_{\ell m} \,. \end{aligned} \tag{C.6}$$

We can apply multiple raising and lowering operators to obtain any spherical harmonic, given that $\ell \geq \max\{|m|, |s|\}$,

$$\begin{aligned} {}_sY_{\ell m}(\theta,\varphi) = (-1)^m \sqrt{\frac{2\ell+1}{4\pi}(\ell+m)!(\ell-m)!(\ell+s)!(\ell-s)!} \\ \times \sum_{k=0}^{\ell-s} \frac{(-1)^m \left(\sin\frac{\theta}{2}\right)^{m+s+2k} \left(\cos\frac{\theta}{2}\right)^{2\ell-m-s-2k}}{k!(\ell-m-k)!(\ell-s-k)!(m+s+k)!} e^{im\varphi} \end{aligned} \tag{C.7}$$

For this work, will be useful to list the lowest dipole ($s=-1$, $\ell=1$) spherical harmonics

$$\begin{aligned} {}_{-1}Y_{1,\pm1}(\theta,\varphi) &= -\sqrt{\frac{3}{8\pi}}\sin\theta \,, \\ {}_{-1}Y_{10}(\theta,\varphi) &= -\sqrt{\frac{3}{16\pi}}(\cos\theta \pm 1) e^{\pm i\varphi} \,, \end{aligned} \tag{C.8}$$

while the $s = 1$ harmonics can be obtained using properties

$$\begin{aligned} {}_{-s}Y_{\ell m}(\theta,\varphi)^* &= (-1)^{-s+m}\,{}_sY_{\ell,-m}(\theta,\varphi)\,, \\ {}_{-s}Y_{\ell m}(\pi-\theta,\varphi+\pi)^* &= (-1)^{\ell}\,{}_sY_{\ell m}(\theta,\varphi)\,. \end{aligned} \tag{C.9}$$

Another possible way of writing the spin-weight spherical harmonics is by using the hypergeometric function,

$$\begin{aligned} {}_sY_{\ell m}(\theta,\varphi) = (-1)^m \sqrt{\frac{2\ell+1}{4\pi}\frac{(\ell+m)!(\ell-m)!}{(\ell+s)!(\ell-s)!}}\,\left(\sin\tfrac{\theta}{2}\right)^{m+s}\left(\cos\tfrac{\theta}{2}\right)^{2\ell-m-s} \\ \times\, {}_2F_1\left(m-\ell, s-\ell, m+s+1; -\tan^2\tfrac{\theta}{2}\right) e^{im\varphi}\,. \end{aligned} \tag{C.10}$$

The product of two spin-weighted spherical harmonics with the same argument can be written as a linear combination of other harmonics, admitting a Clebsh-Gordon decomposition,

$${}_{s'}Y_{j'm'}\,{}_sY_{jm} = \sum_{S,J,M} C_{SJM}\,{}_SY_{JM}\,, \tag{C.11}$$

where

$$\begin{aligned} C_{SJM} = (-1)^{j+j'-J}\sqrt{\frac{(2j+1)(2j'+1)}{4\pi(2J+1)}} \\ \times\,\langle j', m'; j, m | J, M\rangle \langle j', s'; j, s | J, S\rangle\, \delta_{M,m+m'}\,\delta_{S,s+s'}\,, \end{aligned} \tag{C.12}$$

with the restriction that the triangle inequality must hold, $|j - j'| \leq J \leq j + j'$.

Since these harmonics are generalizations of the standard $s = 0$ spherical harmonics, we expect that for each spin-weight s they for an orthogonal and complete set of functions

$$\begin{aligned} \int \mathrm{d}\Omega\ {}_sY_{\ell'm'}(\theta,\varphi)^*\,{}_sY_{\ell m}(\theta,\varphi) = \delta_{\ell\ell'}\,\delta_{mm'}\,, \\ \sum_{\ell=|s|}^{\infty}\sum_{m=-\ell}^{\ell} {}_sY_{\ell m}(\theta_0,\varphi_0)^*\,{}_sY_{\ell m}(\theta,\varphi) = \delta(\cos\theta-\cos\theta_0)\delta(\varphi-\varphi_0)\,, \end{aligned} \tag{C.13}$$

so that any spin-weighted s function $f(\theta,\varphi)$ can be written as

$$f(\theta,\varphi) = \sum_{\ell=|s|}^{\infty}\sum_{m=-\ell}^{\ell} c_{\ell m}\,{}_sY_{\ell m}(\theta,\varphi)\,, \tag{C.14}$$

so each mode coefficient $c_{\ell m}$ is uniquely defined.

Appendix D

Eigenvalue small-c expansion

Using the Leaver continued fraction equation for the eigenvalue, defined in (3.48), is possible to expand the eigenvalue for $c \ll 1$,

$$ {}_s\mathcal{A}_{\ell m} = \sum_{p=0}^{\infty} f_p \, c^p \, . \tag{D.1} $$

Directed substitution into the continued fraction is done in [36, 37], where the coefficients are presented up to $\mathcal{O}(c^6)$. Defining

$$ h(\ell) = \frac{\left(\ell^2 - s^2\right)\left[\ell^2 - (k_+ - k_-)^2\right]\left[\ell^2 - (k_+ + k_-)^2\right]}{2\ell^3\left(\ell^2 - \frac{1}{4}\right)} = \frac{2\left(\ell^2 - m^2\right)\left(\ell^2 - s^2\right)^2}{\ell^3\left(4\ell^2 - 1\right)} \tag{D.2} $$

we may list the series coefficients below,

$$ f_0 = \ell(\ell+1) - s(s+1) \, , \tag{D.3a} $$

$$ f_1 = -\frac{2ms^2}{\ell(\ell+1)} \, , \tag{D.3b} $$

$$ f_2 = h(\ell+1) - h(\ell) - 1 \tag{D.3c} $$

$$ f_3 = 2ms^2\left[\frac{h(\ell)}{(\ell-1)\ell^2(\ell+1)} - \frac{h(\ell+1)}{\ell(\ell+1)^2(\ell+2)}\right] , \tag{D.3d} $$

$$ \begin{aligned} f_4 = {} & 4m^2s^4\left[\frac{h(\ell+1)}{\ell^2(\ell+1)^4(\ell+2)^2} - \frac{h(\ell)}{(\ell-1)^2\ell^4(\ell+1)^2}\right] + \frac{h(\ell+1)^2}{2(\ell+1)} - \frac{h(\ell)^2}{2\ell} \\ & + \frac{(\ell-1)h(\ell-1)h(\ell)}{2\ell(2\ell-1)} + \frac{h(\ell)h(\ell+1)}{2\ell(\ell+1)} - \frac{(\ell+2)h(\ell+1)h(\ell+2)}{2(\ell+1)(2\ell+3)} \, , \end{aligned} \tag{D.3e} $$

$$
\begin{aligned}
f_5 = {} & 8m^3s^6\left[\frac{h(\ell)}{(\ell-1)^3\ell^6(\ell+1)^3}-\frac{h(\ell+1)}{\ell^3(\ell+1)^6(\ell+2)^3}\right] \\
& + 2ms^2\left[\frac{3h(\ell)^2}{2(\ell-1)\ell^3(\ell+1)}-\frac{3h(\ell+1)^2}{2\ell(\ell+1)^3(\ell+2)}+\frac{(3\ell+7)h(\ell+1)h(\ell+2)}{2\ell(\ell+1)^3(\ell+3)(2\ell+3)}\right., \\
& \left. - \frac{(3\ell-4)h(\ell-1)h(\ell)}{2(\ell-2)\ell^3(\ell+1)(2\ell-1)}-\frac{(7\ell^2+7\ell+4)h(\ell)h(\ell+1)}{2(\ell-1)\ell^3(\ell+1)^3(\ell+2)}\right]
\end{aligned}
\tag{D.3f}
$$

$$
\begin{aligned}
f_6 = {} & \frac{16m^4s^8}{\ell^4(\ell+1)^4}\left[\frac{h(\ell+1)}{(\ell+1)^4(\ell+2)^4}-\frac{h(\ell)}{(\ell-1)^4\ell^4}\right] \\
& + \frac{4m^2s^4}{\ell^2(\ell+1)^2}\left[\frac{3h(\ell+1)^2}{(\ell+1)^3(\ell+2)^2}-\frac{3h(\ell)^2}{(\ell-1)^2\ell^3}-\frac{(3\ell^2+14\ell+17)h(\ell+1)h(\ell+2)}{(\ell+1)^3(\ell+2)(\ell+3)^3(2\ell+3)}\right. \\
& \left. + \frac{(11\ell^4+22\ell^3+31\ell^2+20\ell+6)h(\ell)h(\ell+1)}{(\ell-1)^2\ell^3(\ell+1)^3(\ell+2)^2}+\frac{(3\ell^2-8\ell+6)h(\ell-1)h(\ell)}{(\ell-2)^2(\ell-1)\ell^3(2\ell-1)}\right] \\
& + \frac{h(\ell+1)^3}{2(\ell+1)^2}-\frac{h(\ell)^3}{2\ell^2}-\frac{(\ell-1)^2h(\ell-1)^2h(\ell)}{4\ell^2(2\ell-1)^2}+\frac{(\ell-1)(7\ell-3)h(\ell-1)h(\ell)^2}{4\ell^2(2\ell-1)^2} \\
& + \frac{(2\ell^2+4\ell+3)h(\ell)^2h(\ell+1)}{4\ell^2(\ell+1)^2}-\frac{(2\ell^2+1)h(\ell)h(\ell+1)^2}{4\ell^2(\ell+1)^2} \\
& - \frac{(\ell+2)(7\ell+10)h(\ell+1)^2h(\ell+2)}{4(\ell+1)^2(2\ell+3)^2}+\frac{(\ell+2)^2h(\ell+1)h(\ell+2)^2}{4(\ell+1)^2(2\ell+3)^2} \\
& + \frac{(\ell+3)h(\ell+1)h(\ell+2)h(\ell+3)}{12(\ell+1)(2\ell+3)^2}+\frac{(\ell+2)(3\ell^2+2\ell-3)h(\ell)h(\ell+1)h(\ell+2)}{4\ell(\ell+1)^2(2\ell+3)^2} \\
& - \frac{(\ell-1)(3\ell^2+4\ell-2)h(\ell-1)h(\ell)h(\ell+1)}{4\ell^2(\ell+1)(2\ell-1)^2}-\frac{(\ell-2)h(\ell-2)h(\ell-1)h(\ell)}{12\ell(2\ell-1)^2}\,.
\end{aligned}
\tag{D.3g}
$$

Bibliography

[1] B. P. Abbott et al., *Observation of Gravitational Waves from a Binary Black Hole Merger*, Phys. Rev. Lett. **116**, 061102 (2016), arXiv:1602.03837 .

[2] R. H. Dicke, *Coherence in Spontaneous Radiation Processes*, Phys. Rev. **93**, 99 (1954).

[3] Y. B. Zel'dovich, *Generation of Waves by a Rotating Body*, JETP Lett. **14**, 180 (1971), [Zh. Eksp. Teor. Fiz. Pis'ma Red. **14**, 270 (1971)].

[4] Y. B. Zel'dovich, *Amplification of Cylindrical Electromagnetic Waves Reflected from a Rotating Body*, Sov. Phys. JETP **35**, 1085 (1972), [Zh. Eksp. Tear. Fiz. **62**, 2076 (1972)].

[5] S. W. Hawking, *Particle Creation by Black Holes*, Commun. Math. Phys. **43**, 199 (1975), [Erratum: Commun.Math.Phys. 46 (1976) 206].

[6] A. A. Starobinsky, *Amplification of waves reflected from a rotating "black hole"*, Sov. Phys. JETP **37**, 28 (1973), [Zh. Eksp. Teor. Fiz. **64**, 48 (1973)].

[7] A. A. Starobinsky and S. M. Churilov, *Amplification of electromagnetic and gravitational waves scattered by a rotating "black hole"*, Sov. Phys. JETP **38**, 1 (1974), [Zh. Eksp. Teor. Fiz. **65**, 3 (1973)].

[8] N. Deruelle and R. Ruffini, *Quantum and classical relativistic energy states in stationary geometries*, Phys. Lett. **52B**, 437 (1974).

[9] N. Deruelle and R. Ruffini, *Klein Paradox in a Kerr Geometry*, Phys. Lett. **57B**, 248 (1975).

[10] R. Wald, *General Relativity* (University of Chicago Press, 1984).

[11] P. K. Townsend, *Black holes: Lecture notes*, (1997), arXiv:gr-qc/9707012 [gr-qc] .

[12] S. A. Teukolsky, *Rotating Black Holes: Separable Wave Equations for Gravitational and Electromagnetic Perturbations*, Phys. Rev. Lett. **29**, 1114 (1972).

[13] S. A. Teukolsky, *Perturbations of a rotating black hole. I. Fundamental equations for gravitational electromagnetic and neutrino field perturbations*, Astrophys. J. **185**, 635 (1973).

[14] E. Newman and R. Penrose, *An Approach to Gravitational Radiation by a Method of Spin Coefficients*, J. Math. Phys. **3**, 566 (1962).

[15] R. Brito, V. Cardoso and P. Pani, *Superradiance: Energy Extraction, Black-Hole Bombs and Implications for Astrophysics and Particle Physics*, Lecture Notes in Physics, Vol. 906 (Springer International Publishing, 2015) arXiv:1501.06570v3 .

[16] O. Klein, *Die Reflexion von Elektronen an einem Potentialsprung nach der relativistischen Dynamik von Dirac*, Z. Phys. **53**, 157 (1929).

[17] F. Sauter, *Uber das Verhalten eines Elektrons im homogenen elektrischen Feld nach der relativistischen Theorie Diracs*, Z. Phys. **69**, 742 (1931).

[18] C. A. Manogue, *The Klein paradox and superradiance*, Ann. Phys. **181**, 261 (1988).

[19] C. Itzykson and J. Zuber, *Quantum Field Theory*, Dover Books on Physics (Dover Publications, 2012).

[20] R. G. Winter, *Klein Paradox for the Klein-Gordon Equation*, Am. J. Phys. **27**, 355 (1959).

[21] K. Schwarzschild, *On the gravitational field of a mass point according to Einstein's theory*, Sitzungsber. Preuss. Akad. Wiss. Berlin (Math. Phys.) **1916**, 189 (1916), arXiv:physics/9905030 [physics] .

[22] R. P. Kerr, *Gravitational Field of a Spinning Mass as an Example of Algebraically Special Metrics*, Phys. Rev. Lett. **11**, 237 (1963).

[23] M. Heusler, *Black Hole Uniqueness Theorems*, Cambridge Lecture Notes in Physics, Vol. 6 (Cambridge University Press, 1996).

[24] B. Carter, *Axisymmetric Black Hole Has Only Two Degrees of Freedom*, Phys. Rev. Lett. **26**, 331 (1971).

[25] S. A. Teukolsky, *The Kerr metric*, Class. Quantum Grav. **32**, 124006 (2015), arXiv:1410.2130v2 .

[26] R. H. Boyer and R. W. Lindquist, *Maximal Analytic Extension of the Kerr Metric*, J. Math. Phys. **8**, 265 (1967).

[27] S. W. Hawking and G. F. R. Ellis, *The Large Scale Structure of Space-Time*, Cambridge Monographs on Mathematical Physics (Cambridge University Press, 2011).

[28] J. D. Bekenstein, *Extraction of Energy and Charge from a Black Hole*, Phys. Rev. **D7**, 949 (1973).

[29] S. Chandrasekhar, *The Mathematical Theory of Black Holes*, Oxford Classic Texts in the Physical Sciences (Clarendon Press, 1998).

[30] S. A. Teukolsky and W. H. Press, *Perturbations of a rotating black hole. III. Interaction of the hole with gravitational and electromagnetic radiation*, Astrophys. J. **193**, 443 (1974).

[31] W. Kinnersley, *Type D Vacuum Metrics*, J. Math. Phys. **10**, 1195 (1969).

[32] W. H. Press and S. A. Teukolsky, *Perturbations of a Rotating Black Hole. II. Dynamical Stability of the Kerr Metric*, Astrophys. J. **185**, 649 (1973).

[33] E. Berti, V. Cardoso and M. Casals, *Eigenvalues and eigenfunctions of spin-weighted spheroidal harmonics in four and higher dimensions*, Phys. Rev. **D73**, 02401 (2006), [Erratum: Phys. Rev. **D73**, 109902 (2006)], arXiv:gr-qc/0511111v4 [gr-qc] .

[34] E. W. Leaver, *An Analytic Representation for the Quasi-Normal Modes of Kerr Black Holes*, Proc. R. Soc. A Math. Phys. Eng. Sci. **402**, 285 (1985).

[35] E. W. Leaver, *Solutions to a generalized spheroidal wave equation: Teukolsky's equations in general relativity, and the two-center problem in molecular quantum mechanics*, J. Math. Phys. **27**, 1238 (1986).

[36] E. D. Fackerell and R. G. Crossman, *Spin-weighted angular spheroidal functions*, J. Math. Phys. **18**, 1849 (1977).

[37] E. Seidel, *A comment on the eigenvalues of spin-weighted spheroidal functions*, Class. Quantum Grav. **6**, 1057 (1989).

[38] J. G. Rosa, *Superradiance in the sky*, Phys. Rev. **D95**, 064017 (2017), arXiv:1612.01826 [gr-qc] .

[39] S. W. Hawking and J. B. Hartle, *Energy and angular momentum flow into a black hole*, Commun. Math. Phys. **27**, 283 (1972).

[40] E. Poisson, *A Relativist's Toolkit: The Mathematics of Black-Hole Mechanics* (Cambridge University Press, 2004).

[41] G. B. Cook and M. Zalutskiy, *Gravitational perturbations of the Kerr geometry: High-accuracy study*, Phys. Rev. **D90**, 1 (2014), arXiv:1410.7698 .

[42] G. F. Torres del Castillo, *3-D Spinors, Spin-Weighted Functions and their Applications* (Birkhäuser Boston, 2003).

[43] F. Pacini, *Rotating Neutron Stars, Pulsars and Supernova Remnants*, Nature **219**, 145 (1968).

[44] J. D. Jackson, *Classical Electrodynamics*, 3rd ed. (Wiley, 1998).

[45] J. A. H. Futterman, F. A. Handler and R. A. Matzner, *Scattering from Black Holes*, Cambridge Monographs on Mathematical Physics (Cambridge University Press, 1988).

[46] J. N. Goldberg, A. J. Macfarlane, E. T. Newman, F. Rohrlich, and E. C. G. Sudarshan, *Spin-s Spherical Harmonics and* $\eth$, J. Math. Phys. **8**, 2155 (1967).

[47] J. J. G. Scanio, *Spin-weighted spherical harmonics and electromagnetic multipole expansions*, Am. J. Phys. **45**, 173 (1977).